ISTANBUL TECHNICAL UNIVERSITY ★ GRADUATE SCHOOL

CASE STUDY ON SELECTING OPTIMAL MAIN CENTRAL CONE OF LOW EARTH ORBIT SATELLITE

M.Sc. THESIS

Semih TÜRKOĞLU

Department of Aeronautics and Astronautics Engineering

Aeronautics and Astronautics Engineering Programme

MAY 2023

ISTANBUL TECHNICAL UNIVERSITY ★ GRADUATE SCHOOL

CASE STUDY ON SELECTING OPTIMAL MAIN CENTRAL CONE OF LOW EARTH ORBIT SATELLITE

M.Sc. THESIS

Semih TÜRKOĞLU
(511201142)

Department of Aeronautics and Astronautics Engineering

Aeronautics and Astronautics Engineering Programme

Thesis Advisor: Assoc. Prof. Dr. Özge ÖZDEMİR

MAY 2023

ISTANBUL TEKNİK ÜNİVERSİTESİ ★ LİSANSÜSTÜ EĞİTİM ENSTİTÜSÜ

ALÇAK YÖRÜNGE UYDULARI İÇİN OPTİMUM MERKEZİ KONİ TASARIMININ BELİRLENMESİ ÇALIŞMASI

YÜKSEK LİSANS TEZİ

Semih TÜRKOĞLU
(511201142)

Uçak ve Uzay Mühendisliği Anabilim Dalı

Uçak ve Uzay Mühendisliği Programı

Tez Danışmanı: Doç. Dr. Özge ÖZDEMİR

MAYIS 2023

Semih Türkoğlu, a M.Sc. student of İTU Graduate School student ID 511201142, successfully defended the thesis entitled "CASE STUDY ON SELECTING MAIN CENTRAL CONE OF LOW EARTH ORBIT SATELLITE", which he prepared after fulfilling the requirements specified in the associated legislations, before the jury whose signatures are below.

Thesis Advisor : **Assoc. Prof. Dr. Özge ÖZDEMİR** ....
İstanbul Technical University

Jury Members : **Prof. Dr. Metin Orhan KAYA** ....
Istanbul Technical University

Assis. Prof. Dr. Serhat YILMAZ ....
National Defense University

Date of Submission : 08 May 2023
Date of Defense : 25 May 2023

To my family,

FOREWORD

In this thesis, main central cones for large Low Earth Orbit satellite is designed with considering different design concepts to determine and select the most optimal design concept. For get the results of this study, six different central cones are designed and analyzed with respect to same design requirements and limitations.

First of all, I would like to thank my mother Şerife Türkoğlu and father Oğuz Türkoğlu who have always supported me and always make me feel I can solve all the problems. There is a special thanks to my advisor Assoc. Prof. Dr. Özge Özdemir who always supported me throughout my master degree period and believed in me even in the most difficult times at the thesis stage. I also thanks to my colleagues Mevlüt Demir and Emre Boran Karhan who are two people always answered my questions during the analysis phases of the thesis. Thanks to my mentor at Turkish Aerospace Onur Çakmakçı who always forced me to done great successes. I would like to thank to my head engineer Duygu Çakmakçı who is continued to support my master degree process even at the hardest times.

Finally, thanks to my friends Onur Alan and Sima Aslım Yakut who are support and make me enjoy during the thesis process.

May 2023

Semih TÜRKOĞLU
(Astronautical Engineer)

TABLE OF CONTENTS

Page

ABBREVIATIONS

AL	: Aluminium
CAD	: Computer Aided Design
CC	: Central Cone
CFRP	: Carbon Fiber Reinforced Polymers
CTE	: Coefficient of Thermal Expansion
ECSS	: European Cooperation for Space Standardization
ESA	: European Space Agency
FEA	: Finite Element Analysis
FEM	: Finite Element Model
FOSY	: Factor of Safety Yielding
FOSU	: Factor of Safety Ultimate
GA	: Genetic Algorithm
GEO	: Geostationary Earth Orbit
GSO	: Geosynchronous Earth Orbit
HEO	: High Earth Orbit
LEO	: Low Earth Orbit
LVA	: Launch Vehicle Adapter
MEO	: Medium Earth Orbit
MMPDS	: Metallic Materials Properties Development and Standardization
MOS	: Margin of Safety
NC	: Numeric Contral machining
PSD	: Power Spectral Density
QSL	: Quasi-static Loads
SOL	: Solver
SRS	: Shock Response Spectra
UD	: Unidirectional

SYMBOLS

FsL	**:** Allowable core shear stress in the L direction
FsW	**:** Allowable core shear stress in the W direction
f/f_n	**:** Ratio of forcing frequency to natural frequency
G13	**:** Shear Modulus in the 13 Direction
G23	**:** Shear Modulus in the 23 Direction
M	**:** Mass
λ	**:** Critical Buckling Load Factor
σ_{yield}	**:** Yielding stress
$\sigma_{VonMises}$	**:** Von-Mises stress
τ_{xz}	**:** Interlaminar shear stress in the XZ direction
τ_{yz}	**:** Interlaminar shear stress in the YZ direction

LIST OF TABLES

Page

LIST OF FIGURES

Page

CASE STUDY ON SELECTING OPTIMAL MAIN CENTRAL CONE OF LOW EARTH ORBIT SATELLITE

SUMMARY

In this thesis, determination and selection of the most optimum central cone design concept for low orbit satellites of 1000 kg and above from large class satellites is explained. The designs of the cone and cone assembly parts in the study were made with Siemens NX, and the analyzes applied for comparisons were made with Simcenter 3D. The study consists of two stages, in the first stage, a total of 6 cones, 3 different design concepts from 2 different materials, were compared and two cones were selected after the trade-off study. In the second stage, after the iterations on these two cones, the most optimum central cone design was decided by repeating the trade-off study.

While determining the design constraints and requirements of the central cones, Göktürk-Y was chosen as the reference satellite in accordance with the conditions determined in the thesis. Possible launch vehicles were identified while determining the constraints and requirements. In line with the restrictions, the volume envelope and dimensions were determined. One of the most important parts affecting the dimensions is the launch vehicle adapter and it is produced by the launchers in standard diameters. The LVA diameter chosen for the thesis study is Ø1194 mm. Since they provide direct connection with the cone and the LVA, it has been very effective in determining the cone dimensions. At the same time, stiffness, strength and buckling strength requirements were determined. For rigidity, the first natural frequency value of the central cones and their assemblies must be 140 Hz and above. For the strength and buckling strengths, the calculated safety margin values should be positive. In comparisons, it was decided to use cone mass, cone assembly mass, cone stiffness value, cone assembly stiffness value, cone strength and cone buckling strength values.

In the cone designs, aluminum and CFRP materials, which are most frequently used in space applications, were selected. Six cones are designed with aluminum and CFRP versions as semi-monocoque, grid and sandwich design concepts. Cone assemblies consist of launch vehicle adapter, horizontal structural panel and NC bracket in line with mounting requirements. All cones and mounting parts were designed using Siemens NX and mass comparisons were made by entering material properties. As a result of mass comparisons, sandwich cones were the lightest cones, while the CFRP semi-monocoque cone was the lightest central cone when cone assemblies were compared. This is because NC brackets are not used in the mounting designs of the semi-monocoque cones.

To meet the requirements, 3 basic analyzes were performed on the cones. These are modal analysis, static structural analysis and buckling analysis. Modal analysis was applied both to the central cone itself and to its assembly, while static and buckling analyzes were applied for assembly only. Finite element models and connection conditions were created on Simcenter 3D and the determined analyzes were solved with Simcenter 3D using Nastran solvers. In the thesis study, details about the creation

of finite element models, element types and numbers, connection types are given for all cones and assemblies.

After modeling, modal analysis was performed for 6 central cones. In the modal analysis results, all central cones exceed the design requirement of 140 Hz. In the modal analysis results, the cones from the best to the worst were ranked as CFRP semi-monocoque, CFRP sandwich, Aluminum semi-monocoque, CFRP grid, Aluminum sandwich and finally Aluminum grid cone. For the CFRP semi-monocoque cone with the best results, the result is 485.55 Hz and the follower CFRP sandwich cone is 329.76 Hz. Central cone assemblies meet the requirement of all cones in the modal analysis results. Similarly, the results for the CFRP semi-monocoque cone are the best, but after mounting analyses, the results of the CFRP sandwich cone approached the semi-monocoque version. They are ranked from best to worst as CFRP semi-monocoque, CFRP sandwich, Aluminum sandwich, Aluminum semi-monocoque, CFRP grid and finally Aluminum grid central cone.

As the second type of analysis, static structural analysis was applied on central cone assemblies. For the static analysis, the load condition to be applied on the cones was applied with reference to the reference satellite mass of 1000kg. The cones were loaded from the upper part where they would connect with the satellite with a force of 100 kN, affecting the satellite 10 g, and were included in the static analysis. The calculation method and safety factor to be used in the margin of safety calculations were used as specified in ECSS. As a result of the analyzes made, the best static strength results were obtained with the Aluminum grid cone. From good to bad, they are listed as Aluminum grid, Aluminum semi-monocoque, CFRP semi-monocoque, CFRP sandwich, Aluminum sandwich and finally CFRP grid cone. Metallic cones which designed with classical methods gave the best results in terms of static strength.

As the final analysis type, buckling analysis, which is very important in cone or cylinder type structures, has been applied on central cone assemblies. The loads applied in the static analysis were also used in the buckling analysis. Factor of safety values were applied as specified in ECSS. In the buckling analysis, critical buckling load factor results were obtained with Nastran SOL 105 solver. The critical buckling load factor is the ratio of the design limit load (critical load) of the structure to the defined load envelope and shows how many times the structure can withstand the defined load. As expected, the cones with the sandwich design concept turned out to be the best. All cones have a positive margin of safety. The best result was the CFRP sandwich center cone with 21.695, followed by the Aluminum sandwich cone with 15.31. Third best central cone is CFRP semi-monocoque cone, came with 5.505. They are ranked from best to worst as CFRP sandwich, Aluminum sandwich, CFRP semi-monocoque, Aluminum semi-monocoque, Aluminum grid and finally CFRP grid cone.

The first stage resulted in the trade-off study after all the design and analysis activities were completed. All cones were compared by defining different weights for the categories determined in the trade-off study. The aim of the first stage is to select the best 2 central cones among the 6 central cones. After the study, the two best central cones are CFRP sandwich and CFRP semi-monocoque central cones. The CFRP sandwich central cone is in the best position with a score of 8.4937 out of 10, while the CFRP semi-monocoque central cone scored 8.1125.

The second phase continued with design optimizations of CFRP sandwich and CFRP semi-monocoque central cones. These optimizations aimed not to decrease the strength of the structures while gaining mass. The first optimization for the CFRP sandwich center cone is to have the NC bracket removed from the assembly. The second change is the density change of the honeycomb used in the sandwich structure. After these optimizations, the CFRP sandwich central cone assembly has lightened 6.29 kg in total. The analyzes made in the first stage were repeated. The modal analysis results improved at 8.26 Hz for the cone and 25.78 Hz for the assembly level compared to the first situation. Similarly, static analysis results have also improved. The safety margin value of the structure has been increased from 0.266 to 1.123. The buckling analysis has also become better as in other analyses. The initial result, which was 21.695, improved to 24.925 after optimization.

Optimization studies for CFRP semi-monocoque cone include thickness optimizations. The overall cone thickness has been reduced from 3mm to 1.6mm. As a result of this iteration study, a gain of 2.37 kg was achieved. Modal analysis results were improved at 9.94 Hz for the central cone and 73.18 Hz for the assembly. Static analysis results got better, but there was no noticeable improvement. The Tsai-Wu failure index score increased from 0.303 to 0.293. The results of the buckling analysis have worsened after the thinning of the structure, but still meet the requirements. While the initial results were 5.505, this value decreased to 3.37 after design updates.

In the second stage, a trade-off study including only CFRP sandwich and CFRP semi-monocoque central cones was conducted in line with the categories determined in the first stage. With a score of 9.5875 out of 10, the CFRP sandwich cone was the most optimal cone of the study.

Within the scope of the results, different central cone design concepts were designed for the 1000kg low orbit satellite and compared to obtain the most optimal design. As a result of the studies, the CFRP sandwich central cone was selected as the most suitable cone to be used in such satellites. Future studies can focus on further optimization studies for this cone, and the analysis can be verified by testing and manufacturing.

ALÇAK YÖRÜNGE UYDULARI İÇİN OPTİMUM MERKEZİ KONİ TASARIMININ BELİRLENMESİ ÇALIŞMASI

ÖZET

Bu tez çalışmasında büyük sınıf uydulardan 1000kg ve üstü alçak yörünge uyduları için en optimum merkezi koni tasarım konseptinin belirlenmesi ve seçilmesi anlatılmıştır. Çalışmada yer alan koni ve koni montaj parçalarının tasarımları Siemens NX, karşılaştırmalar için uygulanan analizler ise Simcenter 3D ile yapılmıştır. Çalışma iki aşamadan oluşmaktadır, birinci aşamasında 2 farklı malzemeden 3 farklı tasarım konsepti olmak üzere toplam 6 adet koni karşılaştırılmış ve yapılan getiri-götürü çalışması sonrasında iki adet koni seçilmiştir. İkinci aşamasında ise bu iki koni üzerinde yapılan iterasyonlar sonrasında tekrarlanan getiri-götürü çalışması ile en optimum merkezi koni tasarımına karar verilmiştir.

Merkezi konilerin tasarım kısıtlamaları ve gereksinimleri belirlenirken referans uydu olarak tezde belirlenen şartlara da uygun olarak Göktürk-Y seçilmiştir. Kısıtlamalar ve gereksinimler belirlenirken muhtemel fırlatıcı araçları belirlenmiştir. Kısıtlamalar doğrultusunda hacim zarfı ve boyutlar belirlenmiştir. Boyutları etkileyen en önemli parçalardan birisi ayrılma halkasıdır ve fırlatıcılar tarafından standart çaplarda üretilmektedir. Tez çalışması için seçilen ayrılma halkası çapı Ø1194 mm'dir. Koni ile ayrılma halkası direkt bağlantı sağladıkları için koni boyutlarının belirlenmesinde çok etkili olmuştur. Aynı zamanda katılık, mukavemet ve burkulma mukavemeti gereksinimleri belirlenmiştir. Katılık için merkezi konilerin ve onların montajlarının birinci doğal frekans değerinin 140 Hz ve üzerinde olması gerekmektedir. Mukavemet ve burkulma mukavemetleri için ise hesaplanan güvenlik marjı değerlerinin pozitif olması gerekmektedir. Karşılaştırmalarda koni kütlesi, koni montajı kütlesi, koni katılık değeri, koni montaj katılık değeri, koni mukavemeti ve koni burkulma dayanımı değerleri kullanılması kararlaştırılmıştır.

Koni tasarımlarında uzay uygulamalarında en sık kullanılan aluminyum ve CFRP malzemeler seçilmiştir. Koniler kısmi-monokok, ızgara ve sandviç tasarım konseptleri olmak üzere aluminyum ve CFRP versiyonları ile 6 adet tasarlanmıştır. Koni montajlarında ayrılma halkası, yatay yapısal panel ve montaj gereksinimleri doğrultusunda NC braketten oluşmaktadır. Tüm koniler ve montaj parçaları Siemens NX kullanılarak tasarlanmış ve malzeme özellikleri girilerek kütle karşılaştırmaları yapılmıştır. Kütle karşılaştırmaları sonucunda sandviç koniler en hafif koniler olurken koni montajları kıyaslandığı zaman CFRP kısmi-monokok koni en hafif merkezi koni olmuştur. Bunun sebebi kısmi-monokok konilerin montaj tasarımlarında NC braket kullanılmamış olmasıdır.

Gereksinimleri karşılamak için koniler üzerine 3 temel analiz yapılmıştır. Bunlar, modal analiz, statik yapısal analiz ve burkulma analizidir. Modal analiz hem merkezi konileirn kendisine hem de montajına uygulanmıştır, statik ve burkulma analizleri ise sadece montaj için uygulanmıştır. Sonlu eleman modelleri ve bağlantı koşulları Simcenter 3D üzerinden oluşturulmuş olup belirlenen analizler yine Simcenter 3D ile Nastran çözücüsü kullanılarak çözdürülmüştür. Tez çalışmasında sonlu eleman

modellerinin oluşturulması, eleman tipleri ve sayıları, bağlantı tiplerine dair detaylar tüm koni ve montajları için verilmiştir.

Modellemeler sonrasında 6 merkezi koni için modal analiz yapılmıştır. Modal analiz sonuçları sonrasında tüm merkezi koniler tasarım gereksinimi olan 140 Hz sınırını aşmaktadır. Modal analiz sonuçları sonrasında en iyi sonuçtan en kötüye koniler CFRP kısmi-monokok, CFRP sandviç, Aluminyum kısmı-monokok, CFRP ızgara, Aluminyum sandviç ve son olarak Aluminyum ızgara koni şeklinde sıralanmıştır. En iyi sonuçlara sahip olan CFRP kısmi-monokok koni için sonuç 485.55 Hz şeklindedir ve takipçi olan CFRP sandviç koni 329.76 Hz'dir. Merkezi koni montajları modal analiz sonuçlarında yine tüm koniler gereksinimi karşılamaktadır. Benzer şekilde CFRP kısmi-monokok koni için çıkan sonuçlar en iyisidir fakat montaj analizleri sonrasında CFRP sandviç koni sonuçları kısmi-monokok versiyonuna yaklaşmıştır. En iyiden en kötüye CFRP kısmi-monokok, CFRP sandviç, Aluminyum sandviç, Aluminyum kısmi-monokok, CFRP ızgara ve son olarak Aluminyum ızgara merkezi koni olarak sıralanmıştır.

İkinci tip analiz olarak statik yapısal analiz merkezi koni montajları üzerinde uygulanmıştır. Statik analiz için koniler üzerine uygulanacak yük durumu referans uydu kütlesi olan 1000kg referans alınarak uygulanmıştır. Koniler uydu 10g etki edecek şekilde 100 kN'luk bir kuvvet ile uydu ile bağlantı yapacakları üst kısmından yüklenerek statik analizlere sokulmuştur. Güvenlik marjı hesaplamalarında kullanılacak hesaplama yöntemi ve güvenlik faktörü ECSS'te belirtildiği gibi kullanılmıştır. Yapılan analizler sonucunda en iyi statik mukavemet sonuçları Aluminyum ızgara koni ile gelmiştir. İyiden kötüye Aluminyum ızgara, Aluminyum kısmi-monokok, CFRP kısmi-monokok, CFRP sandviç, Aluminyum sandviç ve son olarak CFRP ızgara koni olarak sıralanmıştır. Klasik yöntemler ile tasarlanan metalik koniler statik dayanımları olarak en iyi sonuçları vermiştir.

Son analiz tipi olarak koni veya silindir tipi yapılarda yapılması çok önemli olan burkulma analizi merkezi koni montajları üzerine uygulanmıştır. Statik analizde uygulanan yükler aynı şekilde burkulma analizlerinde de kullanışmıştır. Güvenlik faktörü değerleri ECSS'te belirtildiği gibi uygulanmıştır. Burkulma analizinde Nastran SOL 105 çözücüsü ile burkulma yük faktörü sonuçları elde edilmiştir. Burkulma yük faktörü ise, yapının tasarım limit yükünün (kritik yük) belirlenen yük zarfına oranıdır ve yapının belirlenen yüke kaç kat dayanabileceğini göstermektedir. Analiz sonuçları beklendiği gibi sandviç tasarım konseptine sahip koniler en iyi çıkmıştır. Tüm koniler pozitif güvenlik marjına sahiptir. En iyi sonuç 21.695 ile CFRP sandviç merkezi koni ile gelmiştir ve onu Aluminyum sandviç koni 15.31 ile takip etmektedir. Dikkat edilmesi gereken kısım 3. En iyi koni olan CFRP kısmi-monokok konini 5.505 ile gelmiştir. En iyiden en kötüye CFRP sandviç, Aluminyum sandviç, CFRP kısmi-monokok, Aluminyum kısmi-monokok, Aluminyum ızgara ve son olarak CFRP ızgara koni olarak sıralanmıştır.

Birinci aşama yapılan tüm tasarım ve analiz faaliyetleri tamamlandıktan sonra yapılan getiri-götürü çalışması ile sonuçlanmıştır. Getiri-götürü çalışmasında belirlenen kategoriler farklı ağırlıklar tanımlanarak tüm koniler karşılaştırılmıştır. Birinci aşamanın amacı 6 merkezi koni arasından en iyi 2 merkezi koninin seçilmesidir. Yapılan çalışma sonrasında en iyi iki merkezi koni CFRP sandviç ve CFRP kımi-monokok merkezi konilerdir. CFRP sandviç merkezi koni 10 üzerinden 8.4937 puan alarak en iyi konumdadır, CFRP kısmi-monokok merkezi koni ise 8.1125 puan almıştır.

İkinci aşama CFRP sandviç ve CFRP kısmi-monokok merkezi konilerin tasarım optimizasyonları ile devam etmiştir. Bu optimizasyonlar kütle kazanımları olurken yapıların dayanımlarının düşmemesini hedeflemiştir. CFRP sandviç merkezi koni için ilk yapılan optimizasyon NC braketin montajdan çıkarılmış olmasıdır. İkinci değişiklik olarak ise sandviç yapıda kullanılan honeycomb'ın yoğunluk değişikliğidir. Bu optimizasyonlar sonrasında CFRP sandviç merkezi koni montajı toplam 6.29 kg hafiflemiştir. Birinci aşamada yapılan analizler tekrar edilmiştir. Modal analiz sonuçları ilk duruma göre koni özelinde 8.26 Hz ve montaj seviyesinde 25.78 Hz iyileşmiştir. Benzer şekilde statik analiz sonuçları da iyileşmiştir. Yapının güvenlik marjı değeri 0.266'dan 1.123'e çıkarılmıştır. Burkulma analizi de yine diğer analizlerde olduğu gibi daha iyi duruma gelmiştir. 21.695 olan ilk sonuç, optimizasyon sonrasında 24.925 olarak iyileşmiştir.

CFRP kısmi-monokok koni için optimizasyon çalışmaları kalınlık optimizasyonları içermektedir. Tüm koni kalınlığı 3mm'den 1.6 mm'ye düşürülmüştür. Bu iterasyon çalışması sonucunda 2.37 kg kazanç sağlanmıştır. Modal analiz sonuçları merkezi koni özelinde 9.94 Hz, montaj kapsamında ise 73.18 Hz iyileştirilmiştir. Statik analiz sonuçları daha iyi hale gelmiş fakat gözle görülür bir iyileşme olmamıştır. Tsai-Wu hata indeks puanı 0.303'ten 0.293'e gelmiştir. Burkulma analizi sonuçları ise yapının incelmesi sonrasında daha kötü bir hale gelmiş fakat hala gereksinimleri karşılar durumdadır. İlk sonuçlar 5.505'ken tasarım güncellemeleri sonrasında bu değer 3.37'ye düşmüştür.

İkinci aşama ilk aşamada da belirlenen kategoriler doğrultusunda sadece CFRP sandviç ve CFRP kısmi-monokok merkezi konileri içeren bir getiri-götürü çalışması yapılmıştır. 10 üzerinden 9.5875 puan ile CFRP sandviç koni çalışmanın en optimum konisi olmuştur.

Sonuçlar kapsamıında 1000kg'lık alçak yörünge uydusu için farklı merkezi koni tasarım konseptleri tasarlanıp, en optimum tasarımı elde etmek için karşılaştırılmıştır. Yapılan çalışmalar sonucunda CFRP sandviç merkezi koni bu tarz uydularda kullanılmak üzere en uygun koni seçilmiştir. Gelecek çalışmalarda bu koni için daha fazla optimzasyon çalışması yapılmasına odaklanılabilir ve üretim yapılarak testler ile yapılan analizler doğrulanabilir.

1. INTRODUCTION

Today, satellites with different mission definitions are in orbit with various sizes and masses. Various types of satellites contain different subsystems in order to perform their duties. Different types of subsystems are used by satellites to carry out their functions. During the lifetime of the satellite, all of them should function together without any issues. One of the subsystems for satellites is the structural subsystem, which serves to protect and keep together other subsystems as well as endure stresses during launch. The structural subsystem has primary, secondary, and tertiary structures to accomplish this goal. Primary structures are fundamental parts of structural subsystem which is standing out against main load path and holding all other subsystems.

Central cones or cylinders can be described as the backbones of satellites. As a primary structure, central cones are directly having interfaces with launch vehicle adapters and resist the main load path and vibrations comes from launcher. Because of being the main component of the structural subsystem in the satellite to withstand the loads from launcher, the strength of the central cones should be high to resist. By improving technology in the spacecraft structures, the production type and material usage for primary structures for satellite is also vary. There are different types of approaches on the central cone or cylinder design concepts with considering production capability, cost, easy to integrate, space qualified products and physical properties which are size, mass, strength, stiffness of the structure.

To select a design concept for primary structure of satellite as central cones, the defined design requirements and restrictions are considered and evaluated by engineers. In that evaluation phase of the projects generally heritage and know-how of the engineers have critical role. That is why engineers tends to go with the design of traditional concepts and materials in the satellite design phases. However, the traditional concepts or materials can be change by using new technologies. New materials and concepts may increase the structure performance during the tests and in the orbit of the spacecraft. That is why all around the world and in Turkiye, companies or institutes studies on the development of different types of production and usage of new structures for satellites.

1.1 Purpose of Thesis

The purpose of the thesis is comparing and selecting the optimum design concept of central cone for large satellites around 1000kg in the Low Earth Orbit (LEO) with using the ECSS standards to verification by analyzes. For comparison, the categories are selected as mass of central cones, mass of their assemblies, stiffness of central cones, stiffness of their assemblies, strength of central cone assemblies and buckling strength of the central cone assemblies.

There are two phases in the thesis to determine the optimum design of central cone. There are six different design of central cone which are three different design concepts with CFRP and aluminium materials. The design concepts are semi-monocoque, grid and sandwich structures.

Design requirements and limitations are defined with considering a reference satellite which is an Earth Observation Satellite with 1000kg. For all the central cones, same limitations and requirements applied.

In the first phase of the study there are six different types of central cone designed by using Siemens NX. All central cones and their assemblies are compared between each other with analyzes done by using Simcenter 3D. The analyzes performed in the study are modal analysis, static structural analysis and buckling analysis. At the end of the phase one, there is a trade-off study with defined categories to compare the design solutions for the thesis.

In the second phase of the study, first two central cone design solution selected by using trade-off study in phase one and optimizations on the central cones done for that two cone assemblies. Same with the phase one, in the phase two also same type of analyzes performed with considering ECSS. Optimized central cones are compared between each other to select the optimum design of central cone at the end of the thesis with using same categories with phase one.

1.2 Literature Review

There are various space projects which are using central cylinder or central cone in their structural design. Material, type, shape or size of the central structure of the spacecraft affect the selection of the design concept. On the other hand, from past to now, engineers are working on the make structures lighter without losing any performance effect. For make this dream come true, different types of designs, production technologies, materials are selecting with serious optimizations on traditional structures.

As a monocoque central cone design example, Euclid spacecraft can be an example [1]. From the structural architecture of the Euclid spacecraft there is a central cone in the service module of the spacecraft. Central cone of the Euclid spacecraft provides connection with launch vehicle and, also the monocoque reverse central cone holding the propellant tank and its hardware of the spacecraft. So, the central cone inside of the Euclid spacecraft is supporting the satellite and as an additional role, holding the propulsion subsystem.

For grid typed central cylinder structure example, Express-2000 ISS-Reshetnev is an example [2]. There is a composite lattice typed central cylinder inside of the satellite. That satellite is a communication satellite and in orbit currently. Also, in the paper of Morozov, E.V and Lopatin, A.V. [2] the Express-2000 ISS-Reshetnev satellite has a composite lattice central cylinder and connected to launcher with composite lattice central cone. When these structures are subjected to high intensity loadings during the launch and injection into orbit, the lattice shells should deliver the required level of mechanical structural performance. Axial compression, transverse and simple bending, and torsion are typically included. One of these shells' usual mechanisms of failure is buckling under these loads.

Sandwich central cones are another type of design concepts for satellites. Sentinel-3 satellite of ESA’s has a sandwich central cone inside of it as a primary structure [3]. The skins of the sandwich central cone are CFRP and core of the sandwich is aluminium honeycomb. It is also used as primary load path which is directly connecting with LVA by using glue and rivets.

Except from central cone examples, there are some studies on the optimization of central cylinders or cones. From the paper of Abay M. M., Atak A., İzgü O., Şahin M.

[4] there are some optimization studies on CFRP central cylinder for a large communication satellite. The topologic shape optimization process was carried out utilizing various types of holes after determining the best lay-up, orientations, and number of laminate layers for the CFRP sandwich cylindrical shell based on the loads, which vary with location. The form of the holes was chosen following topologic optimization based on elimination of the lowest stressed regions.

There is another optimization study about composite grid type central cylinder from Pavlov, L., Smeets, B., Simonian, S. M. [5]. According to them compared to conventional structural topologies, lattice composite structures provide a number of potential benefits for aerospace applications, including reduced manufacturing costs and structure mass. For composites, a semi-automatic optimization technique made up of CAD, FEA and GA pieces has been created. It is utilized to solve the lattice satellite central cylinder variant of the EDRS-C satellite's minimum-mass optimization issue.

Afonso, S. M. B., Sienz, J., Belblidia, F. [6] stated the strategies and optimization processes for monocoque and semi-monocoque cylinders and cones. Their study demonstrated the application of many optimization techniques to produce an ideal design for plates and shells. Procedures for structural form optimization and topology optimization were both taken into consideration. These two optimization applications, when used separately, result in new designs that are vastly improved over the original ideas.

Guerrera A. and Varbaro A. [7] studied on launch vehicle adapter design optimizations with using reverse engineering method for Ariane 5 conical shaped PAS 1194VS and PAS 1194C. By performing static and dynamic analysis on the modelled PAS 1194VS and PAS 1194C, the weight optimization done 30% from the original designs. All analyses were carried out to assess the structure's optimization for strength, stability, and weight.

There is also a paper from Günal A.B., Atak A. and Şahin M. [8] which is objected to create a methodology of trade-off study on central cylinder of satellites. The satellite referenced in the study is a communication satellite. The study also attempts to increase the design option selection techniques' objectivity in the area. By evaluating the measurable criteria using analytical findings, the most widely used approach, the Decision Matrix, is enhanced. Eleven Point Scaling categories are redesigned to be suitable with applications for space systems design. In order to evaluate the design possibilities subjectively and find team consensus, a belief map is designed.

2. SATELLITE TYPES, SUBSYSTEMS AND DESIGN LOADS

2.1 Satellite Classifications

Satellites can be classified in different ways. One of the most important factors in this classification is the main task of the satellite. That is because the main purpose of the satellite generally also defines the orbit of the satellite and generally payload of the satellite. When we define the payload of the satellite at the beginning of the project, we also get some performance requirements which are guide the determination of the satellite mass. First of all, satellites are named according to the orbit they serve. These orbits are also classified between each other with different cases, but I will focus on the altitude classifications of the orbits for satellites which are [9]:

- Low Earth Orbit (LEO)
- Medium Earth Orbit (MEO)
- Geostationary or Geosynchronous Orbit (GEO and GSO)
- High Earth Orbit (HEO)

LEO is the type of orbit closest to the earth in terms of distance. The distance of LEO satellites to the Earth varies between 180-2000 km. It is the type of orbit used by earth observation satellites. MEO covers a distance of 2000–35000 km from the Earth's surface. It is the type of orbit generally used by GPS satellites and earth observation satellites produced to observe certain places. GEO is a specific orbit which is 35786 km above the Earth. Satellites at GEO or GSO need to point particular place on Earth which are generally communication satellites. HEO is further than 35000 km and generally meteorological satellites are using this orbit.

Secondly, satellites can be classified depends on the purpose. As I mentioned before the main objective of the satellites also define the payload types. The shape, size, mass, etc. can be change depends on the payload and its performance that is why it is leading the general size and shape of the satellite. According to usage we can define satellites as [9]:

- Military Satellites
- Communication Satellites

- Earth Observation Satellites
- Meteorological Satellites
- Navigation Satellites
- Astronomical Satellites

Finally, satellites can be named according to their masses as shown in below: [10]

- Large Satellites (M > 1000 kg)
- Medium-sized Satellites (500 kg < M < 1000 kg)
- Minisatellite (100 kg < M < 500 kg)
- Microsatellite (10 kg < M < 100 kg)
- Nanosatellite (1 kg < M < 10 kg)
- Picosatellite (M < 1 kg)

2.2 Satellite Subsystems

Satellites have different kind of subsystems to perform their duties. All of them should work seamlessly during the lifetime of the satellite. Generally, satellites have these subsystems:

- Structural Subsystem
- Thermal Control Subsystem
- Attitude and Orbit Control Subsystem
- Power Subsystem
- Command and Data Handling Subsystem
- Communication Subsystem
- Payload Subsystem (differ according to mission)

The main functions and purposes of these subsystems are summarized. The function of the Thermal Control Subsystem is to maintain all spacecraft, Payload components and subsystems within the required temperature limits for each mission phase. Power Subsystem's purpose is generating and arranging the power needed by the satellite, perform distribution and storage functions to other systems. As mentioned in the name Attitude and Orbit Control Subsystem is responsible of controlling the attitude and the orbit of the satellite with using sensors, actuators and software. Command and Data Handling Subsystem has the brain of the satellite which is controlling the other subsystems sometimes automatically or with telemetry coming from ground stations. It is also handling data from ground station and also from satellite payload or other subsystems, and it can store the same data. The main function of the Communication Subsystem is communicating with ground station. Payload Subsystem can be differed according to the mission. For this thesis, I will focus and assume a satellite which is an Earth Observation and Reconnaissance Satellite. That means, Payload Subsystem for these kinds of satellites is Electro-Optic Camera and its components. At Figure 2.1 an example of Earth Observation and Reconnaissance Satellite is shown.

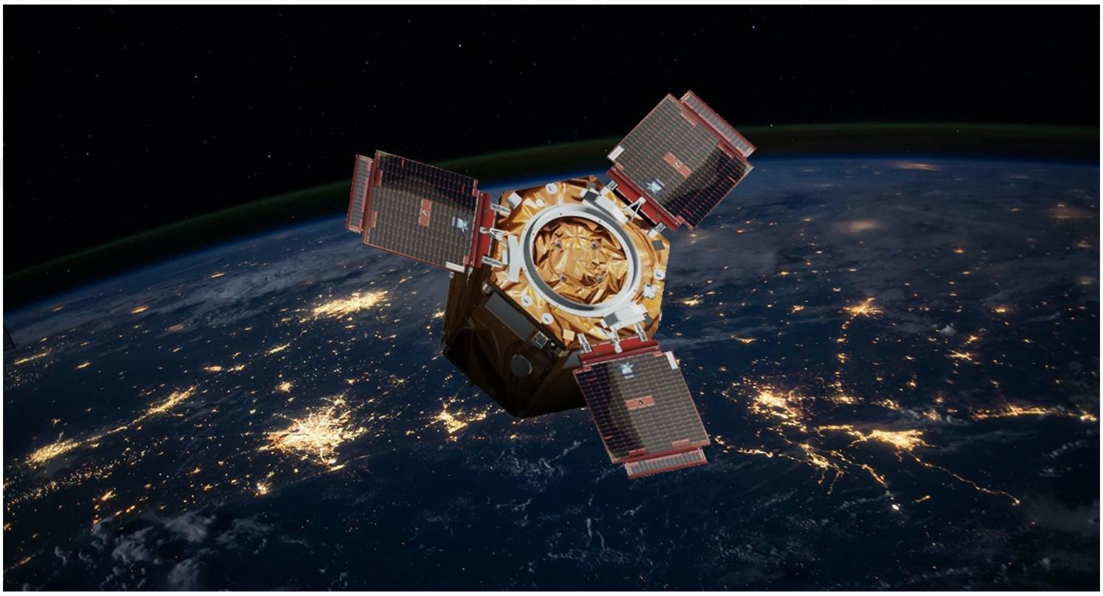

Figure 2.1 : Göktürk – 2 Satellite as an example of Earth Observation and Reconnaissance Satellite [11]

The fundamental function of the Structural Subsystem is supporting all the other subsystems together. Structural Subsystem should ensure to withstand all the mechanical loads to protect satellite. Generally, these mechanical loads are coming from handling and launch phase. Moreover, Structural Subsystem should maintain alignment of sensors, antennas and moving parts. In addition to all structural functions, Structural Subsystem has some nonstructural functions too. As an example for that are conducting electricity and transferring or isolating from heat [12]. There is some space environment affects which structure of the satellite withstand at space. These space environments are [13]:

- Thermal environment
- Vacuum environment

- Neutral particles
- Plasma (low-energy charged particles)
- Charged-particle radiation (high energy)
- Micrometeoroids and debris

Satellite structures can be divided into three parts as primary structures, secondary structures and tertiary structures. [13]

1- Primary structure: It is holding all other subsystems together and also withstand and support the most critical loads. Main load path from spacecraft to launcher is using primary structure.
   a. Central body structure (Structural panels, central cylinders, shear panels, etc.)
   b. Launch vehicle adapter
2- Secondary structure: It can be brackets for equipment or structural panels. This kind of structures are not the main load path but also supporting and withstanding loads for components which they support.
   a. Appendages
   b. Support trusses
   c. Antenna dishes
   d. Propellent tanks and lines
   e. Instruments and mechanisms
3- Tertiary structure: Structures generally using for mounting.
   a. Component housings
   b. Bolts and rivets
   c. Electronic components
   d. Soldered joints

As a part of the primary structure of the satellite, central cone is a crucial part of load path from satellite to launcher. Being a lighter spacecraft is vital for space industry. And if, the load from payload follows directly the side panels or struts, satellite can be heavier than using conical or cylindrical shaped structures. The main philosophy of using the central cone is attaching the cone directly to the launch vehicle adapter. It can be shear panels or trusses for transferring the load from payload to central cone and, central cone can transfer the load to the launcher.

2.3 Mechanical Design Loads

Structural assemblies and components must be designed to endure the loads applied by the mechanical environments to which they are exposed throughout their lifetime. According to ECSS (European Cooperation for Space Standardization) lifetime of a spacecraft shall include transportation, handling, testing, storage, pre-launch, launch, operation and descent if it is necessary [14]. During the validation event, on the satellite the worst combinations of the loads should be applied. To simulate the worst condition which is generally launch phases, there are some tests and test loads applied to satellite on the ground with specific launch phase load types. In addition to tests, the ground events have also some loads on the structure of the satellite which are generally minimal if there is a comparison with launch phases.

2.3.1 Launch loads

Regarding to the satellite volume envelope, mission orbit or mass of the satellite, projects are selecting the launchers to carry them to their orbit or transfer orbit. In the design phases of the projects, engineers are designing the satellite structure with considering the given load envelopes from launcher user manuals. In the launcher user manuals, it is defined that what kind of environment will affect the satellite and what kind of requirements to comply with design. At Figure 2.2 it is shown that as an example of launcher design.

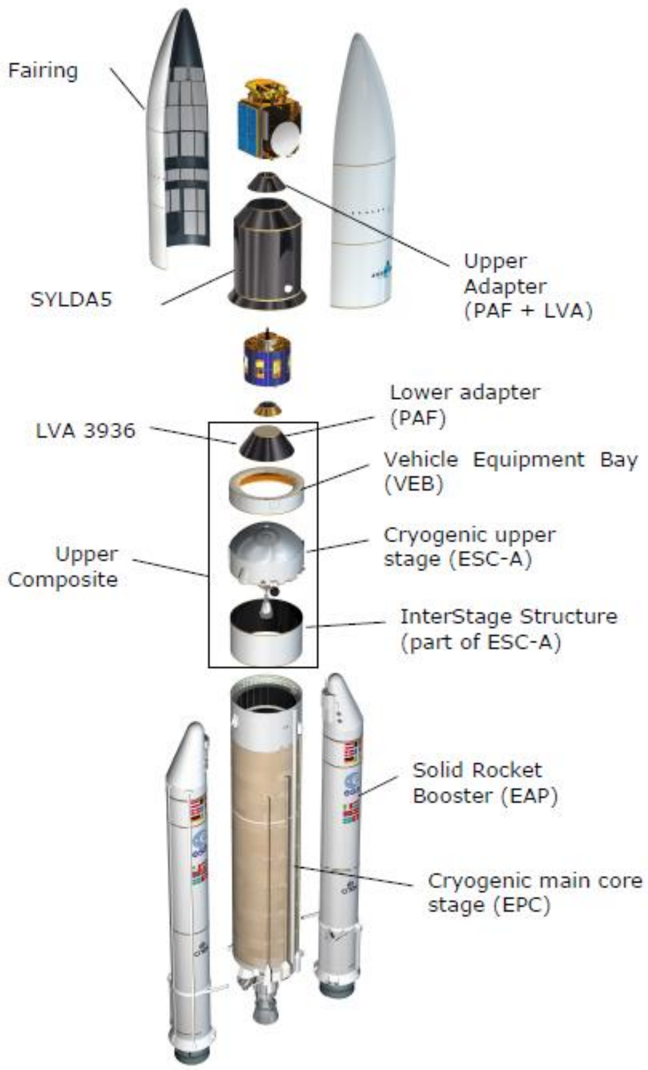

Figure 2.2 : Ariane – 5 Launcher Design [15]

2.3.1.1 Quasi-static loads

At different stages of the launch, different level and types of loads are applied on the launcher's payload which is satellite in this case. As an example of that in Soyuz's user manual for quasi-static accelerations or loads (QSL) it is described in the Figure 2.3 in which phase what kind of 'g' levels are occurred on payload.

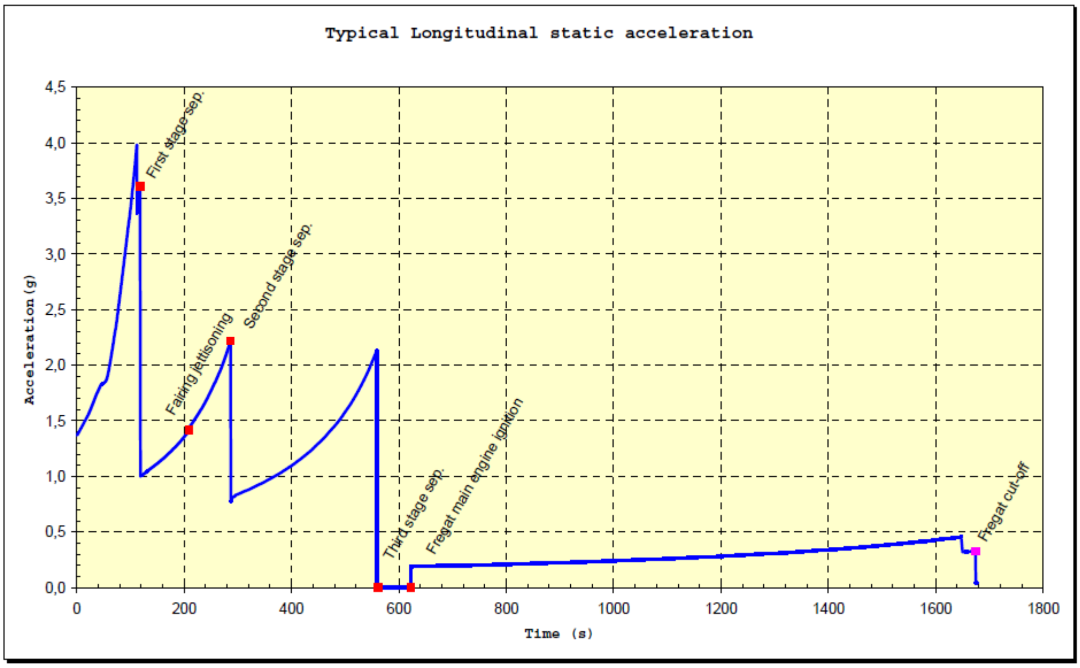

Figure 2.3 : Typical Longitudinal Static Acceleration [16]

The load events on Figure 2.3 are listed at Figure 2.4 for QSL of Soyuz and also at Figure 2.5 the load envelope for QSL is shown.

Load Event		QSL (g) (+ = tension; − = compression)					
		Lateral			Longitudinal		
		Static	Dynamic	Total	Static	Dynamic	Total
0	Ground transportation	-	±0,3	±0,3	−1,0	±0,3	min −1,3 max −0,7
1	Lift-off	±0,2	±1,6	±1,8	−1,0	±0,6	min −1,6 max −0,4
2	Flight with maximum dynamic pressure (Qmax)	±0,4	±0,7	±1,1	−2,4	±0,4	min −2,8 max −2,0
3	First-stage flight with maximal acceleration	±0,1	±0,8	±0,9	−4,3	±0,7	min −5,0 max −3,6
4	Separation between first and second stages	±0,2	±0,9	±1,1	−4,1 −1,0	±0,2 ±0,4	min −4,3 max −0,6
5	Second-stage flight	±0,1	±1,1	±1,2	−1,0 −2,6	±0,4 ±1,4	min −4,0 max −0,6
6	Separation between second and third stages	±0,2	±0,6	±0,8	−2,6 −0,2	±0,7 ±1,5	min −3,3 max +1,3
7	Beginning of third-stage flight	±0,2	±0,6	±0,8	−1,0	±1,9	min −2,9 max +0,9
8	Third-stage engine cutoff	±0,1	±0,3	±0,4	−4,0 0,0	0,0 ±1,8	min −4,0 max +1,8

Figure 2.4 : Design Limit Load Factors of Soyuz [16]

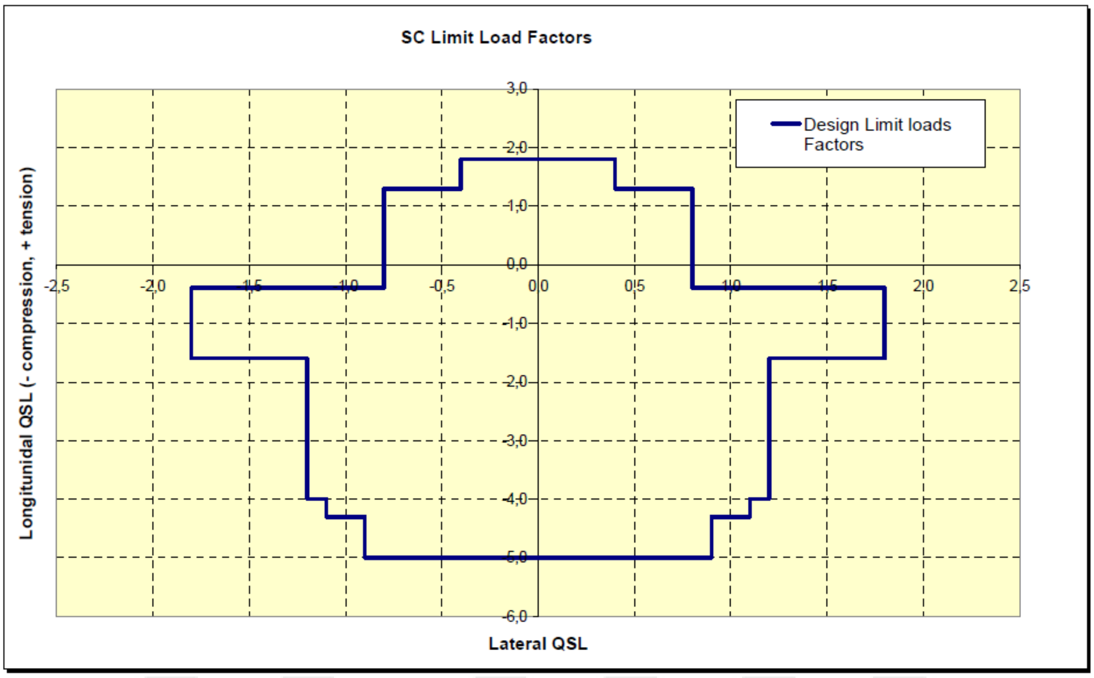

Figure 2.5 : Spacecraft Design Limit Loads [16]

Before the launcher selection, all the candidate launchers' load envelopes are bringing together and the worst case of the load factors are becoming the load envelope to use it in the designs.

2.3.1.2 Sine vibration

During the launcher flight especially at atmospheric flight phase, there are some sinusoidal vibration effects on the satellite. These phases are typically occurring on the satellite around 6 minutes. In the launchers' user manuals, the longitudinal and lateral sine amplitude with respect to a range of frequency band is given. These sine amplitudes are limit sine vibration load limits at satellite's adapter interface with launcher. In the Figure 2.6 and Figure 2.7, limit load levels are shown at equivalent sine environment for Soyuz [16].

Direction	Frequency Band (Hz)						
	1 – 5	5 – 10	10 – 20	20 – 30	30 - 40	40 - 60	60 – 100
	Sine Amplitude (g)						
Longitudinal	0.4	0.5	0.8	0.8	0.5	0.5	0.3
Lateral	0.4	0.6	0.6	0.4	0.4	0.3	0.3

Figure 2.6 : Limit Load Levels of Soyuz at equivalent sine environment [16]

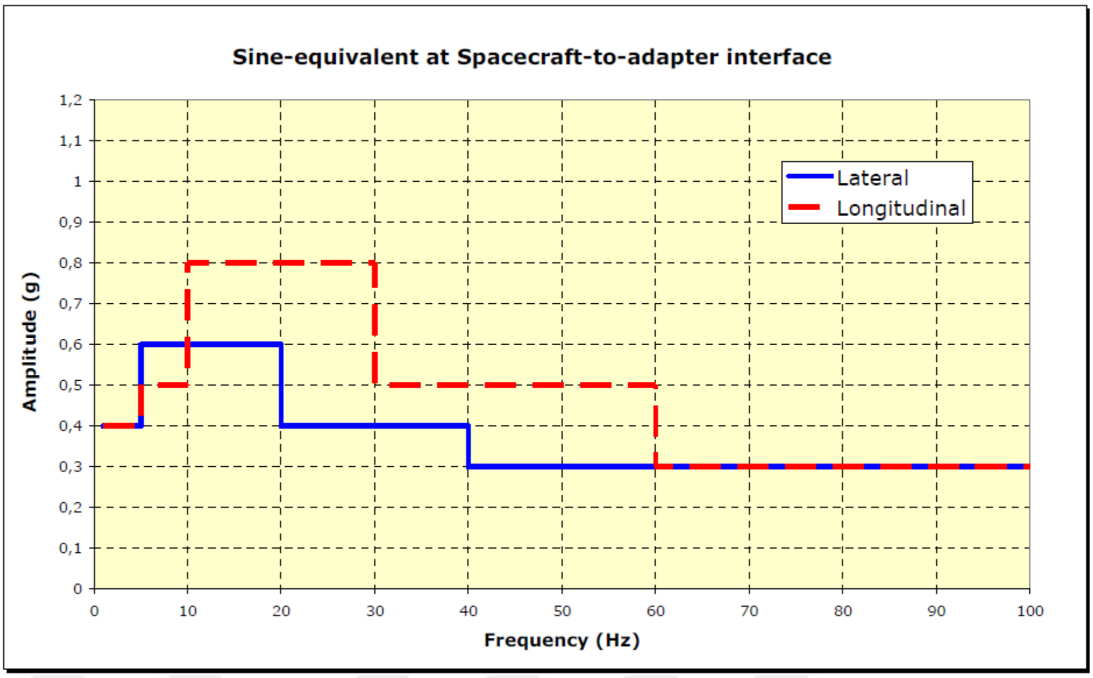

Figure 2.7 : Sine equivalent vibration at adapter interface for Soyuz [16]

2.3.1.3 Random vibrations

Random Vibration affects are kind of different than previous load cases. It is because of for some launchers, it is covered from acoustic load cases above 100 Hz and covered from sine load cases under 100 Hz. However, random vibration has important role on designing a spacecraft and need qualification tests before flight with respect to given load cases from launchers before flight. These loads are occurred on the top of launch vehicle adapter interface of launcher side. As described before, from Falcon 9 launch vehicle user manual that frequency levels are divided into 3 main stages as low frequency (0-100 Hz), mid frequency (100 – 600 Hz) and high frequency (600 – 2000 Hz) [17]. These stages and Power Spectral Density (PSD) are shown in Figure 2.8.

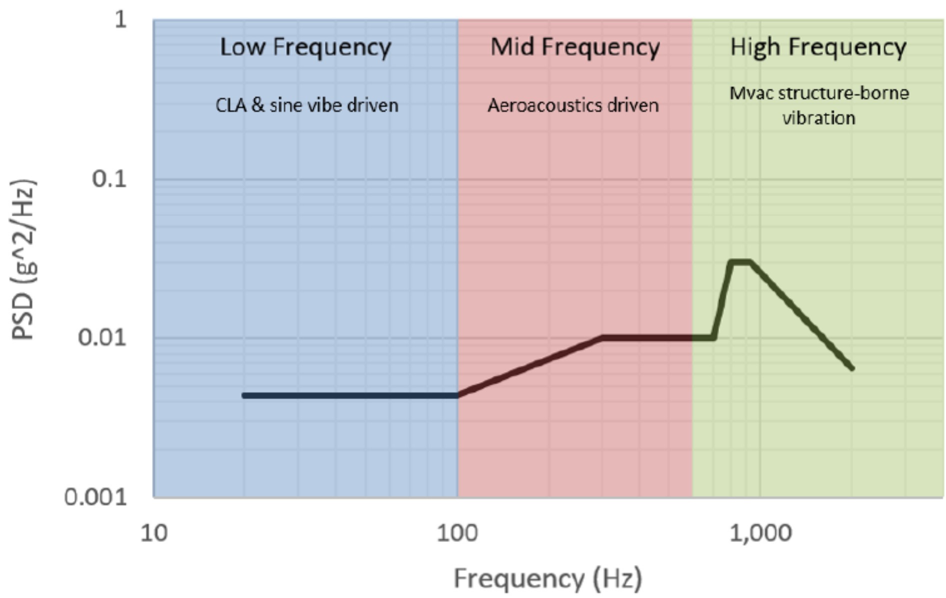

Figure 2.8 : Falcon 9 random vibration environment (5.12 grms) [17]

2.3.1.4 Acoustic vibrations

Acoustic vibration can be occurred on ground and during flight. Generally, because of the venting holes on fairing of launchers there are not any acoustic vibration effects on ground. In flight, it is produced by acoustic pressure fluctuations under the hood, the impingement of engine smoke on the pillow during lift-off, and unstable aerodynamic events transmitted from the upper composite structures during atmospheric flight. Except for the take-off and transonic phase, the acoustic levels are significantly lower than the values specified below [18]. For Vega-C launcher, acoustic vibration levels and load envelopes are shown at Figure 2.9 and Figure 2.10.

Octave center frequency (Hz)	**Flight limit level (dB)** (reference: 0 dB = 2 x 10^{-5} Pa)	
	Lift-off (H0 → H0+3s)	Atmospheric phase (from H0+3s)
31.5	112	110
63	123	120
125	126	122
250	136	127
500	139	130
1000	127	127
2000	122	118
OASPL(1) (20 – 2828 Hz)	141.2	133.7
Duration	3 seconds	55 seconds

Figure 2.9 : Overall Acoustic Pressure Levels [18]

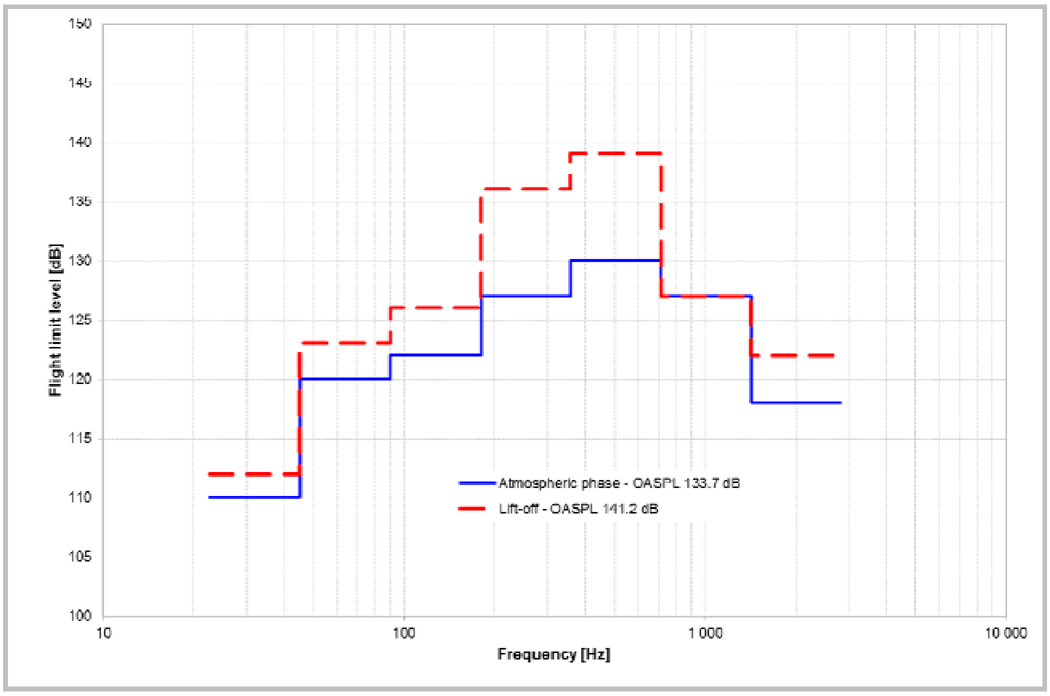

Figure 2.10 : Acoustic Vibration Limit Levels in Fairing [18]

2.3.1.5 Shock

Shock load are applied on the satellite during the launchers' stage separations, fairing jettisoning and most effectively separation from launchers. The satellite separation shock is produced directly at the base of the satellite which has interface with launchers and adapter type has a key role on the shock load levels, since the interface diameter and the separation system have a direct effect. For different interface diameters and flight events it is shown at Figure 2.11 that with different frequency ranges how much Shock Response Spectra (SRS) on the satellite [16]. Also at Figure 2.12, it is shown in the graph [16].

Flight Event	Frequency (Hz)		
	100–1000	1000–2000	2000–5000
	SRS, Shock Response Spectra (Q = 10) (g)		
Fairing & stages separations	15–350	350	350–200

Spacecraft Adapter Interface Diameter	Frequency (Hz)	
	100–1000	1000–10000
	SRS, Shock Response Spectra (Q = 10) (g)	
Ø 937, Ø 1194, Ø 1666	20–1000	1000-700

Figure 2.11 : SRS Values for Soyuz [16]

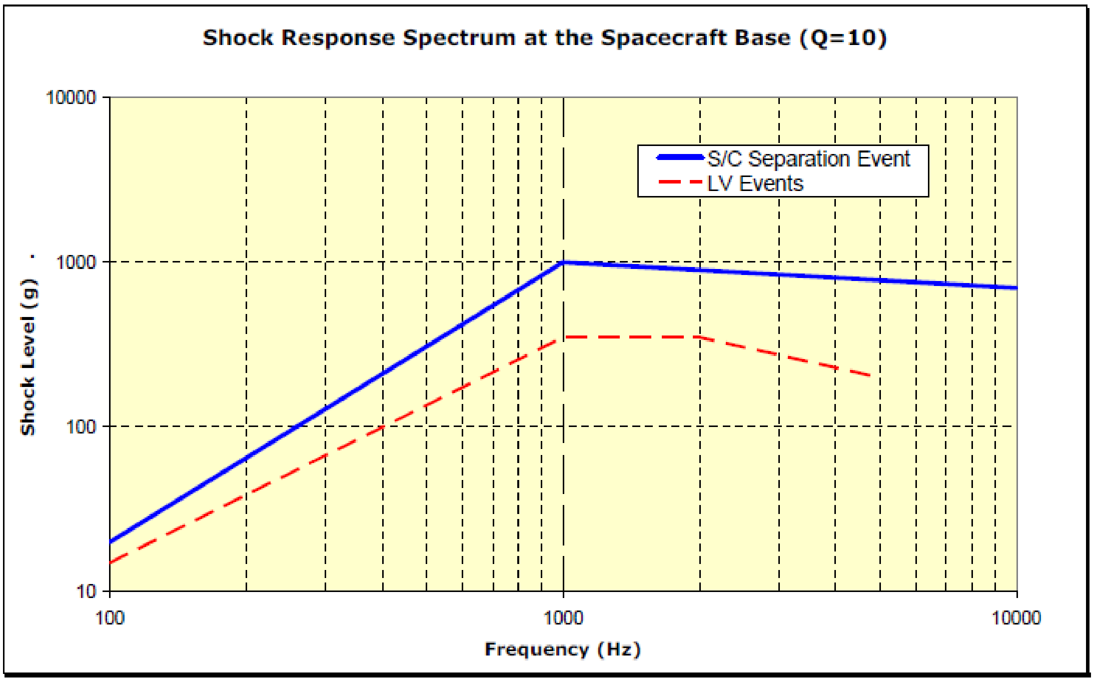

Figure 2.12 : SRS Envelope for Soyuz [16]

2.4 Material

A crucial step in the design process is the selection of materials for a satellite structure. There are some fundamental properties for material selection on space industry. These properties are; strength values of material, modulus of elasticity, fatigue life, fracture toughness, density, thermal behaviour and conductivity, coefficient of thermal expansion (CTE), corrosion resistance, price, availability, machinability and weldability [19]. Mass efficiency has a key role on selecting the material because especially with less weight during the launch the cost of the projects are decreasing a lot. Highly charged thin-walled shells which are cylinders and cones form the central structure of the satellite. It is designed to support axial compressive loads and bending moments. The primary failure mode is caused by buckling of cylinders or cones that is why during the design and material selection buckling strength has important role. Lightweight and rigid structures can be obtained by using materials with a high modulus of elasticity [20]. The advantages and disadvantages of the common materials in space industry are shown in the Figure 2.13.

Material	Advantages	Disadvantages
Aluminium	• High Strength vs weight • Ductile • Easy to machine • Low Density; efficient in compression	• Relatively low strength vs. volume • Low hardness • High CTE
Steel	• High strength • Wide range of strength, hardness and ductility obtained by treatment	• High density • Hard to machine • Magnetic
Heat-Resistant	• High strength vs. volume • Ductile • Strength retained at high temperatures	• High density • Not as hard as steels
Magnesium	• Low density	• Sensitive to corrosion • Low strength vs. volume
Beryllium	• High stiffness vs. density	• Low ductility and fracture toughness • Low short transverse properties • Toxic
Titanium	• High strength vs. weight • Low CTE	• Hard to machine • Poor fracture toughness
Composite	• Can be tailored for high stiffness, high strength, and extremely low CTE • Low density • Good in tension	• Costly for low production volume; requires development • Strength depends on workmanship, needs individual proof testing • Laminated composites are not as strong in compression • Brittle

Figure 2.13 : Comparison of Space Material [21]

3. DESIGN CRITERIAS

Göktürk-Y satellite was chosen as the reference satellite while starting the design studies of the central cones. That is because orbit of the Göktürk-Y satellite is LEO and it is an Earth Observation Satellite with a payload of Electro-Optic Camera. Estimated mass of the satellite is around 1000 kg which makes it in large satellite category [22]. All the design criteria are considered to accommodate central cones in Göktürk-Y satellite.

On the other hand, the opposite side boundary conditions for central cones are coming from launcher interfaces. Central cones have direct interfaces with launch vehicle adapters. In this thesis, as referenced satellite, Göktürk-Y has Ø1194 mm standard launch interface which is lead the central cone bottom diameter.

3.1 Physical Restrictions

Physical restrictions and properties are dimensional properties, mass, material properties used on central cones, components used on designs and design concepts of cones.

3.1.1 Dimensional properties

Designed central cones are accommodating on centre of the satellites as mentioned in their names. The important point of defining the sizes of the cone is the requirements of the satellite. For Earth Observation Satellites, generally a huge telescope is accommodating huge volume on the centre of the satellite. For being the satellite stiffer, central cones in that kind of satellites are generally only locating in platform zone which is not having any payload unit.

In this thesis, central cones have interface with satellite's horizontal structural panels on their top side and, cones have interfaces with launch vehicle adapter on their bottom side. Launch vehicle adapter has proper interfaces with PAS 1194 which is a standard adapter sized as Ø1194 mm [15]. The PAS 1194 technical drawings and interfaces with satellites are shown at Appendix A. For the top side of the cone, Ø720 mm selected to have interfaces with satellite.

Equipment layout design of satellite also effects the sizes of the cones. Height of the central cones are selected as appropriate dimensions with considering possible equipment layout of that kind of satellites which is around 840 mm from the reference coordinate system. The important point on these dimensions is all the central cones will have same dimensional properties to compare under same conditions. The general dimensions of central cones are illustrated at Figure 3.1 below.

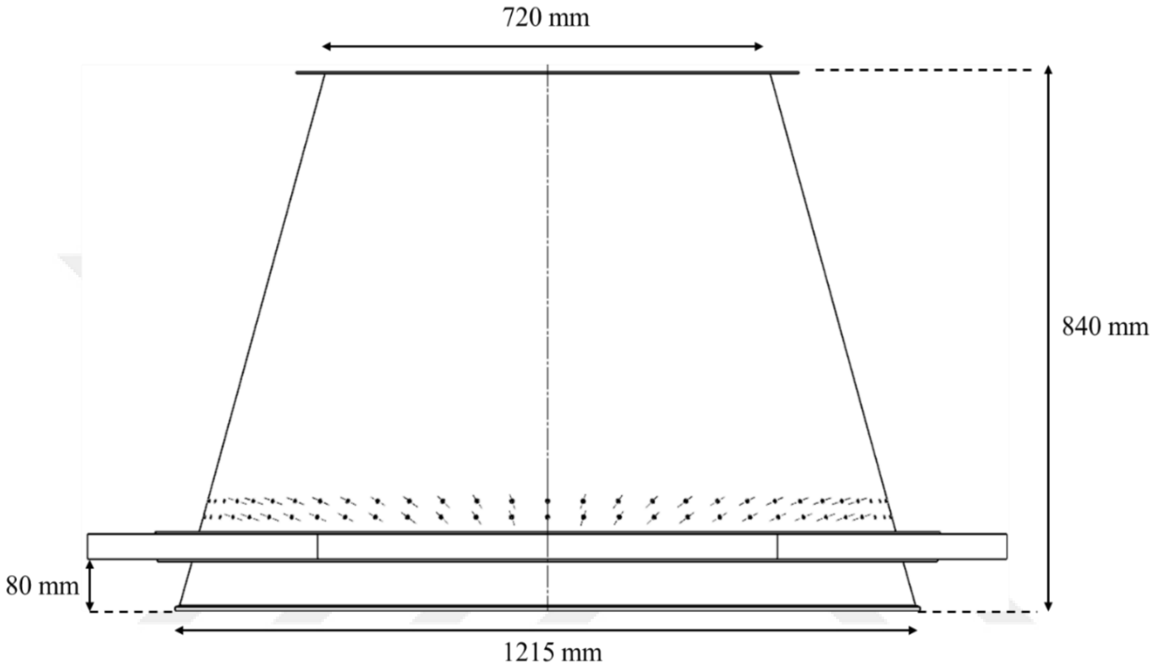

Figure 3.1 : General Dimensions of Central Cone Assemblies

3.1.2 Mass

There is no specific mass restriction for this thesis but, in the space applications, weight has extremely critical role on design. Mass is directly proportional to cost of the projects. Except from money, especially for Earth Observation Satellites, agility is so important because with the movements of the satellite, telescope can capture more images. For getting high agility, moment of inertia (kg x m2) values should be small. Centre of gravity and mass of the satellite are the main objects of the moment of inertia. With considering these facts, mass is affecting moment of inertia and, it is affecting the agility and movement capability of the satellite. To conclude, there is no mass restriction for this study but being a mass efficient product as central cone has critical role on design.

3.1.3 Central cone design concepts

In this thesis, there will be a comparison between six different central cones under same boundary conditions and load cases. These six cones are divided in each other with considering the design concepts and material types of the cones. The main philosophy of the design is defining three different design concepts and applying two types of material on each concept. As a result of that, design concepts are:

- Semi-monocoque cones
- Grid cones
- Sandwich cones

These three design concepts are the main design concepts of the primary structures of satellites for central cylinders and cones [19].

3.1.4 Material properties

Material selection for this study is based on being space compatible. For being space compatible, international standards like European Cooperation for Space Standardization (ECSS) are considering to determine material selection. Materials are chosen as being light, have high strength, have high elastic modulus, size and thickness of the design, form of the design and manufacturing process [23]. Chosen materials for different kind of design concepts of central cones are listed on the Table 3.1.

Table 3.1 : Material List

Cone ID	1	2	3	4	5	6
Design Concept	Semi-monocoque	Semi-monocoque	Grid	Grid	Sandwich	Sandwich
Material	AL 2024	M18 M55J CFRP	AL 7050	M18 M55J CFRP	Skins: AL 2024 HC: AL 5056 (8.1)	Skins: M18 M55J CFRP HC: AL 5056 (6.1)

As shown in the Table 3.1, one type of metal and CFRP selected and applied at different designed central cones. The reason of choosing different aluminium for metallic central cones is the form of the metal. For flat sheets and skins, AL 2024 selected because it is producing as low thickness flat sheets. On the other hand, for the plates which will need NC machine like

Grid cone, AL 7050 selected. That is because, AL 7050 has a form of plate or rod. For sandwich structures, honeycomb parts are selected as same aluminium type which is AL 5056, but the density of the honeycombs are different between each other. The detailed material properties for the metals are listed on Table 3.2. The mechanical properties for the metals are getting from Metallic Materials Properties Development and Standardization (MMPDS), which is an authority from USA to define the metallic material properties [24]. The properties of the aluminium are close to each other except the tensile yield strength and ultimate tensile strength which are key factors on design.

Table 3.2 : AL 2024 and AL 7050 mechanical properties [24]

Metals	AL 2024	AL 7050
Density	2800 kg/m^3	2830 kg/m^3
Modulus of Elasticity	73.1 GPa	71.7 GPa
Poisson's Ratio	0.33	0.33
Shear Modulus	28 GPa	26.9 GPa
Tensile Yield Strength	324 MPa	469 MPa
Ultimate Tensile Strength	469 MPa	524 MPa

For honeycomb materials, detailed mechanical properties are listed at Table 3.3. The 6.1 and 8.1 means that nominal density pounds per cubic foot (pcf) as listed in Hexcel product list. 6.1 pcf is equal to 98 kg/m^3 and 8.1 pcf is equal to 130 kg/m^3. The interlaminar shear stress limits and shear modulus limits are also different with density of honeycomb.

Table 3.3 : Honeycomb AL 5056 (6.1) and AL 5056 (8.1) mechanical properties [18]

Honeycomb	5056 AL (6.1)	5056 AL (8.1)
Density	98 kg/m^3	130 kg/m^3
Shear Modulus (G13)	703 MPa	986 MPa
Shear Modulus (G23)	262 MPa	352 MPa
FsL	4.76 MPa	6.52 MPa
FsW	2.76 MPa	3.86 MPa

For all three central cones have same CFRP material which is space compatible M18 M55J. It is also defined and material properties are shown in ECSS from Airbus' material properties test results [26]. The properties are given for different angles of laminates. Also, for all angle and stress type strength and modulus properties are given. The mechanical material properties are shown in Table 3.4.

Table 3.4 : M18/M55J UD mechanical material properties [26]

CFRP	M18/M55J UD
Density	1580 kg/m^3
UD Tension (0) Strength	1784 MPa
UD Tension (0) Modulus	301 GPa
UD Tension (90) Strength	21 MPa
UD Tension (90) Modulus	5.9 GPa
UD Compression (0) Strength	602 MPa
UD Compression (0) Modulus	293 GPa
In-plane Shear Strength	53 MPa
In-plane Shear Modulus	4.6 GPa

3.1.5 Components used on cone assemblies

One of the main purposes of the satellite primary structure is carrying all the satellite and withstand all loads. Interfaces with launch vehicles and satellites are adapters on both structures. The satellite side is named in the thesis like launch vehicle adapter (LVA). LVAs are the key components for the satellites on their load paths because it is directly transmitting the load to the launchers. Central cones and LVA are connecting to each other from inner face of the cones and outer face of the LVAs. That is resulting with load path directly using central cone for satellite bus. LVA and central cones have also another interface except from direct interface on their inner and outer faces. There is a horizontal structural panel between cones and LVA. It is designed and added to assembly to simulate the connection stresses for lateral connections on central cones. In addition, it is helping to make the assembly stiffer. To conclude, in the thesis for cone assembly designs and analyzes listed components used as below:

- Central cone
- Launch vehicle adapter
- Horizontal structural panel
- Additional structural bracket to connect cone and horizontal panel (if needed)

Last item of the assembly is meaning that additional mass for assemblies which need that component in their designs. Even thought that component make the structural analysis results better and make them compatible with requirements, additional mass has negative effect on the weight comparisons.

3.2 Analysis Types

Some analyzes are made during the design phase to ensure that the satellite is resistant to the loads and effects it will be exposed to during tests, launch and orbit. These analyzes can be described as a simulation of structural behavior under these conditions. Just like the satellite, their primary and secondary structures should also have to withstand loads during those phases of satellite life. Some structural requirements for satellite structure can be detailed into each other to ensure the little parts of it also withstand the effects. Central cones are one of the main primary structure of satellites which can be basically defined as backbone of satellite. That is why some main analyzes for central cones should be considered to compare the optimal design.

3.2.1 Modal analysis

Natural frequency is frequency of a systems which make them vibrate under any external effects [27]. The natural frequency depends on various factors such as the mass, stiffness, and damping of the object. Knowing the natural frequency of an object is crucial because if the object vibrates at a frequency that matches its natural frequency, it can lead to a significant increase in the amplitude of the vibration. This can potentially cause permanent damage to the object, which is why it's important to have an understanding of its natural frequency. Natural frequency is an important concept in physics and engineering, as it can help predict how an object will behave when subjected to external forces or vibrations. It is also a key factor in the design of structures and mechanical systems as satellite structures.

Modal analysis is a type of structural analysis that is used to determine the natural frequencies, mode shapes, and damping properties of a structure. Modal analysis involves analysing the structural member's geometry, material properties, and boundary conditions to predict its natural frequencies and mode shapes [28].

It is important to keep the satellite and launch vehicle natural frequencies separate from each other to ensure there is no resonance. That is why in the launch vehicle user manuals there are described natural frequency requirements. Same as satellite and launch vehicle, components of the satellite are also need to have non-couple natural frequency values from satellite body. Generally, in the launch vehicle user manuals the defined frequency range is up to 100 Hz [15]. As a result of this value with using vibration isolation theory, component natural frequency values can be defined as a requirement before starting to design. From vibration isolation theory, the √2 times defined natural frequency range is assigning the natural frequency lower limits for structural designs. In Figure 3.2, the effect of √2 is shown. At any value smaller than √2 for f/f_n the there is an amplification because transmissibility values are always bigger than 1. On the other hand, if the f/f_n is bigger than √2, it will be an isolation and vibration will be depended on the damping ratios [19].

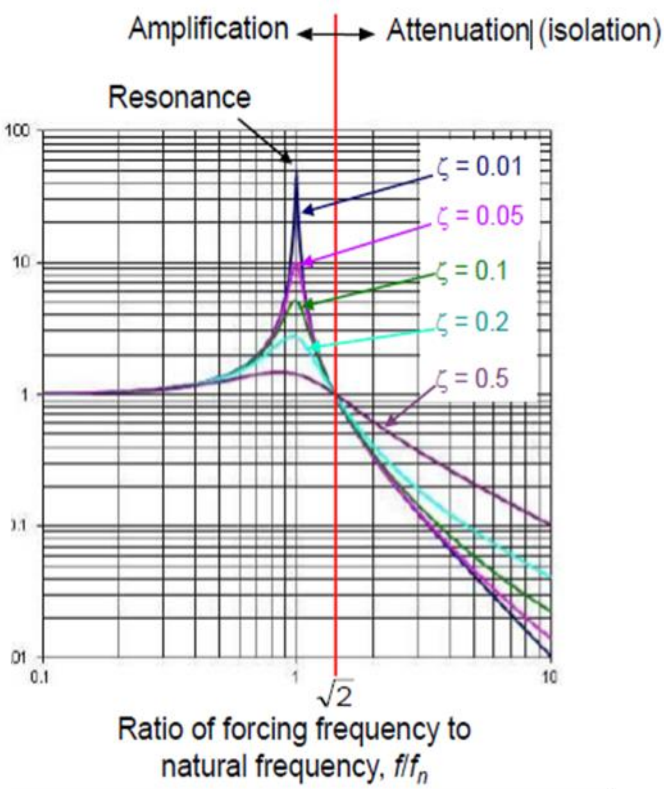

Figure 3.2 : Transmissiblity curve [19]

As a result of that, with considering vibration isolation, the modal analysis results for central cones should have bigger than 140 Hz which is equal to 100 * √2. During the comparisons of the cones, it will be important to be stiffer than other ones which is basically controlling with hard mounted modal analysis of the central cones. Also, the modal analysis of the cone assemblies will be considered on the comparisons for the performance of the assembly.

3.2.2 Static structural analysis

Static analysis is a type of structural analysis that is used to determine the stresses and deformations in a structure under static loading conditions. As part of satellite structures, static analysis is used to predict the stresses and deformations that the structure will experience during launch and in orbit. In global static stress analysis of satellite, load conditions are defining with considering candidate launch vehicle load envelopes. performing linear static analysis on the central cone of a satellite is critical to ensure that the structure can withstand the loads and stresses it will experience during launch and operation.

As mentioned before, central cones are backbone of the satellite structure. It is the main path of loads for satellite. Central cones are carrying all the satellite bus during launch and in orbit. In static view, whole satellite weight with defining acceleration can be load conditions of the central cones. Acceleration values which are ‘g’ values, defining in the launch vehicle user manuals for spacecrafts in global way. To enforce the central cones more, 10g will be applied during the static structural analysis. Central cones are also carrying satellite bus, that is why referenced satellite Göktürk-Y weight will be applied on the upper side of the central cones under acceleration levels. Mass of the Göktürk-Y is almost equal to 1000 kg [22]. With quick mathematics 1000 kg with 10g acceleration is equal to 100 kN.

3.2.3 Buckling analysis

Buckling analysis is a form of structural analysis that predicts the failure mode of a component when subjected to compressive loads. In relation to satellite structures, it is utilized to determine the critical load at which a structural member will buckle or fail due to compressive loading. Buckling analysis involves analysing the structural member's geometry, material properties, and boundary conditions to predict its critical buckling load. In the buckling analysis, the critical buckling load factor which is symbolized as λ obtained from FEA. λ is equal to design limit load (critical load) divided by defined load case [29].

The central cone is another critical component of a satellite structure that provides structural support and stability for other subsystems. Because of its length and slender shape, it is susceptible to buckling when subjected to compressive loads. During the launch phase of the mission, the satellite experiences high levels of acceleration and vibration, which can cause compressive loads on the central cones. Additionally, the central cone must be designed to withstand thermal expansion and contraction during the varying temperature extremes experienced in space. These loads can cause the central cone to buckle if it is not designed to resist buckling. As a thin-walled and slender structure, the central cone of a satellite is susceptible to buckling under compressive loads. Therefore, it is important to perform buckling analysis on the central cone to ensure that it is designed and constructed to resist buckling and can withstand the mechanical loads and stresses it will encounter during launch and operation in space [29].

Same as static analysis, defined load is coming from Göktürk-Y satellite for central cones. Boundary conditions are also same as static analysis, which means that there is a hard mounted LVA under the central cone and the load is occurring on the top side of the central cones in the analysis. With considering Göktürk-Y mass 1000 kg and 10g load level, same as static analysis 100 kN force applied on the central cone assemblies.

4. DESIGN PHASE

The design criteria of the central cones are described in the Section 3. Design phase of the central cones are started with considering design criteria mentioned before. Siemens NX [30] used for 3D designs. It is used because of the user-friendly transitions with analysis application of it which is called Simcenter 3D. It is easy to iterate designs with using same software during the designs. In this section, designs of central cones and their assemblies with mass properties comparisons are shown. These comparisons are the first main part of the trade-off study at the end of the thesis.

4.1 Design Philosophy

It is important to make a decision on the design procedure and phases of a structure. For make the designs more efficient and easier to iterate them, creation of the design process tree has key role. That is why in the beginning of the designs, design process scheme is planned as shown in the Figure 4.1.

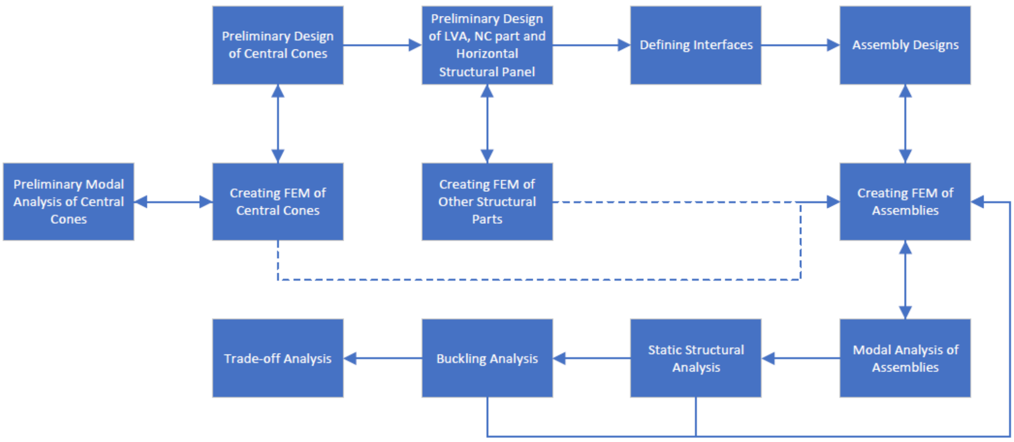

Figure 4.1 : Design Process Scheme

As shown in the figure, it is starting with preliminary design of central cones. In the phase, it is not only the 3D design of the cones, it is also adding material properties on cones. After that there are two ways to continue to designs. First of them is creating the FEM of central cones which is important to apply modal analysis only on central cones and also that FEMs can be imported to assembly FEM. Regarding the preliminary modal analysis results of the central cones, it can be first iterations on the cones in that phase. Second way is continued to design other parts of the central cone assemblies. Same as the cone FEMs that parts also need FEM for applying them on assembly FEM. Material properties of horizontal structural panel, NC part and LVA is also applied in this phase. After those interfaces are defining between cones and other parts of the assemblies. It is important to define number and sizes of the connections here in this phase. After the definitions and design changes, assembly design is starting. Assembly design phase is putting together all the 3D models of central cone assembly parts which are central cone, horizontal structural panel, NC part if needed and also LVA. After this process, it is time to start creating assembly FEMs. The connections between parts are defining and modelling here. Also creating boundary conditions has crucial role in this phase. With finishing assembly FEMs and connections, the analysis phase is starting. In the analysis phase there are three main analyzes which is mentioned before. They are modal analysis, buckling analysis and linear static analysis. All the load definitions and boundary condition definitions for specified analysis is done in that phases. Also, with regarding to analysis results, there can be some design iterations of the central cone assemblies. At the end of the design phase, there is a trade-off study to determine which central cone is optimal solution for a satellite which is orbiting on LEO and more than 1000kg. Until the last one which is trade-off study, all six central cones have the same processes.

4.2 Central Cone Designs

There are three different design concepts for the thesis as mentioned before. These three different design concepts all have two different material type which makes six different central cone to compare. These concepts are semi-monocoque, grid and sandwich design concepts. In the beginning of the designs, concepts have designed with the same dimensional properties within themselves. As an example for that, the thicknesses for aluminium grid cone and CFRP grid cone are same. As a result of all this, concepts of the designs are shown in this section, but with different applied materials the mass properties are differ from each other.

4.2.1 Semi-monocoque cone design

A monocoque shell is a symmetrical shell that lacks any reinforcing elements or circular frames. The limitation of monocoque structure is having less buckling strength. For proper load introduction, it's necessary to distribute the loads evenly across the cross section of the structure. If loads are concentrated in one area, it may lead to premature failure in that specific location. With considering lack of buckling strength of monocoque shells, stiffened monocoque structures seems more convenient for this study. There are two types of them, one of them is stiffened-skin monocoque and semi-monocoque structure. Stiffened-skin monocoque has stiffeners which are longitudinal structural members on the skins. That stiffeners are helping to increase the buckling strength of the structure. Secondly, semi-monocoque structures have intermediate ring frames which are included to enhance the buckling strength of the skin, but there are no axial members present [13]. The shape of the cone is a leading point of the selection of semi-monocoque structure. Another reason of that selection is having less weight than stiffened-skin monocoque structure because of having a smaller number of stiffer members. Also, semi-monocoque structures can be produced both for sheet metals and CFRP.

In the preliminary design phase of the semi-monocoque central cone, thickness values of whole cone used same which is 2 mm. Thickness is an important parameter for the design because of the mass effect of the study. Also, for make the central cone with stiffener members, four longitudinal ring frames used in the design. Rings are not carrying the main load of the satellite but they are helping to rise buckling strength of the cone shell. The general shape of the semi-monocoque central cone is shown at Figure 4.2.

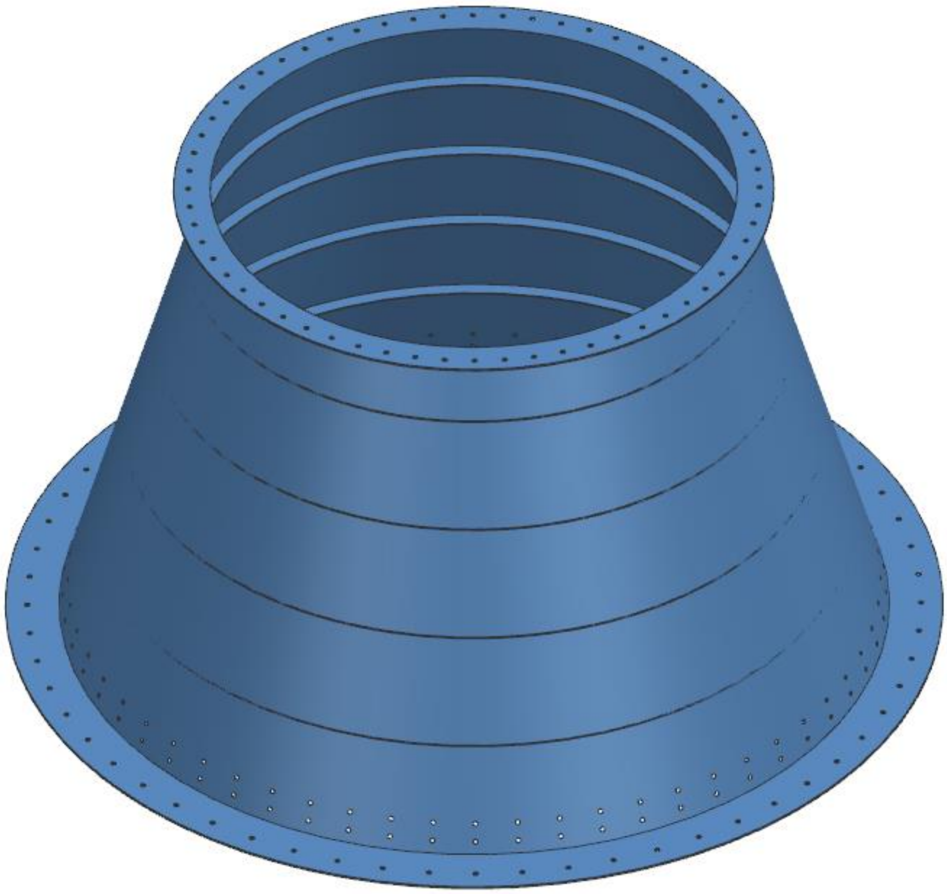

Figure 4.2 : Semi-monocoque Central Cone Preliminary Design

In the first stage of the thesis, aluminium and CFRP central cones both have same dimensional properties. With respect to analysis results, that dimensions can be change because of the optimizations on central cones. The shell and longitudinal rings are 2 mm. The upper and bottom rings are 3 mm which have connections with launch vehicle adapter and satellite. Upper side of the central cone has connections with satellite which the satellite loads are applying. Bottom side of the central cone has interfaces with LVA to carry all the loads to the launchers.

After applying the materials on the central cones first mass information came out. As an Aluminium metal, AL 2024 sheet metal used and for CFRP material M18/M55J UD applied. In the Appendix B, the orientations of the CFRP material are described. Mass results of the semi-monocoque central cones are shown at Table 4.1.

Table 4.1 : Semi-monocoque central cones mass comparison

Central Cones	Aluminium	CFRP
Mass (kg)	16.77	9.41

CFRP semi-monocoque central cone is way much lighter than Aluminium semi-monocoque central cone without assemblies. Even the same dimensions and boundary conditions, because of the high-density, Aluminium central cone is heavier one. From preliminary design results, Aluminium central cone is around 56% heavier than CFRP central cone.

4.2.2 Grid central cone design

The usage of different types of grid structures are used on the space industry is increasing each day. There are several types of that grid structures which are chosen with dependents of specific mission requirements, weight restrictions or cost considerations. Main central cones as a primary structure of the satellite are very suitable for the usage of such structures. There are several common usages of grid structures on central cones or cylinders.

Types of the grid structures have a name with a result of the shape of the grids. Most common types of them are isogrid and orthogrid central cones. The main difference between isogrid and orthogrid structures is their geometry. Isogrid structures have a lattice pattern consisting of interconnected panels, while orthogrid structures have a grid pattern consisting of interconnected beams. Isogrid structures offer enhanced strength and rigidity due to their lattice design, whereas orthogrid structures are less complex to construct and assemble because of their simpler grid pattern. In the thesis, because of the easy to manufacture and design, orthogrid structure selected as base grid central cone design. With considering analysis results, the shapes of the grids can be optimized if it is needed.

The total thickness of the grid central cones is 10 mm. There is a 1 mm shell behind the grids of the central cones. With 4 mm walls between grids, there are 4 grids on the one column of cones. The height of each grid has different values which are 160 mm, 150 mm, 150 mm and 145 mm respectively. The section view of the central cones are shown in the Figure 4.3.

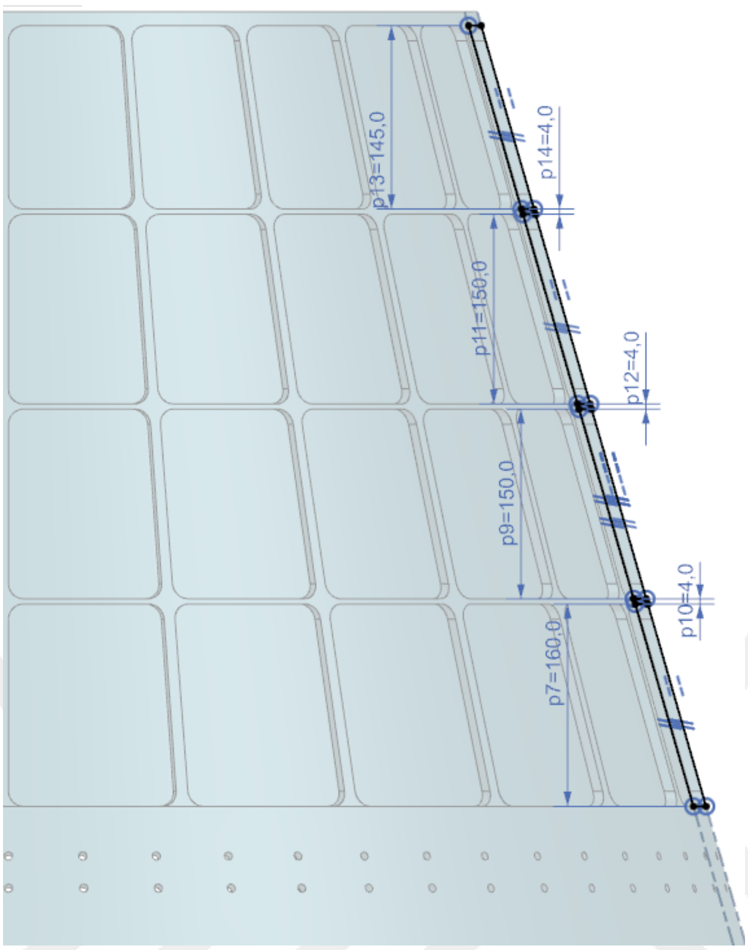

Figure 4.3 : Section view of the grid central cones

Rotation angle of the grids are 14° with respect to reference coordinate system. The total number of the grids around the cone shell is 96. In the preliminary design phase of the study, the dimensions of the grids are defined same for both materials which are Aluminium and CFRP. As Aluminium metal, AL 7050 selected and for CFRP M18/M55J selected like semi-monocoque CFRP cone. In the Appendix C, the orientations of the CFRP on grid central cone are shown. Masses of the grid central cones are listed on the Table 4.2.

Table 4.2 : Grid central cones mass comparison

Central Cones	Aluminium	CFRP
Mass (kg)	21.12	12.32

Same as the semi-monocoque cones, grid central cones have also same mass results regarding to materials. CFRP grid central cone is lighter than Aluminium grid central cone. Aluminium central cone is around 42% heavier than the CFRP one. General view of the grid central cones is shown in Figure 4.4.

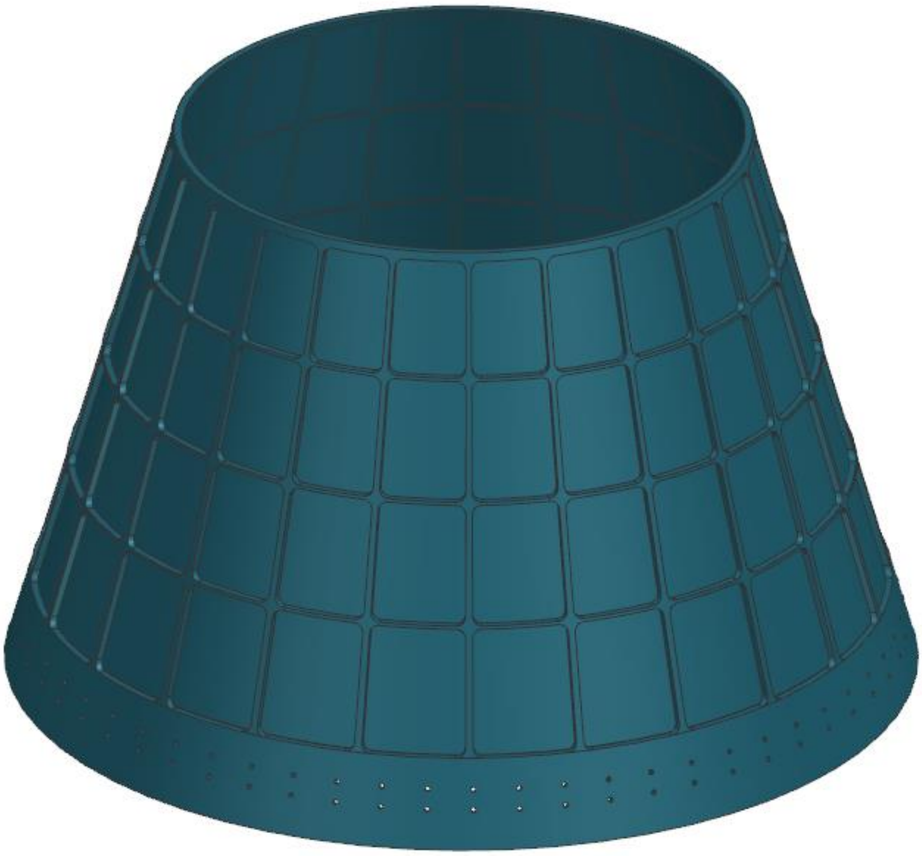

Figure 4.4 : General view of grid central cones

4.2.3 Sandwich central cone design

There are several advantages of sandwich structures for spacecraft design. The major advantages of sandwich structures are being lightweight, have strength, rigidity and buckling strength. The types of the sandwich structures are also changing with respect to materials of the skins or core structure. It is also known that the shape and geometry of the core structure is another difference of sandwich structures. In the satellite industry, especially for primary structural panels, honeycomb sandwiches are using which have hexagonal geometry like honeycombs on the core of the sandwich. The materials of the honeycomb sandwiches are named from upper and lower skins' material generally. That is because for space applications, honeycomb cores are generally aluminium material. Upper and lower skins can be metal or CFRP which is depended to mission selection, requirements and cost efficiency. The general idea of the sandwich panels is shown at Figure 4.5.

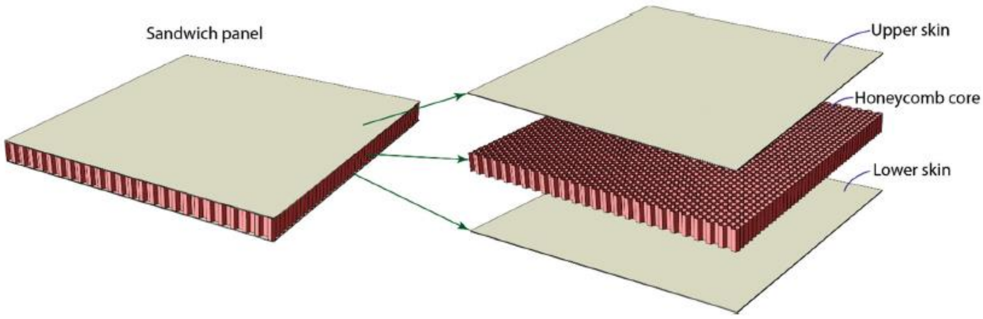

Figure 4.5 : Honeycomb sandwich structure [31]

In the thesis, the dimensional limitations of the sandwich central cones are the same. The chosen materials of the core structure are the same for both cones which only has a difference of honeycomb density. It is 5056 AL with densities of 98 and 130 kg/m^3. Also, the thickness of skins is different than each other for central cones too. Total thickness of both cones is same for them which is 10 mm. Upper and lower skin thicknesses of AL sandwich cone is 0.4mm with AL 2024 sheet. The core thickness of that central cone is 9.2 mm with 98 kg/m^3 5056 AL honeycomb. For CFRP sandwich central cone, upper and lower skin thicknesses are 0.88 mm and core honeycomb thickness is 8.24 mm with density of 130 kg/m^3 5056 AL. The layout of the CFRP is shown at Appendix D. General view for sandwich central cones is shown at Figure 4.6.

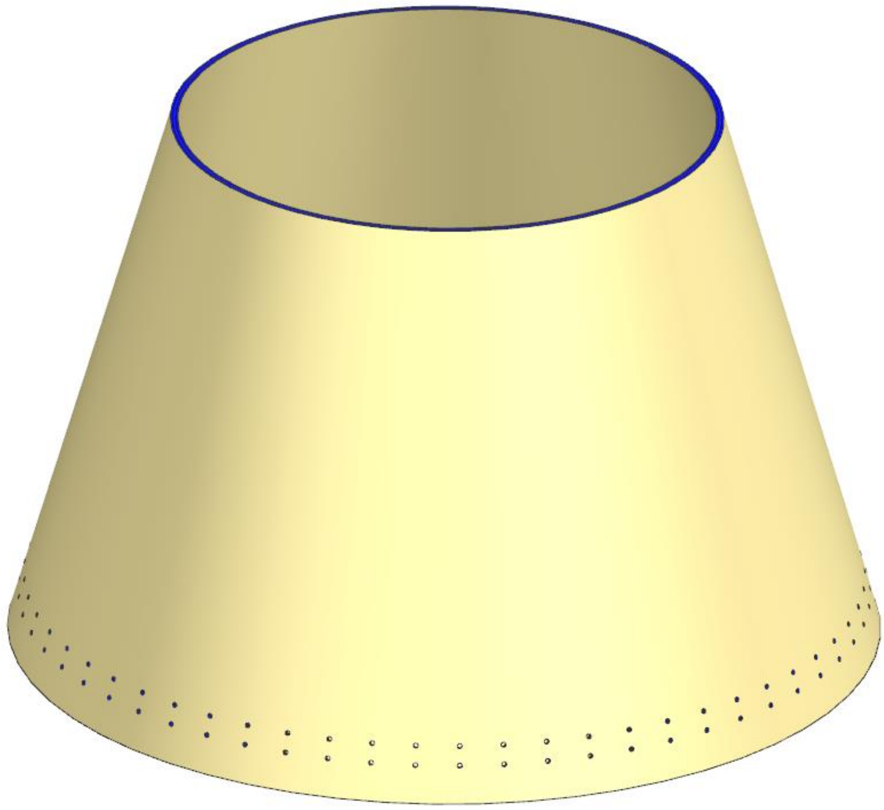

Figure 4.6 : General view of Sandwich Central Cones

Mass comparisons of the sandwich central cones are done after application of materials. The mass results are shown at Table 4.3.

Table 4.3 : Mass comparison of sandwich central cones

Central Cones	Aluminium	CFRP
Mass (kg)	7.92	8.21

The results have different characteristics than other concepts of design. For other two design concepts, metallic central cones are heavier than CFRP central cones. But in this case, CFRP central cone is heavier than Aluminium sandwich cone. This difference is not an anomaly for the study because, the skin thicknesses and core densities are different from each other. The reasons of the differences will be shown at analysis phase of the study. CFRP sandwich central cone is around 3.53% heavier than metallic one.

4.2.4 Central cone mass comparisons

After preliminary designs of the central cones, first mass comparisons between design concepts and types came out. The results are shown at Table 4.4.

Table 4.4 : Mass comparisons of the central cones

Central Cones	AL monocoque	CFRP Monocoque	AL Grid	CFRP Grid	AL Sandwich	CFRP Sandwich
Mass (kg)	16.77	9.41	21.12	12.32	7.92	8.21

With results of the design concept mass comparisons, sandwich central cones are lighter ones. After that, semi-monocoque cones are coming but it is important that CFRP Grid cone is lighter than AL semi-monocoque cone that is why in this stage with averages of the design concepts can be sortable. If the comparison can be one by one without defining the design concepts, AL Sandwich cone is lighter central cone and AL Grid cone is heavier one.

4.3 Assembly Designs

To find the optimal design concept of central cones for LEO satellites, simple assembly designs are created to compare. Central cone assemblies aim to have almost same main components of the satellite structure which is directly connected to central cones and launch vehicles. It is because that load path of from satellite is following the satellite primary structure to central cones and launch vehicle adapter to transfer them to launch vehicles. In the study, assemblies have component listed below:

- Central cones
- Launch vehicle adapter
- Horizontal structural panel
- NC bracket (if needed)

4.3.1 Launch vehicle adapter design

Launch vehicle adapters are the interfaces between spacecrafts and launch vehicles. Depends on the sizes of the spacecraft diameter of the launch vehicle adapter is changing. There are standard sizes of the launch vehicle adapters. Most common sizes are Ø937 mm, Ø1194 mm and Ø1663 mm which are diameters of the interfaces of launch vehicles. In the thesis, with considering the sizes of reference project Ø1194 mm standard LVA chosen. The interfaces of the LVA should be compatible with the launch vehicles which is specified in their user manuals. As a reference adapter of launch vehicle side PAS 1194 selected and technical drawings of that is shown at Appendix A [15].

As an assembly design, LVA has directly connections with central cones from inside of them. Also, LVA has interfaces with horizontal structural panel. The cross section view of the LVA is shown at Figure 4.7 and general view of the LVA is shown at Figure 4.8.

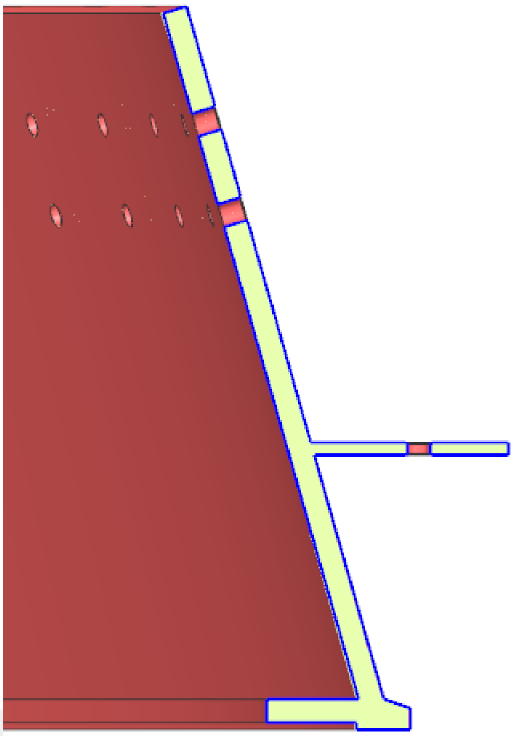

Figure 4.7 : Section view of the LVA

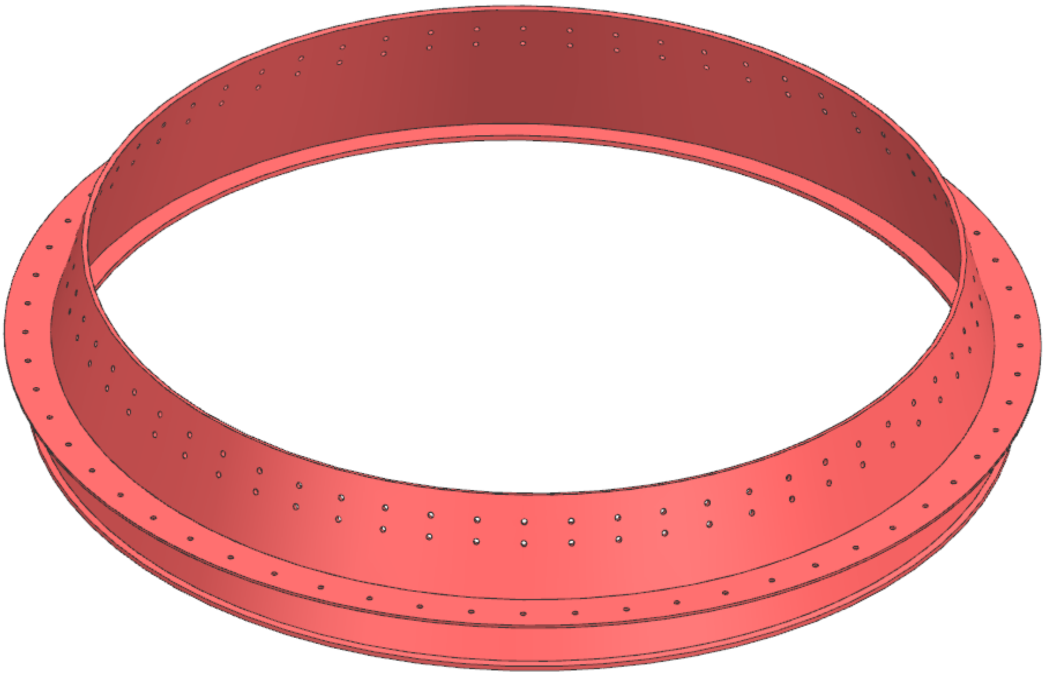

Figure 4.8 : General view of the LVA

The material of the LVA is aluminium which is AL 7075. Mass of the LVA is 19.02 kg. The LVA is same for all assemblies. That is why the mass of the LVA is not a criterion for assembly design of central cones.

4.3.2 Horizontal structural panel

Horizontal structural panel for central cone assembly is actually a main structural panel of satellite. The reason of adding this panel on the central cone assembly is having connections and interfaces with LVA and central cone. That connections from cone to LVA with using horizontal structural panel is another load path for satellite. Horizontal structural panel is a honeycomb sandwich panel which has AL skins and AL honeycomb as core inside. Total thickness of the panel is 40 mm. Skin thicknesses are 0.41 mm with AL 2024 and 39.18 mm honeycomb as AL 5056 with 50 kg/m^3 density. In the assembly designs of the central cones, same horizontal structural panel used and mass results of it is 1.39 kg. It is use same for all assemblies so, it is not affecting the comparisons of the cone assemblies.

General view of the horizontal structural panel is shown at Figure 4.9. The shape of the panel is selected as hexagonal because of the reference project Göktürk-Y. The same shape for the panels used on that project too.

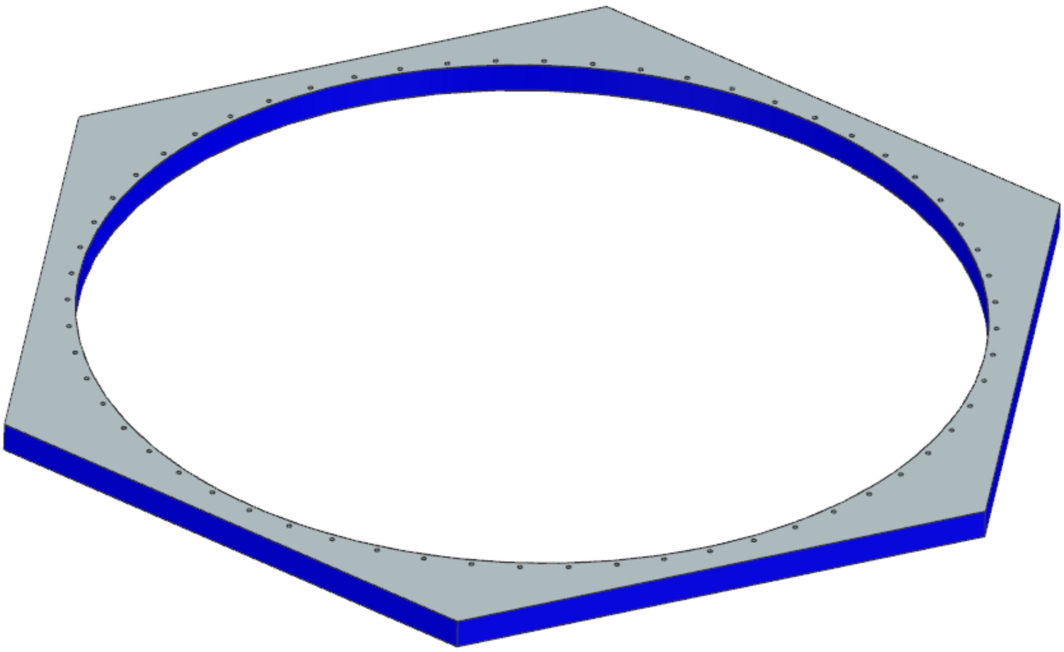

Figure 4.9 : General view of horizontal structural panel

4.3.3 NC bracket

NC bracket is a bracket to connect central cones to horizontal structural panel. It is a secondary structure for the assembly to connect some components. The connection with central cone is also interfaces with LVA with using same tru fasteners. Same as central cone and LVA connection of NC bracket, horizontal structural panel connections of NC bracket are also using same tru fasteners. Material of the NC bracket is AL 7050 which is named the bracket for needs of machining. For design concepts, some of the cone assemblies are not using NC bracket because of their design. This is an advantage for them in case of mass comparison of assemblies. The mass of the NC bracket after applying the material of it is 5.62 kg.

For preliminary design phase Table 4.5 is shown that which central cone assemblies are using NC bracket in their assemblies.

Table 4.5 : Usage of NC bracket in central cone assemblies

Central Cones	AL monocoque	CFRP Monocoque	AL Grid	CFRP Grid	AL Sandwich	CFRP Sandwich
Usage of NC bracket	No	No	Yes	Yes	Yes	Yes

It is important that for both grid and sandwich central cones, design of the NC bracket is same. General view of the NC bracket design is shown at Figure 4.10.

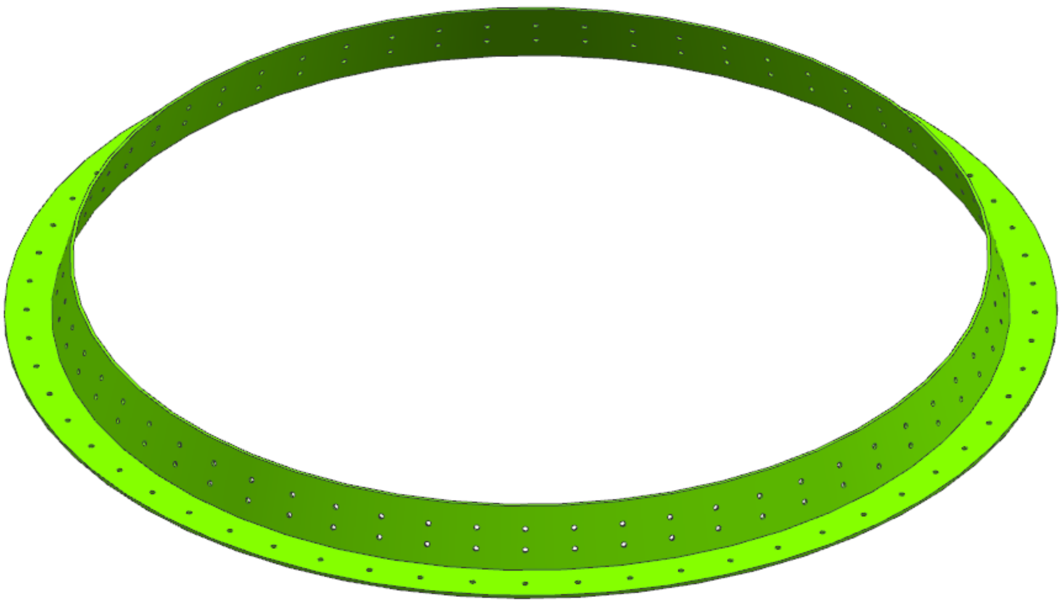

Figure 4.10 : General view of NC bracket design

4.3.4 Interfaces of assemblies

The connections of the components in the assembly are basic in the design. The type of the interfaces is all same in the assemblies. The size of the holes is M6 and number of interfaces between central cones and LVA is 120 which is 60 per circle with 2 columns. With same sizes of holes, the number of connections between central cones and NC bracket is 60 if there is a NC bracket in the assembly and NC bracket has same number of connections with horizontal structural panel. On the other hand, for the assemblies without NC bracket the connection number of the horizontal structural panel and central cone is 60. Horizontal structural panel has also same number of connections with LVA. The material of the connection is selected from NX library and it is Titanium_Ti_6AI-4V. The material properties of the Titanium Alloy are shown at Table 4.6.

Table 4.6 : Titanium alloy material properties [30]

Metal	Titanium_Ti_6AI-4V
Density	4430 kg/m^3
Modulus of Elasticity	131 GPa
Poisson's Ratio	0.34
Tensile Yield Strength	805 MPa
Ultimate Tensile Strength	845 MPa

The details of the connections will be shown at analysis phase.

4.4 Assembly Comparisons

Second main comparison for the central cones is assembly mass comparison which is another important criterion to have less component in their assemblies. Semi-monocoque central cones have an advantage here to not have NC bracket in their designs in the preliminary design phase. In the Figure 4.11, Figure 4.12 and Figure 4.13, general views of the central cone assemblies are shown.

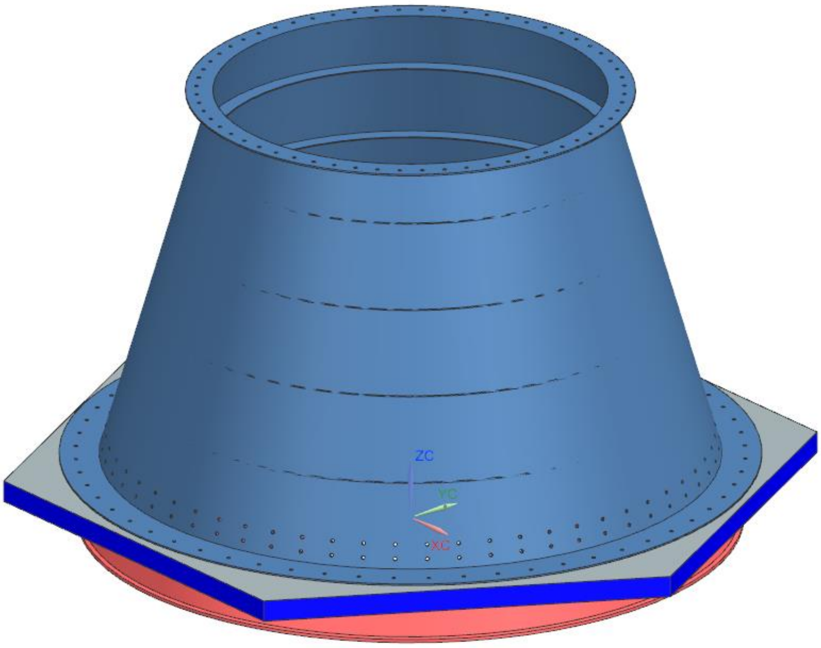

Figure 4.11 : Semi-monocoque central cone assembly

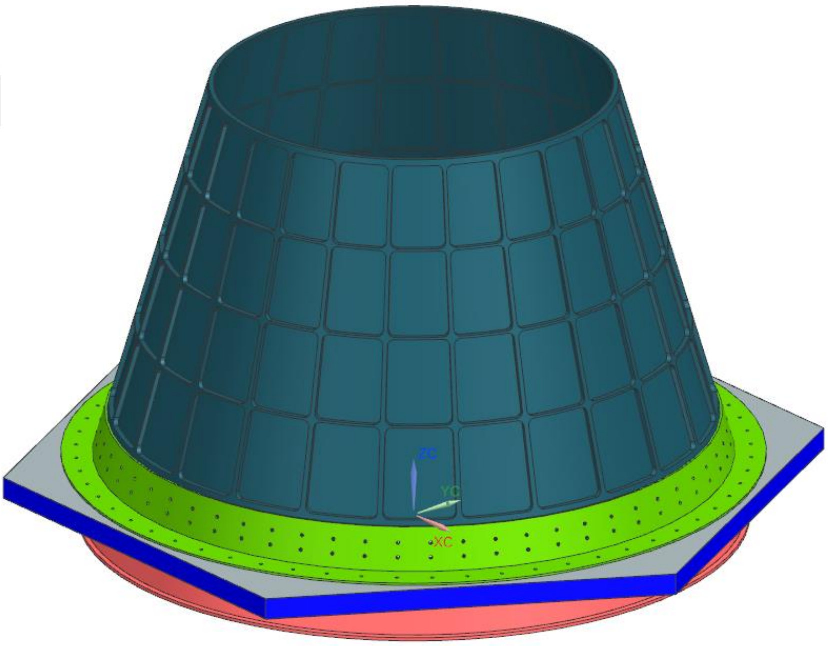

Figure 4.12 : Grid central cone assembly

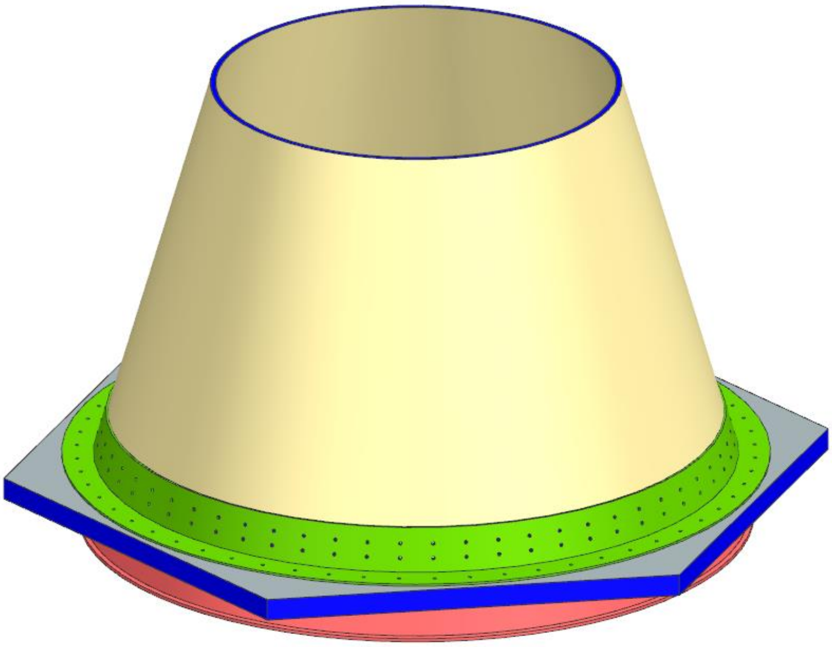

Figure 4.13 : Sandwich central cone assembly

The mass comparisons of the assemblies are shown at Table 4.7.

Table 4.7 : Assembly mass comparisons of central cones

Central Cones Assemblies	AL monocoque	CFRP Monocoque	AL Grid	CFRP Grid	AL Sandwich	CFRP Sandwich
Mass (kg)	37.36	30	47.33	38.53	34.13	34.42

It is clear that as an assembly CFRP monocoque cone is lighter cone of the study. NC bracket mass is a disadvantage for sandwich cones because it makes them heavy even the only central cone masses of them are lighter ones. Grid central cone assemblies are heavier ones and AL Grid cone is worst one.

5. ANALYSIS PHASE

Analysis phase is another important phase of the study. In this phase, the main comparisons of the study will be made. The analyzes of the study are modal analysis on central cone, modal analysis, linear static analysis and buckling analysis on the central cone assemblies. After that four different analyzes, the results came out as final pieces of the trade-off study. At the end of the first trade-off study, there will be a selection between six different central cone assemblies to find optimum one. Two of them will be selected and there will be some design iterations on them to make them optimal. After that, there will be same trade-off study between top two central cone assemblies to find out optimum central cone design concept for LEO satellites more than 1000kg. As an analysis program Simcenter 3D selected [32]. Simcenter 3D and Siemens NX are connected to each other, and with using one of them it is easy to switch between each other.

5.1 Creating FEM of Central Cones

Modelling philosophy of the central cone design concepts are different than each other with respect to material and design type of them. Some of the central cones are modelled as 3D solid meshes and some of them modelled as 2D shell meshes. In this section of the thesis, the modelling philosophy of the central cones will be described one by one.

5.1.1 Creating FEM of semi-monocoque central cones

There are two different finite element modelling method for semi-monocoque central cones. For metallic central cone, 3D solid meshes are used and for CFRP semi-monocoque central cone 2D shell meshes are used.

5.1.1.1 FEM of aluminium semi-monocoque central cone

3D CTETRA meshes selected for Aluminium semi-monocoque central cone. Size of the elements are 9 mm and surface maximum growth rate is 1.3. Element and node numbers for aluminium semi-monocoque central cone is shown at Table 5.1.

Table 5.1 : Element properties of Aluminium semi-monocoque central cone

Central Cone	Aluminium semi-monocoque
Number of elements	278194
Number of nodes	561140
Mesh Type	3D CTETRA
Type of the physical properties	PSOLID

The shape of the elements and meshes are shown at Figure 5.1. Sizes of the elements are adjusted around the holes.

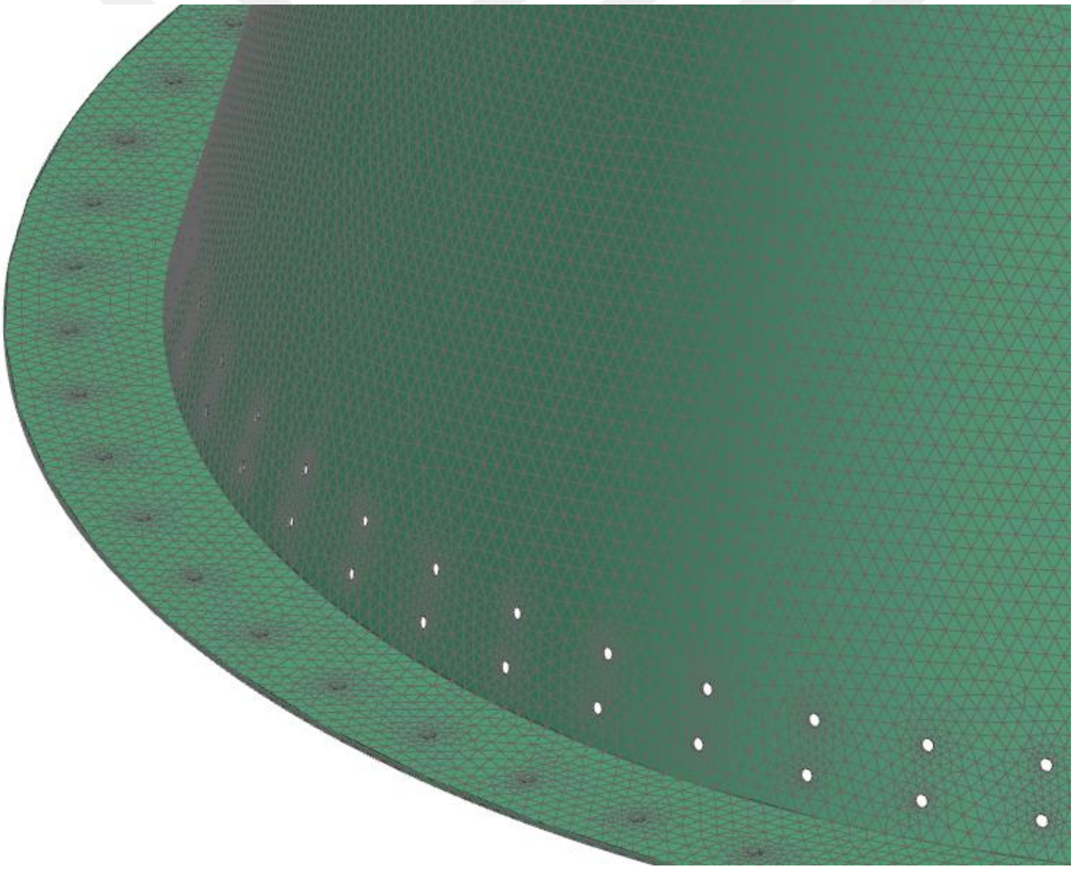

Figure 5.1 : Element shapes of the aluminium semi-monocoque central cone

5.1.1.2 FEM of CFRP semi-monocoque central cone

CFRP semi-monocoque central cone is modelled as 2D thin-shell meshes. The important part for this section is using laminate for layup of CFRP. At Appendix B, the layup and orientation of plies are shown with details. For 2 mm shells, with 0.1mm of thickness, there are 20 plies. For 3 mm parts of the central cone, with 0.1mm of thickness, there are 30 plies. Element properties for CFRP semi-monocoque cone is shown at Table 5.2.

Table 5.2 : Element properties of CFRP semi-monocoque central cone

Central Cone	CFRP semi-monocoque
Number of elements	66714
Number of nodes	35647
Mesh Type	2D CTRIA3
Type of the physical properties	2D Laminate

Element size of the meshes are 12 mm and maximum growth rate of the meshes is 1.3. The shape of the elements and meshes are shown at Figure 5.2. Sizes of the elements are adjusted around the holes.

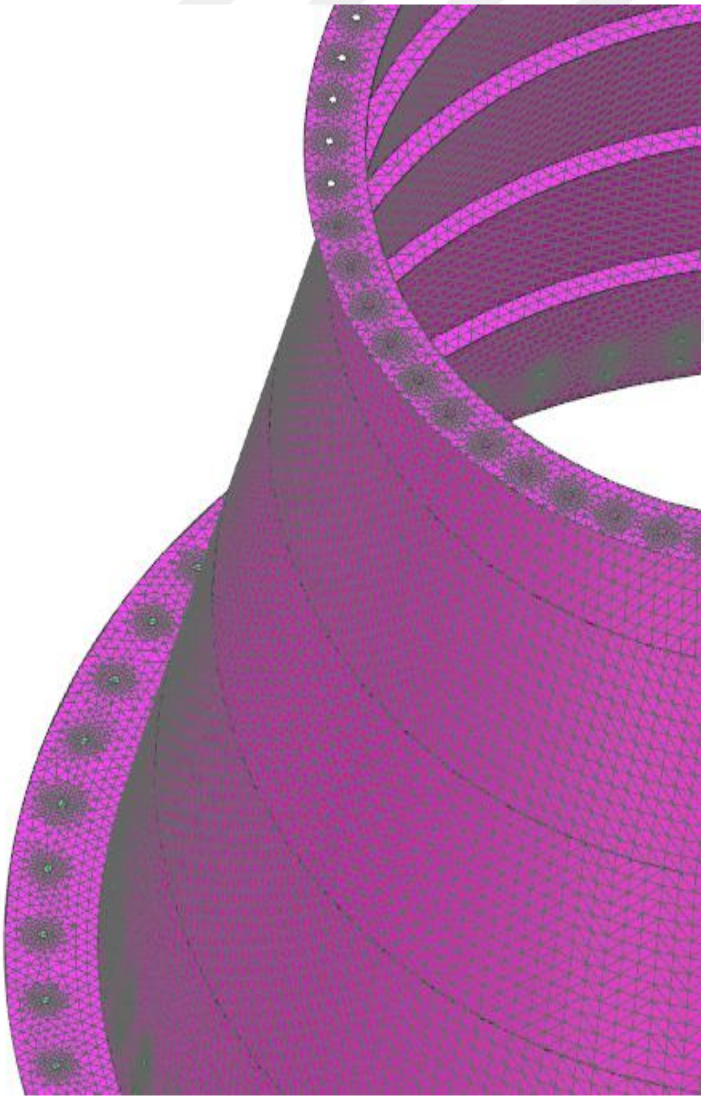

Figure 5.2 : Element shapes of CFRP semi-monocoque central cone

5.1.2 Creating FEM of grid central cones

There are two different finite element modelling method for grid central cones. For metallic central cone 3D solid meshes are used and for CFRP grid central cone 2D shell meshes used.

5.1.2.1 FEM of aluminium grid central cone

3D CTETRA meshes selected for Aluminium grid central cone. Two different 3D solid meshes applied on the central cone. First part of the central cone is grid side of the cone which is upper side of the cone. Other one is bottom part of the central cone which has interfaces with NC bracket and LVA. Both parts have the same 3D CTETRA mesh types. At Figure 5.3, the meshes of Aluminium grid central cone is shown. Green meshes are described as first part of the meshes and blue meshes are second part of them which has interfaces with other parts of assemblies.

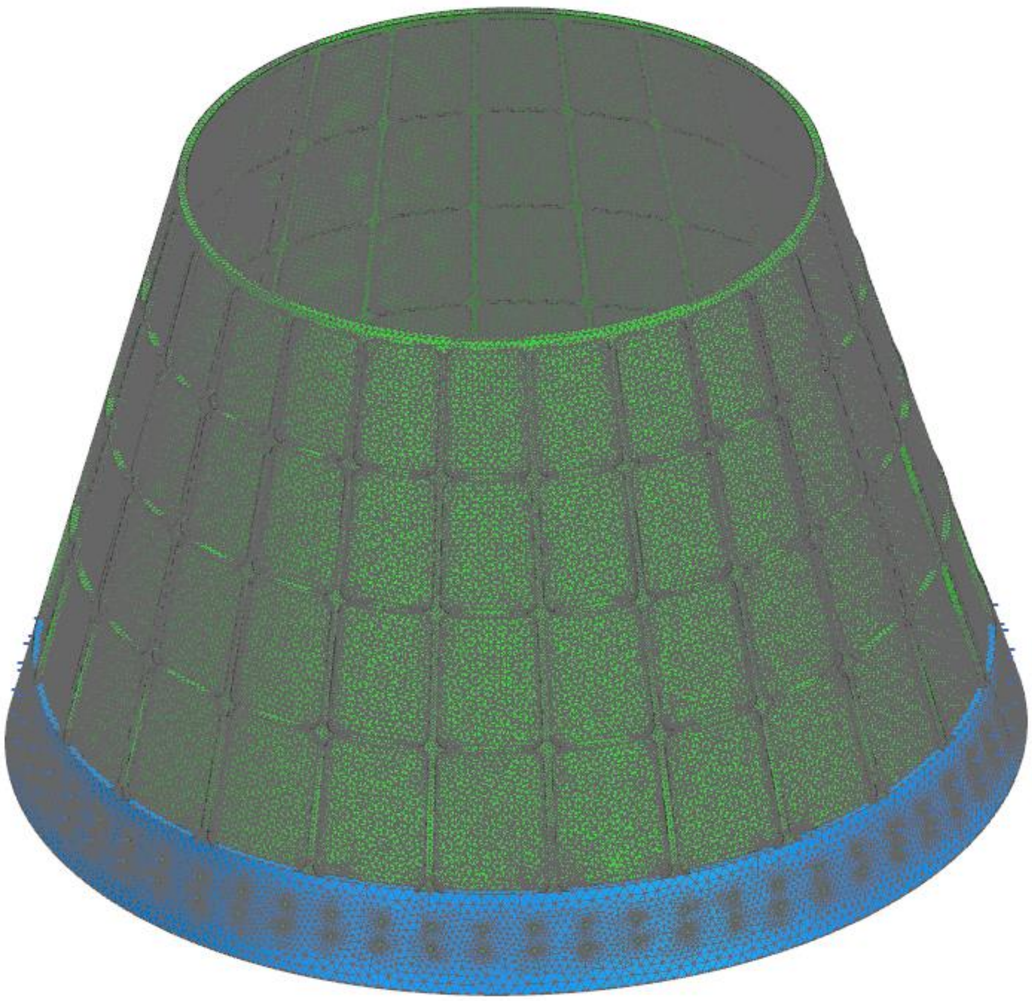

Figure 5.3 : General view of aluminium central cone

Element sizes of the green part is 8 mm with 1.3 maximum growth rate. Element sizes of the blue part is 15 mm with 1.3 maximum growth rate. Element properties are shown for Aluminium grid central cone at Table 5.3. The numbers of the elements and nodes are total numbers for green and blue parts of the meshes.

Table 5.3 : Element properties of the Aluminium grid central cone

Central Cones	Aluminium Grid
Number of elements	420439
Number of nodes	826046
Mesh Type	3D CTETRA
Type of the physical properties	PSOLID

5.1.2.2 FEM of CFRP grid central cone

For grid sides and shell behind the grids, 2D thin-shell elements created for CFRP grid central cone. The important part for this section is using laminate for layup of CFRP for both 2D thin-shells. At Appendix C, the layup and orientation of plies are shown with details for both. For the shell behind with 0.1mm ply thicknesses there are 10 plies at laminate. For grid side of the central cone there are 60 plies with 0.15 ply thickness. The green colour is shown the grid side of the meshes and orange part is shown the shell of the cone at Figure 5.4.

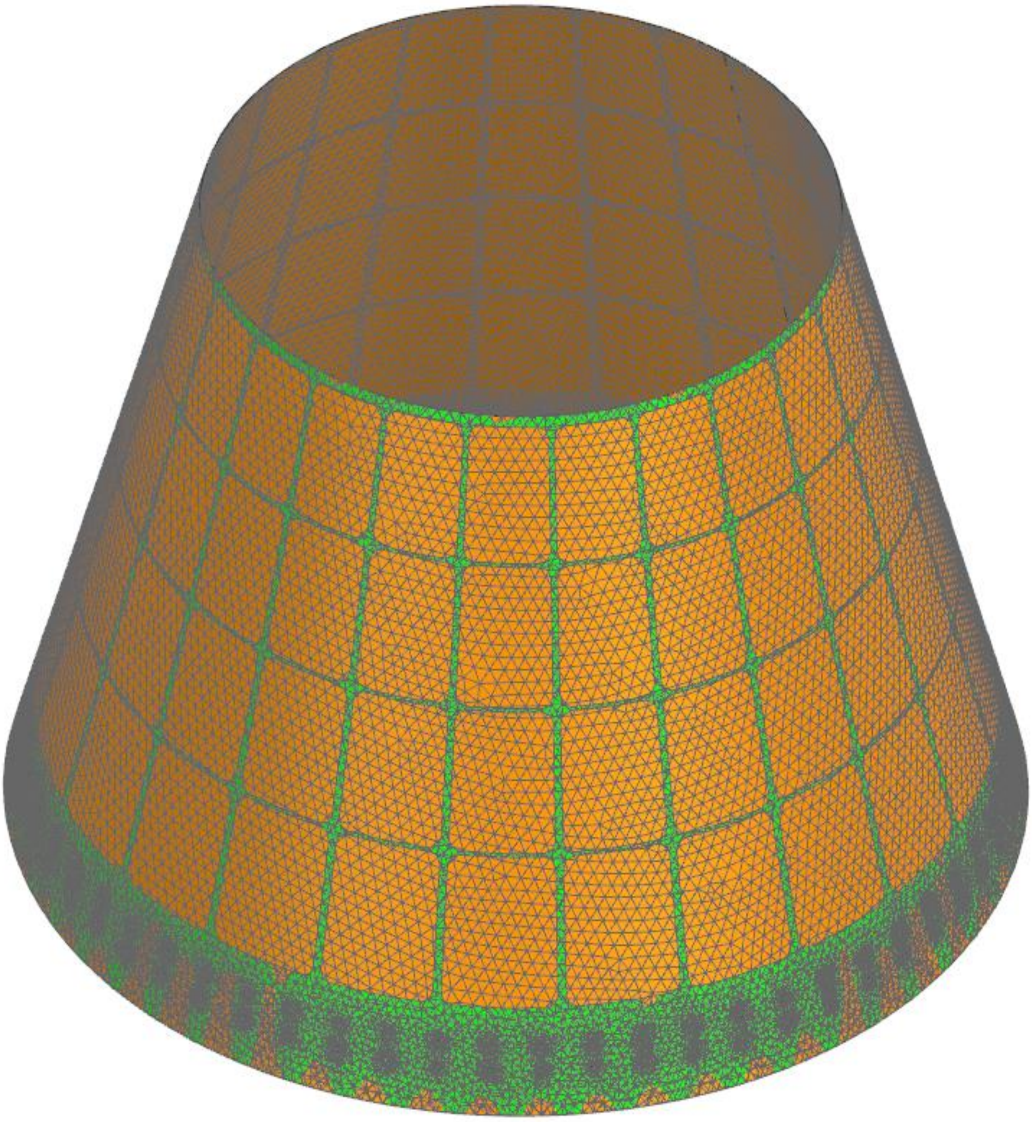

Figure 5.4 : General view of CFRP grid central cone meshes

Orange part of the meshes have 15 mm element size with maximum growth rate 1.3 and green side of the meshes have 12 mm element size with maximum growth rate 1.3. For orange part, layup of the CFRP has an offset on the middle of them but for green side, the offset of the layup is beginning from the bottom of the laminate. Element properties are shown at Table 5.4.

Table 5.4 : Element properties of CFRP grid central cone

Central Cone	CFRP Grid
Number of elements	54342
Number of nodes	29930
Mesh Type	2D CTRIA3
Type of the physical properties	2D Laminate

5.1.3 Creating FEM of sandwich central cone

For sandwich central cones 2D thin shell mesh method used because of having different kind of parts in their design. Difference between metallic and CFRP sandwich cones are type of the physical properties of meshes in their model. 2D PCOMP applied on aluminium sandwich central cone and 2D Laminate applied on CFRP sandwich central cone.

5.1.3.1 FEM of aluminium central cone

2D CQUAD4 mesh type selected for Aluminium sandwich central cone. The mid-surface modelling method used to create a surface in the middle of the design and core and skins of the honeycomb properties added in the FEM of cone with using 2D PCOMP. General element sizes of the elements are 10 mm for the central cone. Skin thickness of the central cone is 0.41 mm and core thickness of the honeycomb is 9.18 mm. Element properties of the aluminium sandwich central cone is shown at Table 5.5.

Table 5.5 : Element properties of Aluminium sandwich central cone

Central Cone	Aluminium Sandwich
Number of elements	32837
Number of nodes	33489
Mesh Type	2D CQUAD4
Type of the physical properties	PCOMP

General view of the FEM of aluminium sandwich central cone is shown at Figure 5.5. Because of only one part of the model, there is only one type of meshes.

Figure 5.5 : General view of Aluminium sandwich central cone FEM

5.1.3.2 FEM of CFRP sandwich central cone

Same as aluminium sandwich central cone, 2D CQUAD4 mesh type is applied on the CFRP sandwich central cone too. Mid-surface method used to create a shell for the modelling elements. The difference from aluminium one is using 2D Laminate on applying the material properties on the central cone. The CFRP ply thicknesses of the honeycomb skin is 0.11 mm with 8 plies for one skin. Honeycomb core thickness of the sandwich central cone is 8.24 mm. Element sizes of the meshes are 10 mm which is same with aluminium sandwich central cone. Element properties of the CFRP sandwich central cone is shown at Table 5.6.

Table 5.6 : Element properties of CFRP sandwich central cone

Central Cone	CFRP Sandwich
Number of elements	32837
Number of nodes	33489
Mesh Type	2D CQUAD4
Type of the physical properties	2D Laminate

Number of elements and nodes are same with Aluminium sandwich central cone because they both using same sizes of elements and types. General view of the meshes are shown at Figure 5.6.

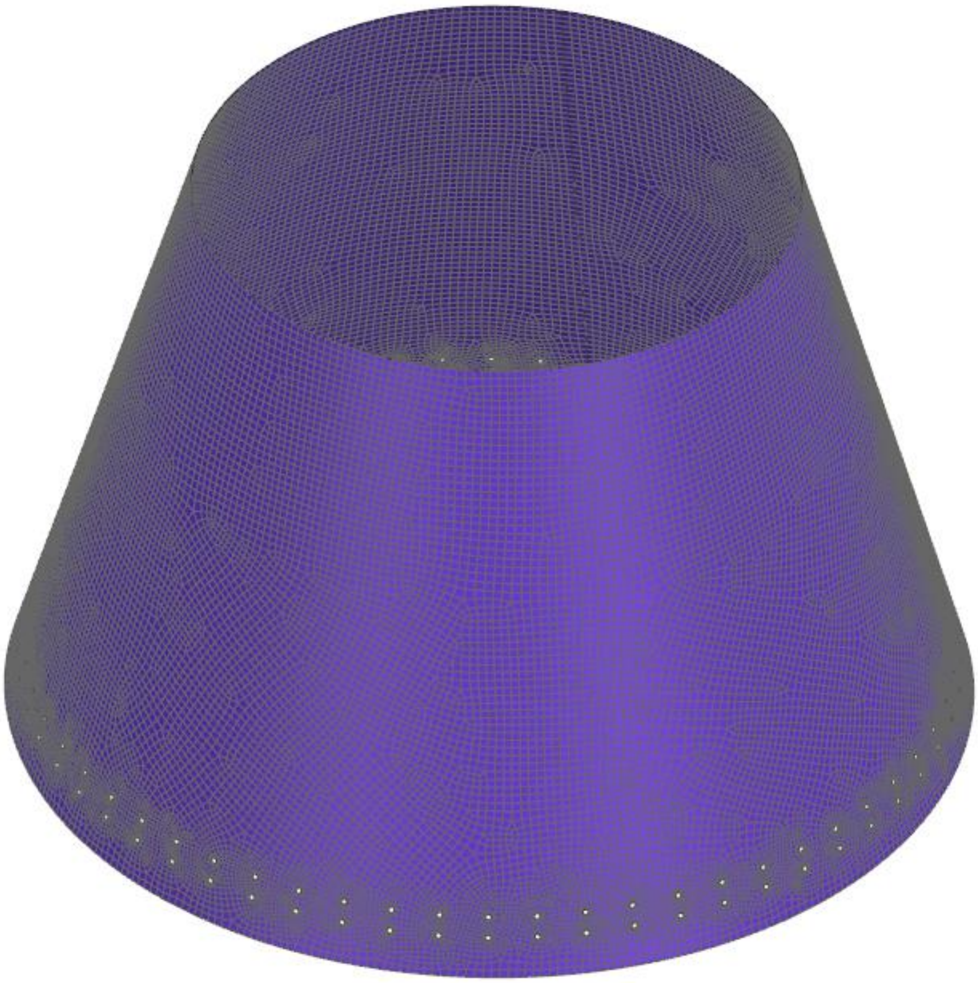

Figure 5.6 : General view of CFRP sandwich central coen FEM

5.2 Modal Analysis of Central Cones

First analysis on the central cones is modal analysis of only central cones. There will be a second modal analysis comparison for the study but it will cover all the assembly of the central cones. In this part of the thesis, the general boundary conditions and modal analysis results will be shown with details. The main boundary condition of the modal analysis is being hard mounted from the bottom of the structure which is basically mounting face of the central cones. Also, there are some simulation objects as glue for CFRP central cones. SOL 103 Real Eigenvalues of Simcenter Nastran solver is used to solve the simulation of the study.

For make the hard mounted surface, there are fixed constraints on the bottom of the central cones. General view of the fixed constraints is shown at Figure 5.7 on Aluminium semi-monocoque central cone as an example of them.

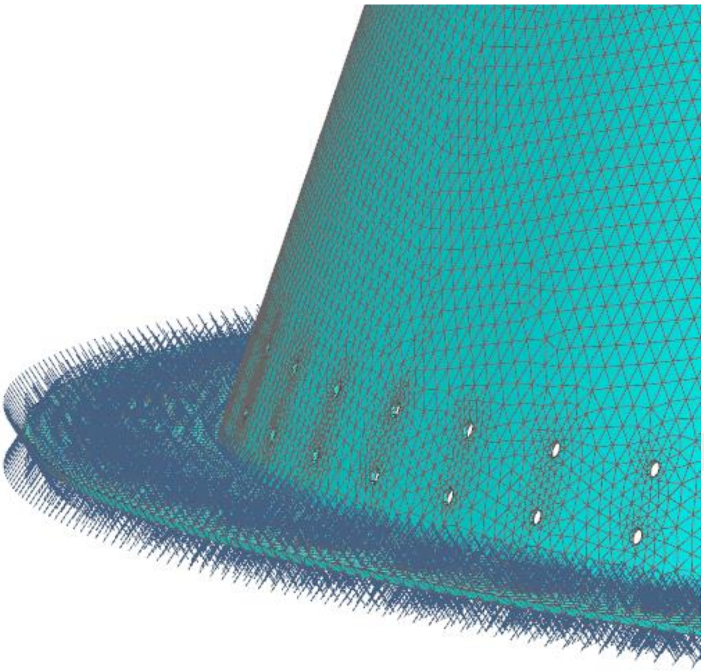

Figure 5.7 : Fixed constraints on central cone

For CFRP semi-monocoque and grid central cones, there are some simulation objects as glue which is connecting parts of the design. The glue is connecting edge of the ribs of semi-monocoque central cone and surface of the cone as shown at Figure 5.8. This is important because making the mid-surface on the designs is cutting the connection between all the edges and surfaces from each other. There are 4 ribs and 2 upper and bottom rings around the CFRP semi-monocoque central cone that is why six different edge gluing applied as simulation object on the analysis of CFRP semi-monocoque central cone. For CFRP grid central cone, there are only 2 parts to glue each other. One of them is grid part of the cone and other one is shell behind the grid. Face gluing is shown at Figure 5.9 which has green and orange parts of meshes to glue each other. Only one face gluing simulation object is enough for this central cone.

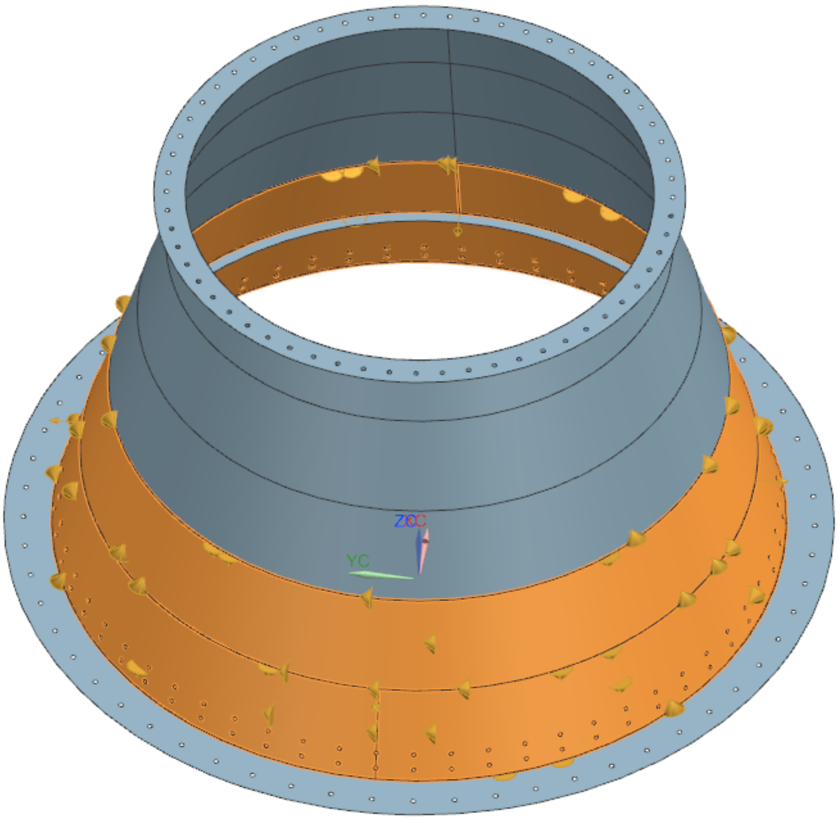

Figure 5.8 : Edge gluing for CFRP semi-monocoque central cone

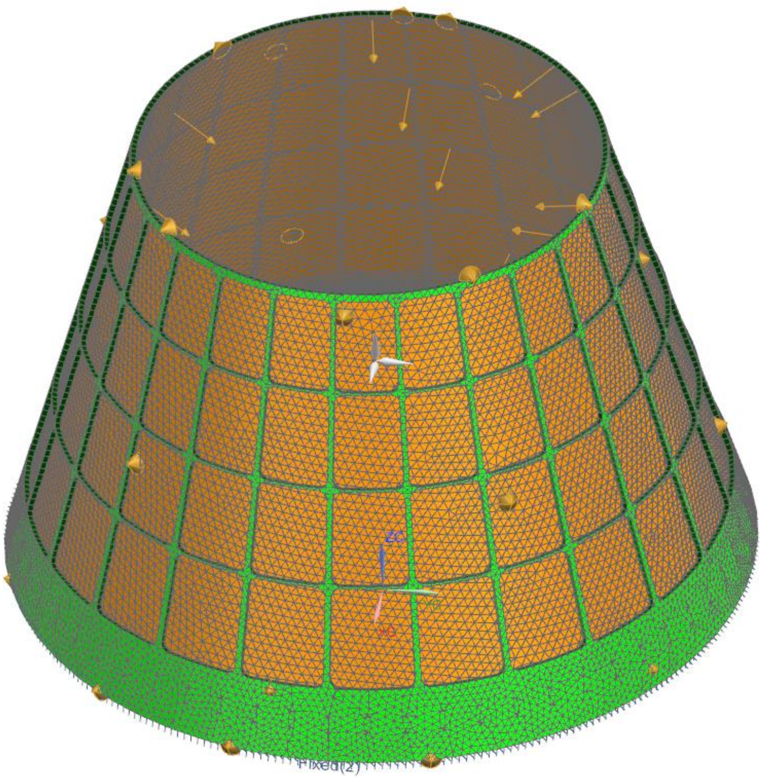

Figure 5.9 : Face gluing of the CFRP grid central cone

In the modal analysis results, there are two critical results to understand the behaviour of the structure. One of them is natural frequency results of the structure and other one is mode shapes of the structure. In the thesis, as a design requirement there is first natural frequency value of the central cones should be upper than 140 Hz. To understand the mode shapes better, model is exaggerating with using 10% model results of the result page of the Simcenter 3D.

5.2.1 Modal analysis of semi-monocoque central cones

5.2.1.1 Modal analysis of aluminium semi-monocoque central cone

For Aluminium semi-monocoque central cone modal analysis results are shown at Table 5.7 for first 10 modes. The important one is results of first natural frequency for the study.

Table 5.7 : Modal analysis results of Aluminium semi-monocoque central cone

Central Cone	Aluminium Semi-monocoque
Mode 1 (Hz)	321.31
Mode 2 (Hz)	322.05
Mode 3 (Hz)	367.20
Mode 4 (Hz)	367.85
Mode 5 (Hz)	392.95
Mode 6 (Hz)	393.66
Mode 7 (Hz)	427.93
Mode 8 (Hz)	428.74
Mode 9 (Hz)	516.97
Mode 10 (Hz)	518.55

Modal analysis results of aluminium semi-monocoque central cone are satisfying the design requirement of having 140 Hz first natural frequency value. Mode shape of first mode is shown at Figure 5.10. The general modes of the central cone are rising in twos, with considering to examine the results of the analysis. Mode 1-2, Mode 3-4, Mode 5-6, Mode 7-8 and Mode 9-10 are almost same values. The results shows that there may be some mass reduction studies if other analysis results can satisfy their requirements too.

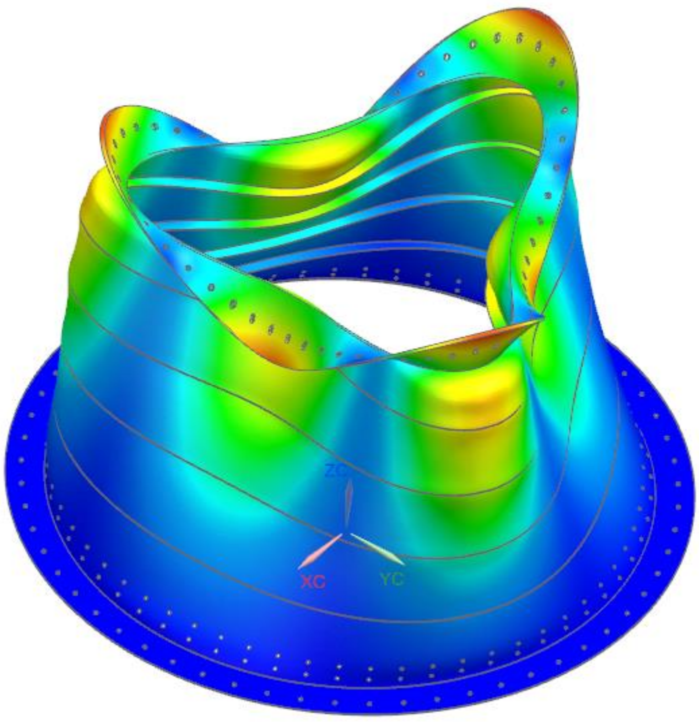

Figure 5.10 : General view of Aluminium semi-monocoque central cone Mode 1 with 10% model

5.2.1.2 Modal analysis of CFRP semi-monocoque central cone

For CFRP semi-monocoque central cone modal analysis results are shown at Table 5.8 for first 10 modes. The important one is results of first natural frequency for the study.

Table 5.8 : Modal analysis results of CFRP semi-monocoque central cone

Central Cone	CFRP Semi-monocoque
Mode 1 (Hz)	485.55
Mode 2 (Hz)	488.48
Mode 3 (Hz)	552.11
Mode 4 (Hz)	553.29
Mode 5 (Hz)	581.57
Mode 6 (Hz)	582.09
Mode 7 (Hz)	632.61
Mode 8 (Hz)	636.11
Mode 9 (Hz)	756.66
Mode 10 (Hz)	766.56

First natural frequency value of CFRP semi-monocoque central cone is higher than 140 Hz which is satisfying the design requirement. The results are better than metallic semi-monocoque central cone with considering to modal analysis. Also, regarding the analysis results it may be some mass optimization on the central cone if it can satisfy other analysis results too. The mode shape of first mode is shown at Figure 5.11. Mode shapes of both semi-monocoque central cones are similar to each other.

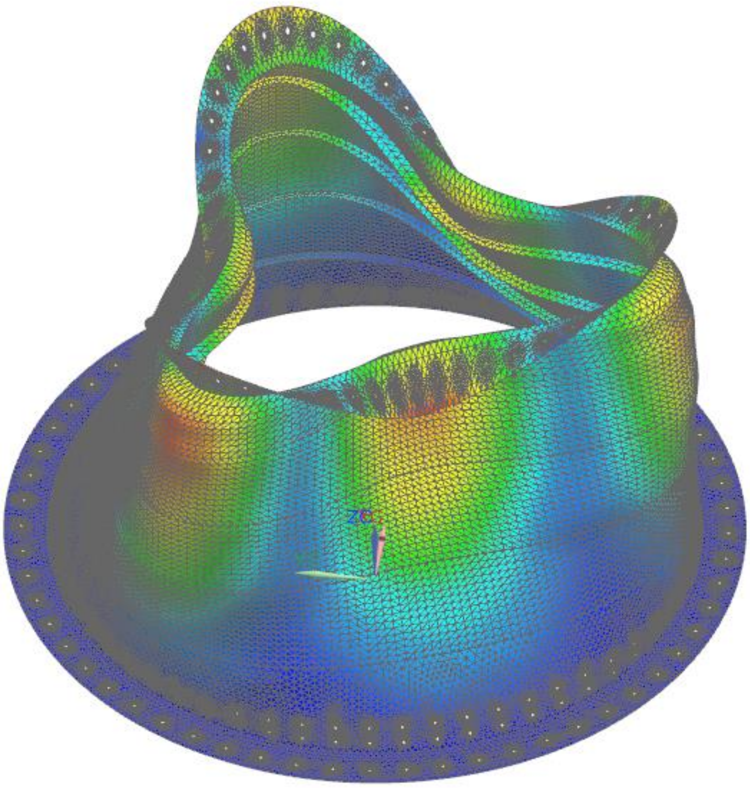

Figure 5.11 : CFRP semi-monocoque central cone mode shape for Mode 1

5.2.2 Modal analysis of grid central cones

5.2.2.1 Modal analysis of aluminium grid central cone

Aluminium grid central cone has same condition with semi-monocoque central cones. The modal analysis results for first 10 modes are shown at Table 5.9.

Table 5.9 : Modal analysis results of Aluminium grid central cone

Central Cone	Aluminium Grid
Mode 1 (Hz)	223.13
Mode 2 (Hz)	223.21
Mode 3 (Hz)	252.17
Mode 4 (Hz)	252.37
Mode 5 (Hz)	258.94
Mode 6 (Hz)	259.20
Mode 7 (Hz)	311.82
Mode 8 (Hz)	311.94
Mode 9 (Hz)	362.43
Mode 10 (Hz)	362.63

First natural frequency value of Aluminium grid central cone is satisfied the design requirements. On the other hand, frequency values are lower than both semi-monocoque central cone results. The shape of the Mode 1 is shown at Figure 5.12 which is similar to semi-monocoque cone mode shapes.

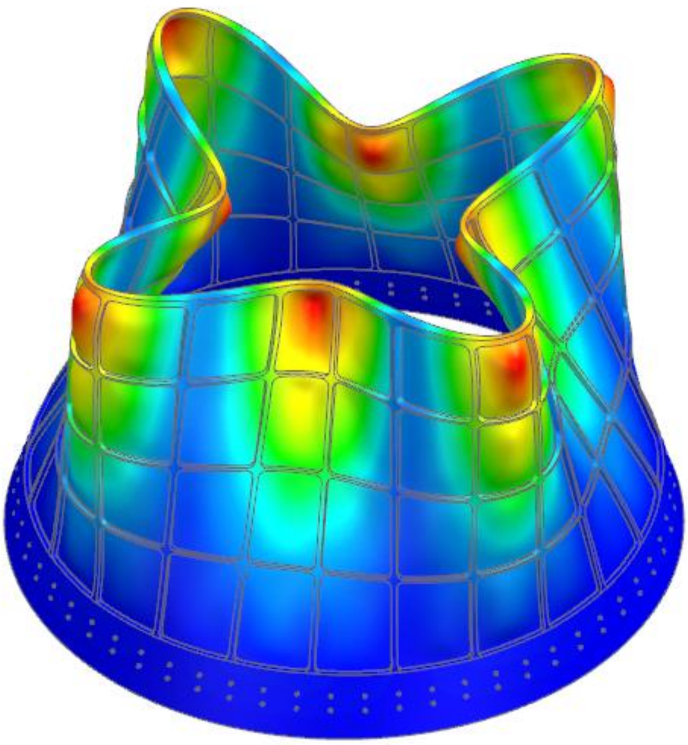

Figure 5.12 : Aluminium grid central cone mode shape for Mode 1

5.2.2.2 Modal analysis of CFRP grid central cone

For CFRP grid central cone same analysis proceed to get natural frequency results. First 10 mode frequency values are shown at Table 5.10.

Table 5.10 : Modal analysis results of CFRP grid central cone

Central Cone	CFRP Grid
Mode 1 (Hz)	272.98
Mode 2 (Hz)	281.64
Mode 3 (Hz)	314.83
Mode 4 (Hz)	317.70
Mode 5 (Hz)	327.97
Mode 6 (Hz)	330.11
Mode 7 (Hz)	368.49
Mode 8 (Hz)	371.89
Mode 9 (Hz)	418.54
Mode 10 (Hz)	421.17

Same with the Aluminium grid central cone, results are lower than the semi-monocoque central cones but still first natural frequency value is higher than the design requirements which is 140 Hz. The shape of the Mode 1 is shown at Figure 5.13.

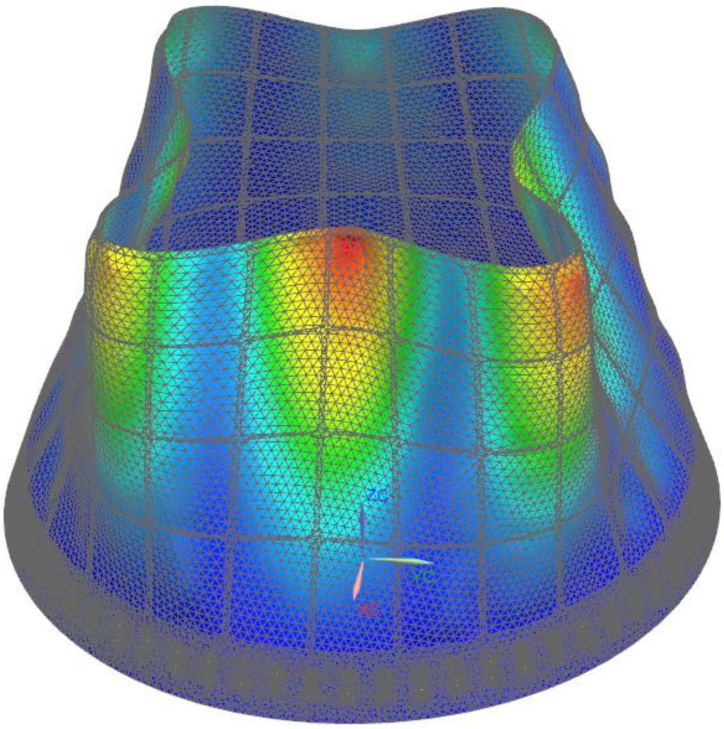

Figure 5.13 : CFRP grid central cone mode shape for Mode 1

5.2.3 Modal analysis of sandwich central cones

5.2.3.1 Modal analysis of aluminium sandwich central cone

Same conditions applied on sandwich central cones too. For Aluminium sandwich central cone modal analysis results of first 10 modes are shown at Table 5.11.

Table 5.11 : Modal analysis results of Aluminium sandwich central cone

Central Cone	Aluminium Sandwich
Mode 1 (Hz)	261.54
Mode 2 (Hz)	261.55
Mode 3 (Hz)	325.88
Mode 4 (Hz)	325.88
Mode 5 (Hz)	353.99
Mode 6 (Hz)	353.99
Mode 7 (Hz)	452.32
Mode 8 (Hz)	452.33
Mode 9 (Hz)	558.27
Mode 10 (Hz)	558.30

Results of Aluminium sandwich central cone modal analysis are around grid central cones and lower than semi-monocoque central cones. However, the results are still satisfied the design requirements. The shape of the Mode 1 is shown at Figure 5.14.

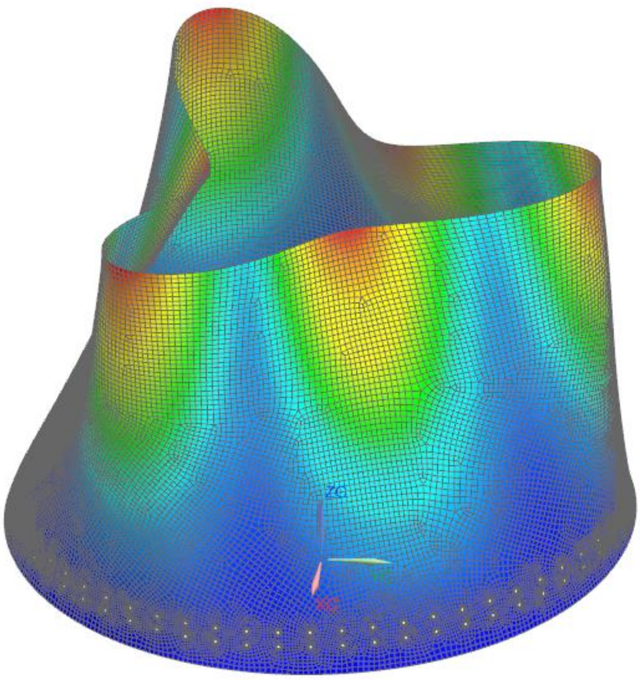

Figure 5.14 : Mode shape of Aluminium sandwich central cone Mode 1

5.2.3.2 Modal analysis of CFRP sandwich central cone

Modal analysis results for CFRP sandwich central cone are listed at Table 5.12.

Table 5.12 : Modal analysis results of CFRP sandwich central cone

Central Cone	CFRP Sandwich
Mode 1 (Hz)	329.76
Mode 2 (Hz)	329.76
Mode 3 (Hz)	369.26
Mode 4 (Hz)	369.27
Mode 5 (Hz)	375.94
Mode 6 (Hz)	375.95
Mode 7 (Hz)	461.23
Mode 8 (Hz)	461.24
Mode 9 (Hz)	514.34
Mode 10 (Hz)	514.37

CFRP sandwich central cone modal analysis results are second best after the CFRP semi-monocoque central cone. Mode shape of mode 1 for CFRP sandwich central cone is shown at Figure 5.15.

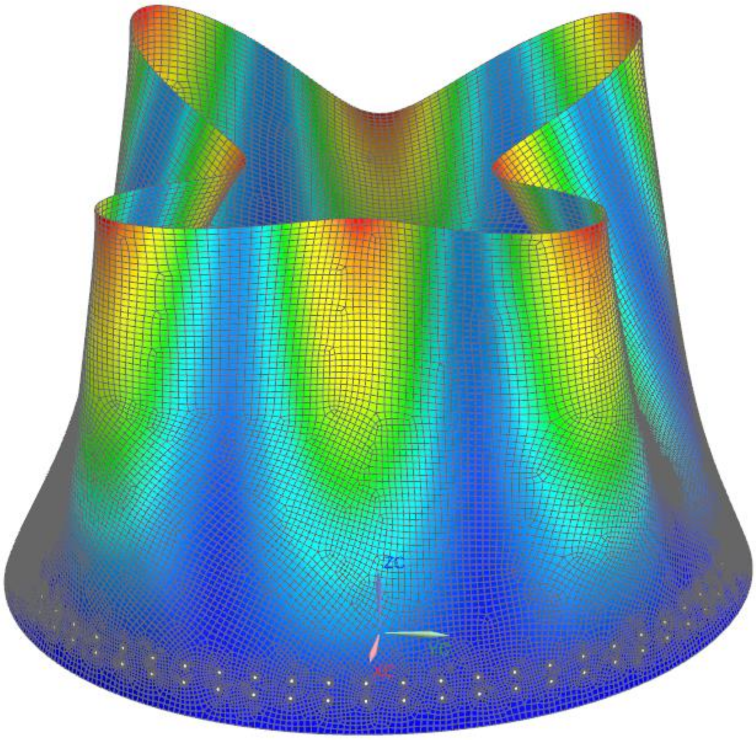

Figure 5.15 : Mode shape of Mode 1 for CFRP sandwich central cone

5.2.4 Modal analysis results comparison for central cones

Third comparison of the study is modal analysis results of the central cones. It is important to known that modal analysis results are giving the stiffness criteria of the central cones and all of them are satisfying the design requirements. That is why with regarding to other types of analysis there can be some iterations to decrease mass and stiffness because requirement is far from current situations. First natural frequency values of the central cones are listed at Table 5.13.

Table 5.13 : Modal analysis results comparison of central cones

Central Cones	AL monocoque	CFRP Monocoque	AL Grid	CFRP Grid	AL Sandwich	CFRP Sandwich
Mode 1 (Hz)	321.31	485.55	223.13	272.98	261.54	329.76

For all type of design concepts CFRP central cones have higher frequency values than Aluminium ones. One of the main reasons of that is having more weight for metallic central cones. Rising mass values are inversely proportional to stiffness values, so modal analysis results are parallel with this fact. The heaviest central cone which is Aluminium grid central cone has lowest natural frequency level.

5.3 Creating FEM of Assembly Components

It is important to create correct finite element model other components and connections of the central cone assemblies. In the previous section, creation of the central cone FEMs described with element types and sizes. Same with central cone FEMs, other components also have different types of elements and sizes. Other components of the central cone assemblies are launch vehicle adapter, horizontal structural panel, NC bracket and connections of them.

With respect to the material type of the component, the modelling philosophy is changing. For metallic structures it is easy and more appropriate to make 3D solid meshes on the other hand for composites like honeycombs, modelling the structure with 2D thin shells is more correct one.

For launch vehicle adapter (LVA) 3D CTETRA (10) meshes applied on the model with element size of 9 mm and maximum growth rate is 1.3. The sizes of the meshes are adjusted around the holes of launch vehicle adapter. Because of being metal, type of the modelling is selected as 3D solid for LVA. Element and node numbers of the LVA is listed at Table 5.14.

Table 5.14 : Element properties of LVA

Assembly Component	LVA
Number of elements	124953
Number of nodes	253295
Mesh Type	3D CTETRA
Type of the physical properties	PSOLID

General view of the FEM of launch vehicle adapter is shown at Figure 5.16.

Figure 5.16 : FEM of LVA

As a composite structure which is honeycomb sandwich panel, horizontal structural panel modelled with 2D thin shells with using mid-surface method. 2D CQUAD (4) meshes applied on the model with element size of 5 mm. Also, around the holes meshes are controlled with number of mesh as six. Element properties of the horizontal structural panel FEM is listed at Table 5.15.

Table 5.15 : Element properties of horizontal structural panel FEM

Assembly Component	Horizontal Structural Panel
Number of elements	17398
Number of nodes	18333
Mesh Type	2D CQUAD
Type of the physical properties	PCOMP

FEM of horizontal structural panel is shown at Figure 5.17.

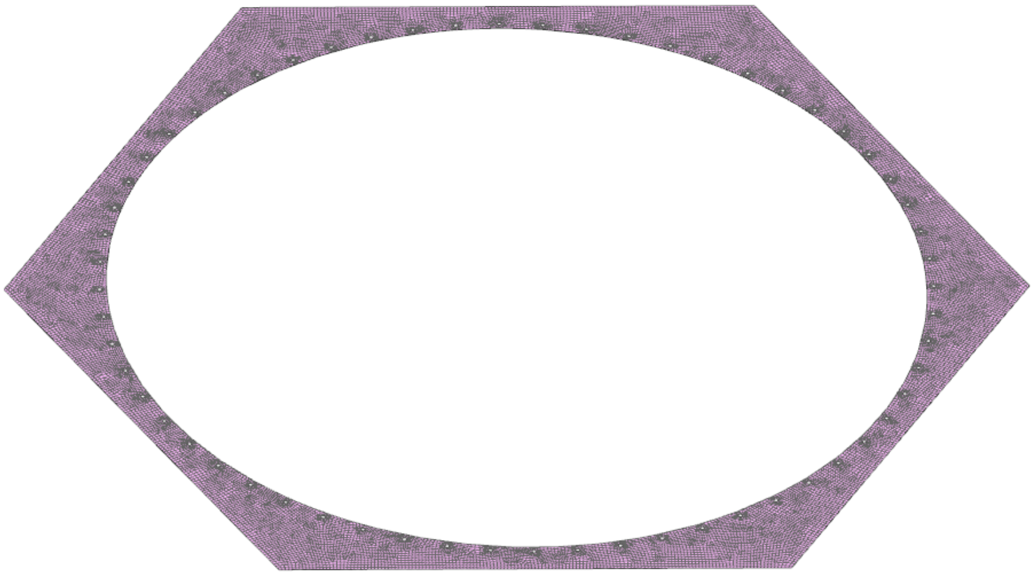

Figure 5.17 : FEM of horizontal structural panel

Last component of the assemblies is NC bracket which is another metallic component of the assembly. That is why NC bracket is also modelled with 3D solid meshes as CTETRA (10). Element sizes of the meshes are 9 mm with maximum growth rete 1.3. Element properties of the NC bracket is listed at Table 5.16.

Table 5.16 : Element properties of NC bracket FEM

Assembly Component	NC Bracket
Number of elements	80020
Number of nodes	165181
Mesh Type	3D CTETRA
Type of the physical properties	PSOLID

General view of NC bracket FEM is shown at Figure 5.18.

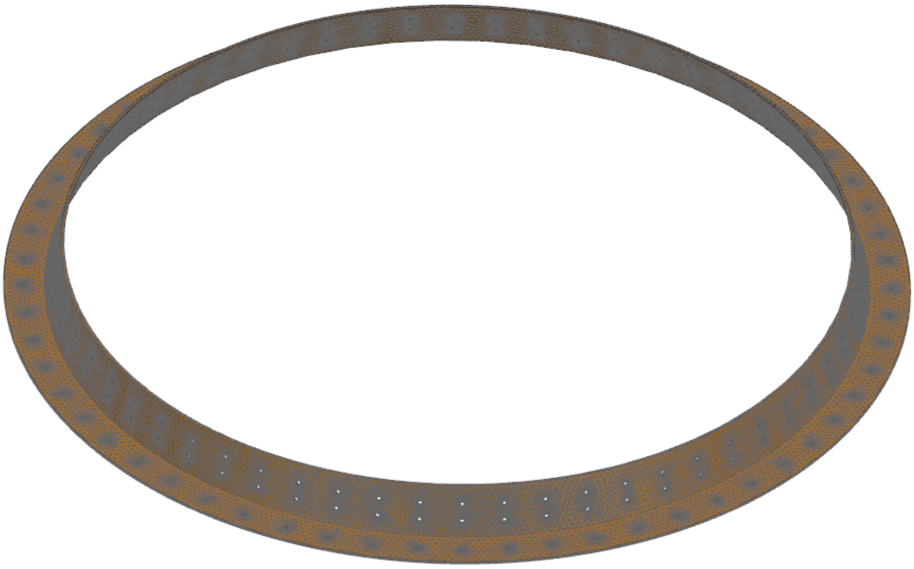

Figure 5.18 : FEM of NC bracket

5.3.1 Connections of the assemblies

For all the connections on the central cone assemblies, same type of connection selected. The member of this connection type is RBE2 and CBAR 1D collectors. RBE2 is kind of spider to connect node to node connections with rigid collector. All the degree of freedoms of the RBE2 connections are rigid for all axis. Also, RBE2 elements have infinite stiffness which makes all the nodes connected with RBE2 moves together [33]. The scheme of RBE2 is shown at Figure 5.19.

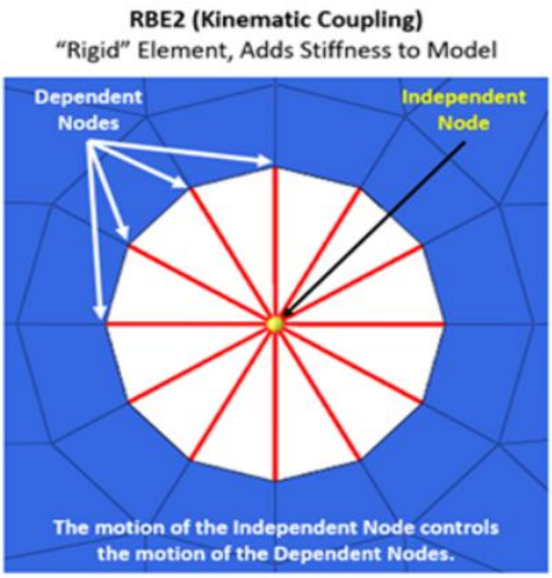

Figure 5.19 : Scheme of RBE2 collector [33]

Another connector is CBAR in assembly FEMs. CBAR is a bar element of Simcenter NASTRAN to provide stiffness to all six DOFs of each node or grid points. Difference from RBE2, it has not infinite stiffness only have stiffness with defined rod diameter with rod material. Rod material is Titanium-Ti-6AI-4V selected from siemens library. CBAR supports tension, compression, torsion and bending in two perpendicular planes, and shear in two perpendicular planes. The definition of the material data is using PBAR module of Simcenter 3D.

Connections of the assemblies are depended on the how many components will connect to each other. There are two types of connection in the central cone assemblies. Two parts are connecting or three parts are connecting to each other. For two parts it's like RBE2-CBAR-RBE2 connection and for three parts it's like RBE2-CBAR-RBE2-CBAR-RBE2. CBARs are connecting the different parts to each other and RBE2s are providing stiffness from centre of the hole to edge of the hole. For 2D surfaces RBE2s are connecting centre node of hole to edge of the holes. For 3D surfaces RBE2s are connecting mid-level node which is geometrically centre of them to inner surface of the holes. CBARs connecting centre nodes of different parts of the assemblies. As an example of that, for three component examples Figure 5.20 is visualize the connection of central cones.

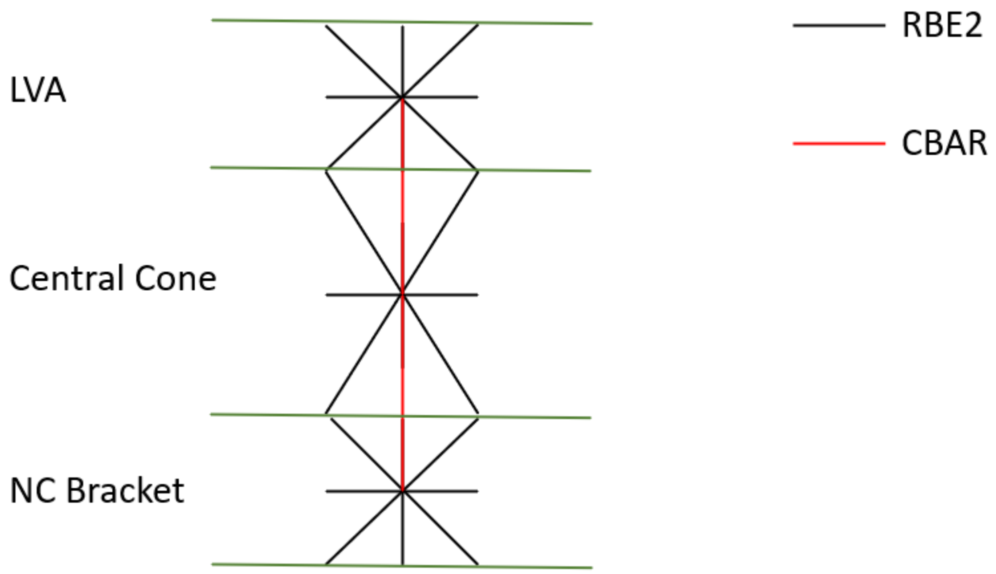

Figure 5.20 : Example connection of central cones

5.4 Modal Analysis of Central Cone Assemblies

Second analysis of the thesis is modal analysis for central cone assemblies. The method of the analysis is almost same with the modal analysis on central cones. Only difference between them is adding new boundary conditions because of the assembly structure of the central cones. In the central cone modal analysis, the fixed constraint boundary condition is applying on the bottom surface of the central cones. On the other hand, for the assemblies, the fixed constraint which is making the structure hard mounted is applying on the bottom surface of the LVA. The reason of that is LVA will be attached to the launch vehicle from the bottom surface of it, and that connection is almost hard mounted connection for FEM. Other 1D connections are explained in the previous section for the assemblies. There is another boundary condition for the central cone assemblies. It is on the top surface of the central cones which is normally attaching to the satellite from that surface. The boundary condition is not a fixed constraint this time, there are RBE2 rigid elements connecting the nodes of the central cone top surface. The boundary condition of the central cone assemblies is shown at Figure 5.21.

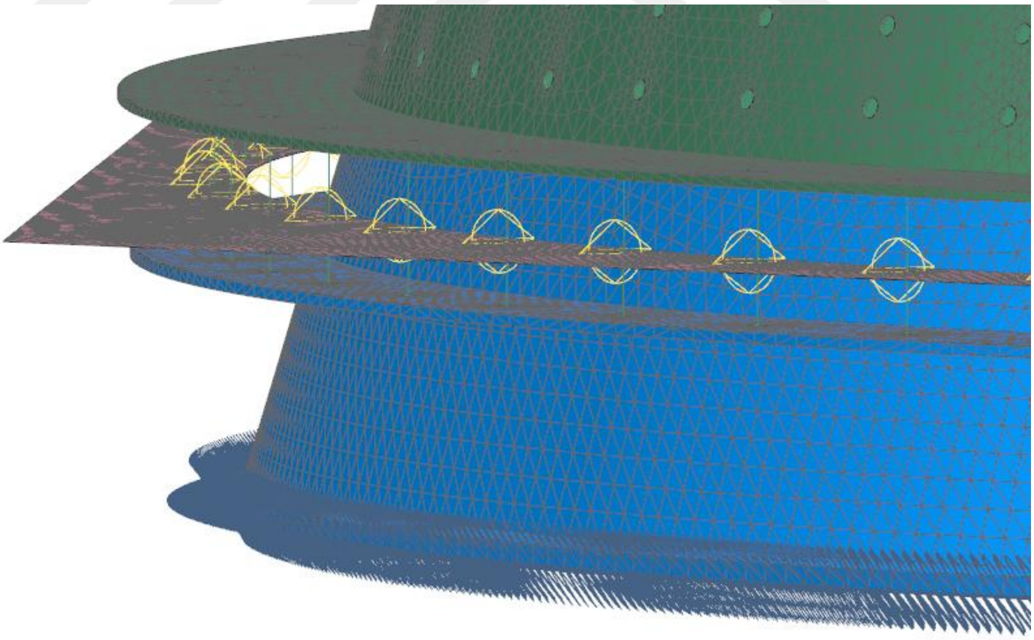

Figure 5.21 : Fixed constraint on the LVA

There are also some simulation objects between the assembly components. That simulation object is 'contact' object which is prevents objects from interfering into each other. For the central cone assemblies for all touching elements, the face contact created in the Simcenter 3D simulation as shown at Figure 5.22 as an example.

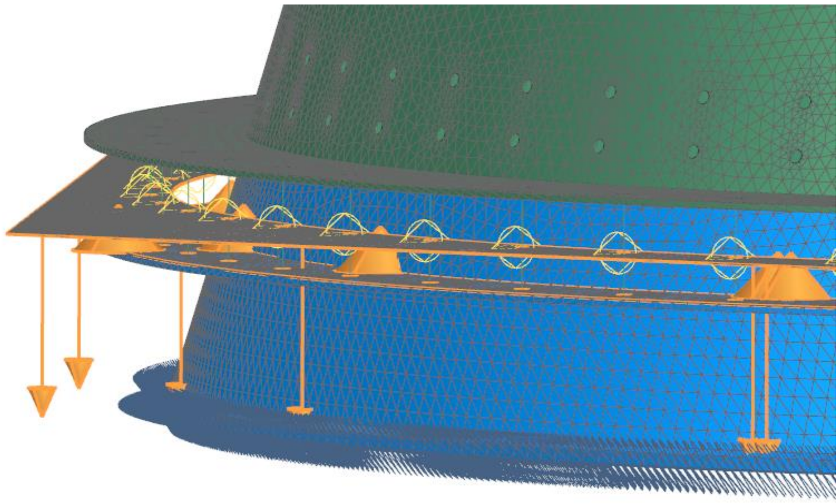

Figure 5.22 : Face contact simulation object example

The important point of the analysis results is to find the first eigen value of the assembly which is natural frequency of it, to understand the mass participation in the assembly on the modes. That is why from the results, the mass participation has crucial role. For some assembly results Mode 1 is not representing the first natural frequency of the system.

5.4.1 Modal analysis of semi-monocoque central cone assemblies

5.4.1.1 Modal analysis of aluminium semi-monocoque central cone assemblies

Modal analysis results of the Aluminium semi-monocoque central cone assembly are listed at Table 5.17.

Table 5.17 : Aluminium semi-monocoque central cone assembly modal analysis results

Central Cone Assy.	Aluminium Semi-monocoque
Mode 1 (Hz)	417.24
Mode 2 (Hz)	418.25
Mode 3 (Hz)	432.52
Mode 4 (Hz)	433.34
Mode 5 (Hz)	505.18
Mode 6 (Hz)	507.06
Mode 7 (Hz)	515.30
Mode 8 (Hz)	516.59
Mode 9 (Hz)	619.41
Mode 10 (Hz)	620.29

Frequency values of the assembly modal analysis results are higher than the central cone modal analysis results. Which is expected before the analysis because of the connections makes the assembly stiffer. With using 10% deformation view of the results, aluminium semi-monocoque central cone assembly modal analysis results and mode shapes are shown at Figure 5.23.

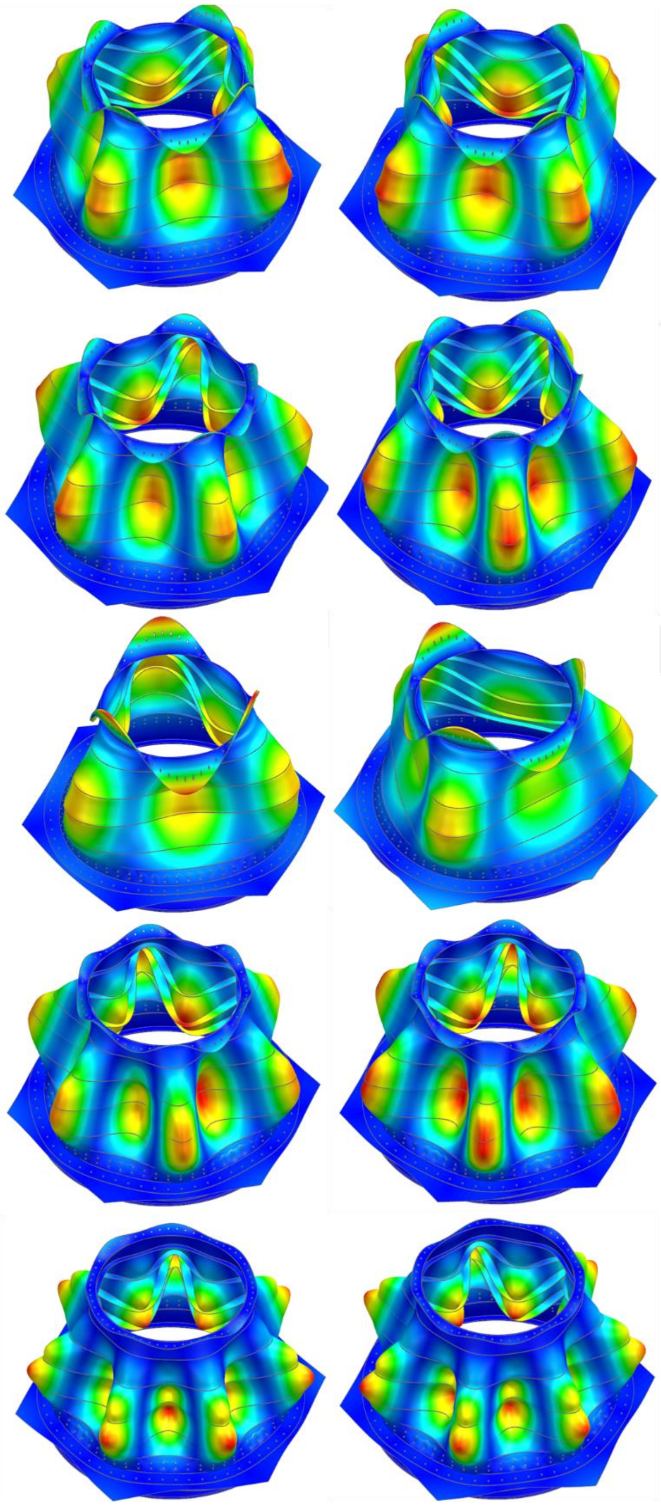

Figure 5.23 : Mode Shapes of Aluminium semi-monocoque central cone assembly

The mode shapes are shown that Mode 1 is the first natural frequency of the Aluminium semi-monocoque central cone assembly because cone of the assembly is participating the deformation.

5.4.1.2 Modal analysis of CFRP semi-monocoque central cone assembly

CFRP semi-monocoque central cone assembly modal analysis conditions are same with the aluminium one. That is why there is no specific explanation for that analysis. The modal analysis results of the CFRP semi-monocoque central cone assembly is listed at Table 5.18.

Table 5.18 : CFRP semi-monocoque central cone assembly modal analysis results

Central Cone Assy.	CFRP Semi-monocoque
Mode 1 (Hz)	615.47
Mode 2 (Hz)	617.86
Mode 3 (Hz)	633.95
Mode 4 (Hz)	636.81
Mode 5 (Hz)	697.78
Mode 6 (Hz)	716.51
Mode 7 (Hz)	718.41
Mode 8 (Hz)	720.40
Mode 9 (Hz)	721.02
Mode 10 (Hz)	724.56

Same with the aluminium semi-monocoque central cone assembly analysis results, CFRP semi-monocoque central cone assembly modal analysis results are also shown that assembly is stiffer than cone itself. With using 10% deformation view of the results, aluminium semi-monocoque central cone assembly modal analysis results and mode shapes are shown at Figure 5.24. After Mode 4, it is shown that the horizontal structural panel is the main component of the assembly which has mode at those frequencies. However, Mode shape 1 is shown that CFRP semi-monocoque central cone is participating the vibration that is why Mode 1 is the primary frequency value for the assembly.

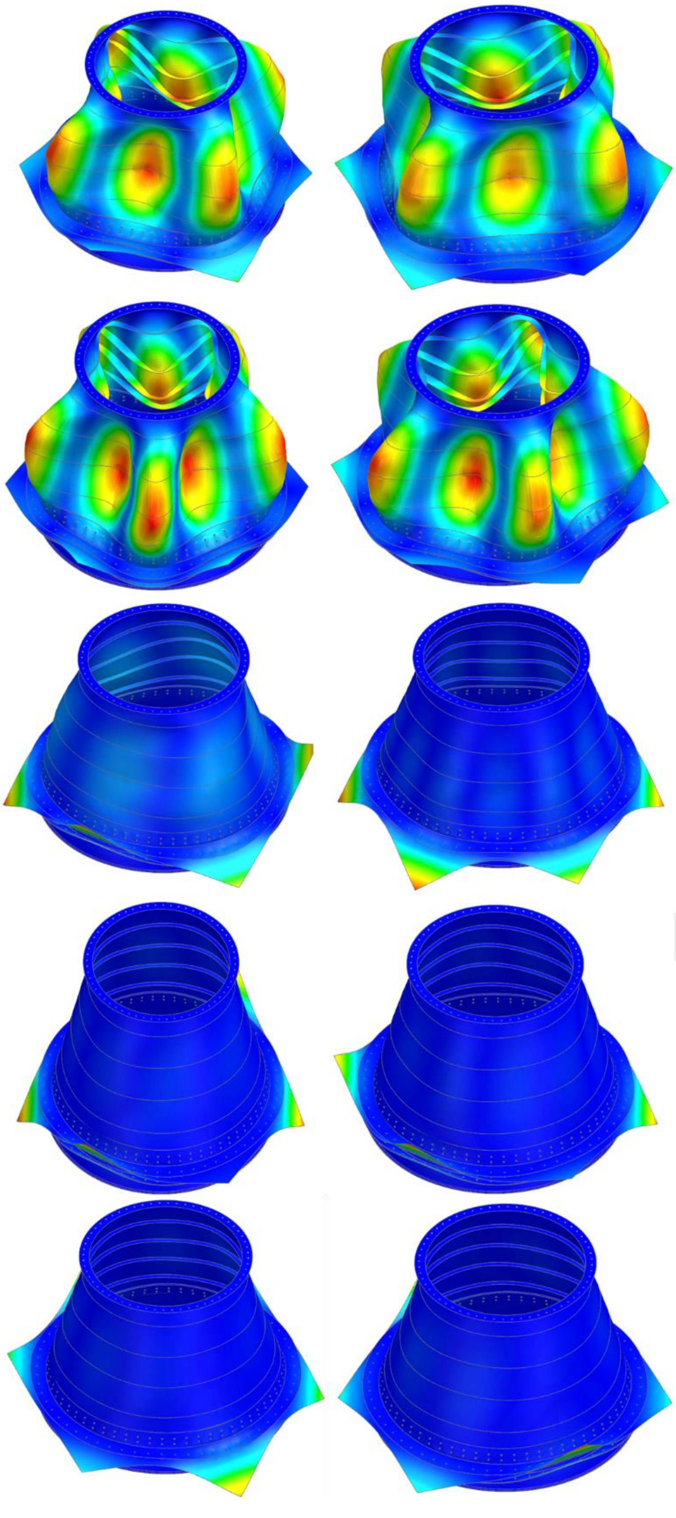

Figure 5.24 : Mode Shapes of CFRP semi-monocoque central cone assembly

5.4.2 Modal analysis of grid central cone assembly

5.4.2.1 Modal analysis of aluminium grid central cone assembly

Grid type central cones have the less frequency values as a comparison between all the design concepts. For Aluminium grid central cone assembly same conditions applied for modal analysis. Only difference between grid assemblies and semi-monocoque assemblies are usage of NC bracket in the assembly. Modal analysis results of the Aluminium grid central cone assembly are shown at Table 5.19.

Table 5.19 : Modal analysis results of Aluminium grid central cone assembly

Central Cone Assy.	Aluminium Grid
Mode 1 (Hz)	328.78
Mode 2 (Hz)	328.95
Mode 3 (Hz)	330.31
Mode 4 (Hz)	330.65
Mode 5 (Hz)	363.79
Mode 6 (Hz)	364.00
Mode 7 (Hz)	370.71
Mode 8 (Hz)	370.85
Mode 9 (Hz)	416.27
Mode 10 (Hz)	416.41

Results of the analysis are again rising with the assembly. However, the frequency values of the aluminium grid central cone assembly modal analysis results are way lower than semi-monocoque central cone assemblies. With using 10% deformation view of the results, aluminium grid central cone assembly modal analysis results and mode shapes are shown at Figure 5.25. The results shown that mode shape of the Mode 1 is the primary mode of the structure and grid cone is participating the deformation.

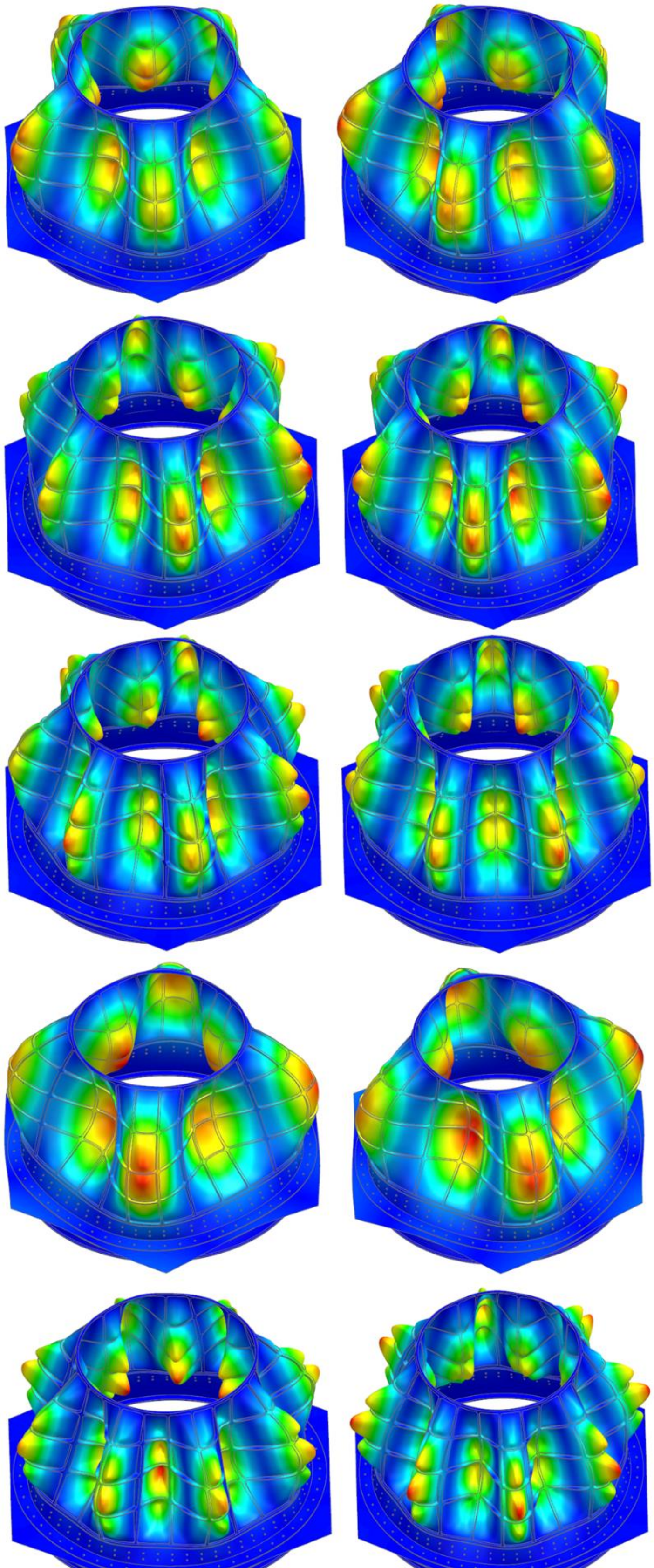

Figure 5.25 : Mode Shapes of Aluminium grid central cone assmebly

5.4.2.2 Modal analysis of CFRP grid central cone assembly

For CFRP grid central cone assembly same analysis done by using same conditions. Results of the modal analysis of CFRP grid central cone assembly is listed at Table 5.20.

Table 5.20 : Modal analysis results of CFRP grid central cone assembly

Central Cone Assy.	CFRP Grid
Mode 1 (Hz)	405.75
Mode 2 (Hz)	408.26
Mode 3 (Hz)	424.21
Mode 4 (Hz)	425.91
Mode 5 (Hz)	445.78
Mode 6 (Hz)	447.66
Mode 7 (Hz)	482.66
Mode 8 (Hz)	486.07
Mode 9 (Hz)	490.78
Mode 10 (Hz)	492.59

CFRP grid central cone assembly modal analysis results are stiffer than aluminium grid central cone assembly as expected because the results of the central cone modal analysis results are also parallel with the assembly results. With using 10% deformation view of the results, CFRP grid central cone assembly modal analysis results and mode shapes are shown at Figure 5.26. The results shown that mode shape of the Mode 1 is the primary mode of the structure and grid cone is participating the deformation.

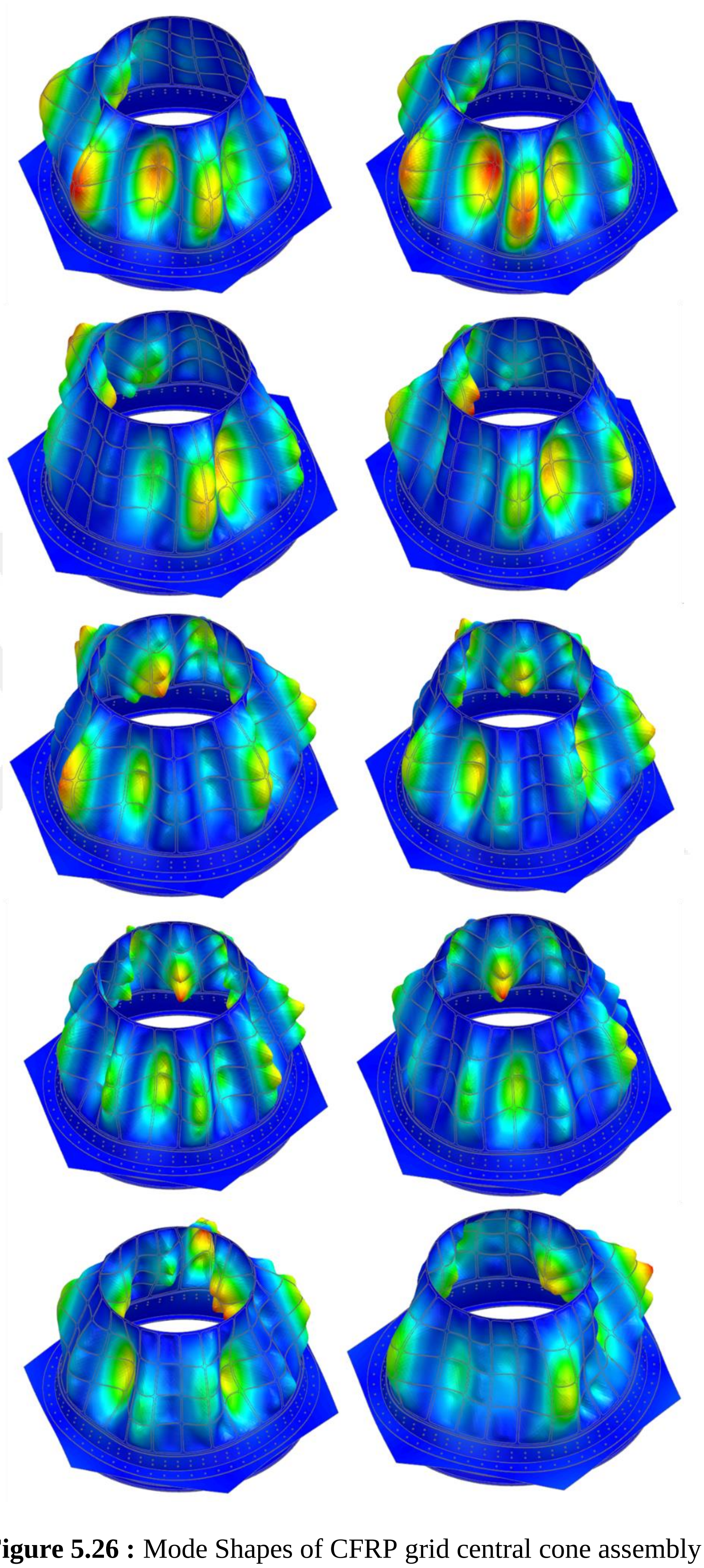

Figure 5.26 : Mode Shapes of CFRP grid central cone assembly

5.4.3 Modal analysis of sandwich central cone assemblies

5.4.3.1 Modal analysis of aluminium sandwich central cone assembly

After semi-monocoque and grid central cone assemblies, sandwich central cone assemblies have also the same conditions in their modal analysis. The usage of NC bracket is also available for sandwich central cones too. Results of the modal analysis of Aluminium sandwich central cone assembly is listed at Table 5.21.

Table 5.21 : Modal analysis results for Aluminium sandwich central cone assemblies

Central Cone Assy.	Aluminium Sandwich
Mode 1 (Hz)	482.89
Mode 2 (Hz)	483.05
Mode 3 (Hz)	526.08
Mode 4 (Hz)	526.17
Mode 5 (Hz)	532.66
Mode 6 (Hz)	535.80
Mode 7 (Hz)	626.09
Mode 8 (Hz)	626.60
Mode 9 (Hz)	660.41
Mode 10 (Hz)	662.13

With using 10% deformation view of the results, Aluminium sandwich central cone assembly modal analysis results and mode shapes are shown at Figure 5.27. The results shown that mode shape of the Mode 1 is the primary mode of the structure and grid cone is participating the deformation.

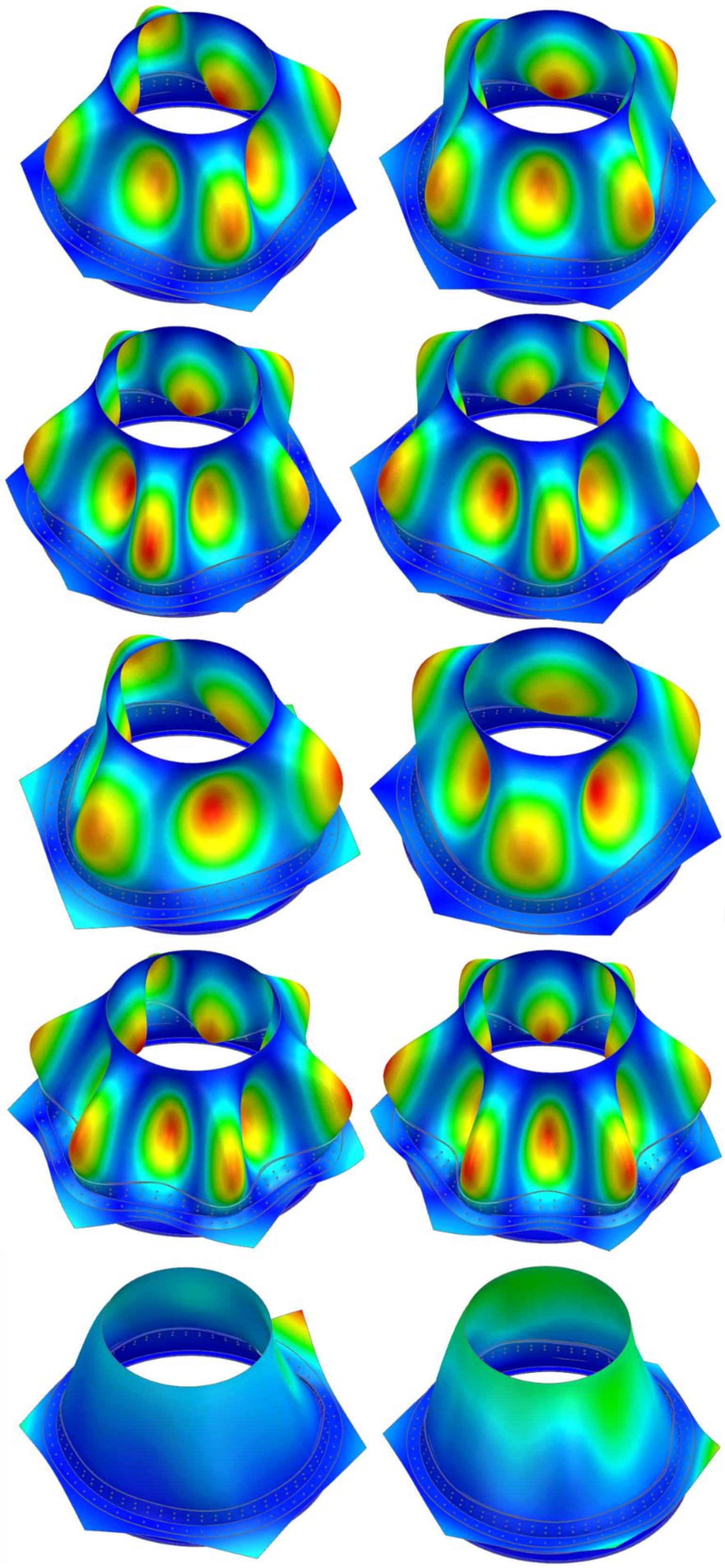

Figure 5.27 : Mode Shapes of Aluminium sandwich central cone assembly

Mode shape 9 and 10 for aluminium sandwich central cone assembly shows that horizontal structural panel is the primary structure of the deformation.

5.4.3.2 Modal analysis of CFRP sandwich central cone assembly

Modal analysis results of the CFRP sandwich central cone assembly are listed at Table 5.22.

Table 5.22 : Modal analysis results of CFRP sandwich central cone assembly

Central Cone Assy.	CFRP Sandwich
Mode 1 (Hz)	553.05
Mode 2 (Hz)	555.75
Mode 3 (Hz)	561.48
Mode 4 (Hz)	562.86
Mode 5 (Hz)	588.25
Mode 6 (Hz)	589.39
Mode 7 (Hz)	605.90
Mode 8 (Hz)	617.43
Mode 9 (Hz)	649.91
Mode 10 (Hz)	653.49

With using 10% deformation view of the results, Aluminium sandwich central cone assembly modal analysis results and mode shapes are shown at Figure 5.28. The results shown that mode shape of the Mode 1 is the primary mode of the structure and grid cone is participating the deformation.

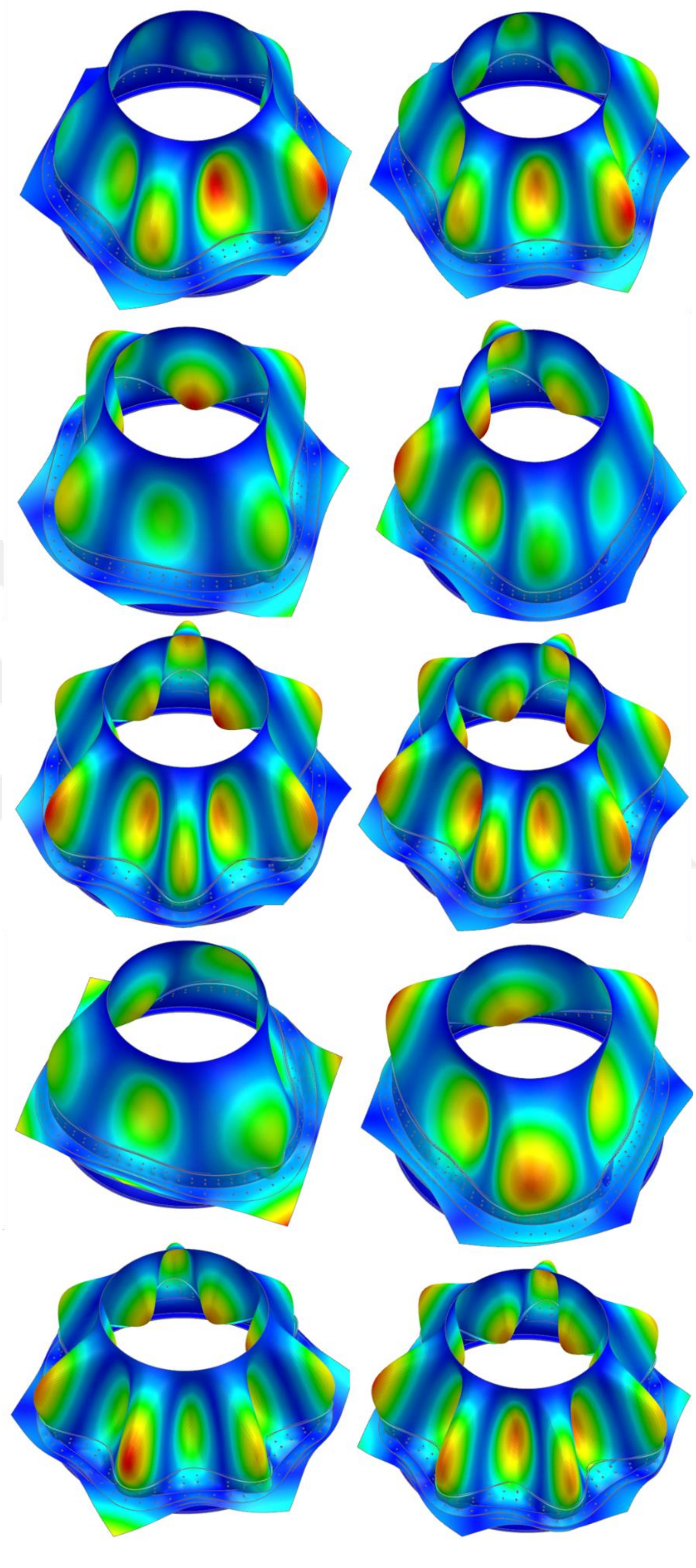

Figure 5.28 : Mode Shapes of CFRP sandwich central cone assembly

5.4.4 Modal analysis results comparison for the central cone assemblies

Forth comparison of the study is modal analysis results of the central cone assemblies. This is also the first analysis result comparison for the central cone assemblies. For all the central cone assemblies the frequency values of the first natural frequency are higher than the design requirement. That is why modal analysis results can be optimized after other structural analysis results. That is because being higher number of frequency values for first primary mode can be over design with using more weight or parts in the design. On the other hand, for comparison under same conditions, it shows that the stiffness values of the central cone assemblies. For satellites, the primary structural members of it have crucial role on the rising the stiffness value of it. The first natural frequency values of the central cone assemblies are listed at Table 5.23.

Table 5.23 : Modal analysis result comparison for central cone assemblies

Central Cone Assy.	AL monocoque	CFRP Monocoque	AL Grid	CFRP Grid	AL Sandwich	CFRP Sandwich
Mode 1 (Hz)	417.24	615.47	328.78	405.75	482.89	553.05

Same with the central cone modal analysis results, for assemblies also all design concepts have same behaviour with considering material type of them. CFRP central cones have higher stiffness values with considering their same design concepts of metallic ones. With considering all the designs, CFRP semi-monocoque central cone assembly is the stiffer assembly of the study. Which is tend to make optimizations for it most. CFRP sandwich central cone assembly is the second best after the CFRP semi-monocoque one. After that, Aluminium sandwich central cone comes with great frequency value which is far from fourth and fifth central cone assemblies. Aluminium semi-monocoque is following the aluminium sandwich central cone assembly and after that with 405.75 Hz frequency value CFRP grid central cone assembly is coming. Like weight and first modal analysis results Aluminium grid central cone has the worst result between the central cones. Grid central cones are heavier central cones between the all assemblies. It is affecting the results of the modal analysis because the geometry of the cones is almost same between each other.

5.5 Static Structural Analysis of Central Cone Assemblies

To determine the stresses and deformations on the central cone assemblies static structural analysis is performed. For define the strength of the central cone assemblies margin of safety is used. Regarding to material and design concept type margin of safety calculation can be change. For comparisons of the static structural analysis results of central cone assemblies same conditions applied on the structure.

As a reference satellite, 1000 kg LEO satellite selected for the thesis. During the loading of the central cone assemblies, same load condition applied on the structure with the same way. To force the structure, the satellite mass was loaded onto the central cone assemblies with 10g of impact. 1000 kg satellite mass with 10g equals to 100 kN downward force applied on the center of the cone top circle. From the center point of the cone top surface there is a node to connect surrounding nodes on the top edge of the central cones with using RBE2 connections. As an example, the force direction and the connection between nodes are shown at Figure 5.29 for Aluminium sandwich central cone assembly. The load case applied on the central cone assemblies with the same method as shown.

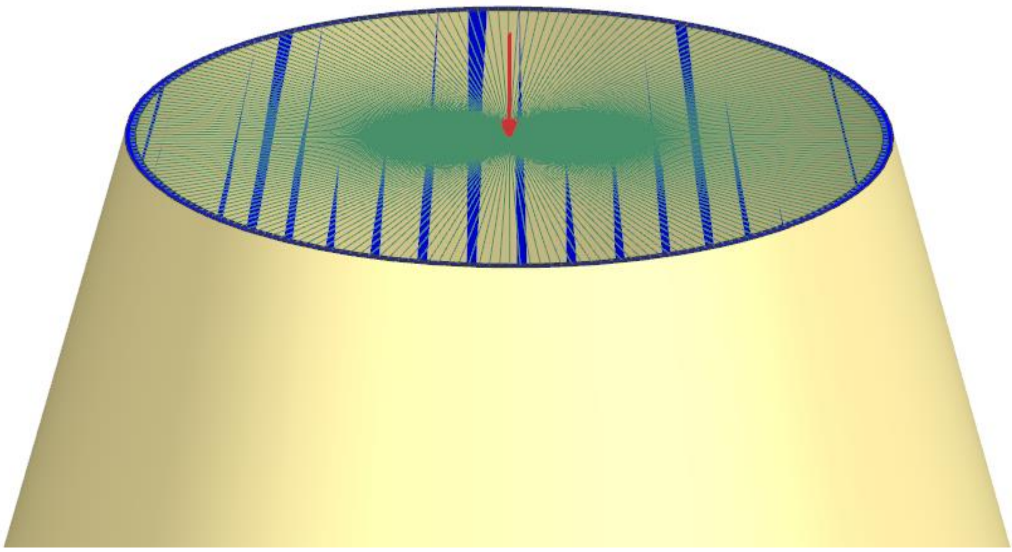

Figure 5.29 : Load container example for static structural analysis on central cone assemblies

There are different type of margin of safety calculations for different materials and design concepts. Factor of safety values are also changing with the type of the spacecraft and type of the material for ECSS. In the margin of safety calculations different FOS values are used with respect to ECSS [34]. The used FOS values are listed at Table 5.24.

Table 5.24 : Selected Factor of Safety (FOS) values at calculations [34]

Structure Type	FOSY	FOSU
Metallic Parts	1.1	1.25
Sandwich Parts (honeycomb shear)	N/A	1.25
CFRP	N/A	1.25

For metallic parts factor of safety yielding is the main safety factor in the calculations. CFRP parts of the central cone assemblies have different approach than others which is depends on the calculation of Tsai-Wu failure criteria. In the thesis, Tsai-Wu failure calculations applied with using Simcenter Nastran solver Tsai-Wu failure calculations which is estimating the failure if the results of the analysis reach the failure index 1 for each laminate of the composite. For margin of safety calculations equation (5.1) and equation (5.2) used.

$$MoS_{Metallic} = \frac{\sigma_{yield}}{FOS_{Metallic}\ x\ \sigma_{VonMises}} - 1 \tag{5.1}$$

$$MoS_{honeycomb} = \frac{1}{\sqrt{(\frac{FOS\ x\ \tau_{xz}}{FsL})^2 + (\frac{FOS\ x\ \tau_{yz}}{FsW})^2}} - 1 \tag{5.2}$$

It is important to having positive MoS values after the calculations. For metallic MoS calculation σ_{yield} is equal to material yielding stress and $\sigma_{VonMises}$ is equal to analysis result as Von-Mises stress on the structure. For honeycomb core, the MoS calculation is depends on the interlaminar shear stresses along the L and W direction of the honeycomb which are shear stresses at xz and yz planes.

5.5.1 Static structural analysis of semi-monocoque central cone assemblies

5.5.1.1 Static structural analysis of Aluminium semi-monocoque central cone

As a metallic structure, aluminium semi-monocoque central cone is used $MoS_{Metallic}$ in the calculations. The stress levels with Von-Mises and deformations on the structure has critical points of the analysis. After the load applied on the central cone the analysis is performed with aluminium semi-monocoque central cone assembly. The Von-Mises stress result and deformation on the structure are shown at Table 5.25.

Table 5.25 : Static structural analysis results of aluminium semi-monocoque central cone assy.

Central Cone Assy.	Aluminium Semi-monocoque
Von-Mises (MPa)	96.07
Deformation (mm)	0.221
$MoS_{Metallic}$	2.066

Deformation on the structure is negligible after the analysis because of the small values. AL 2024 is used for Aluminium semi-monocoque central cone. The yielding stress of the AL 2024 is 324 MPa and as a metallic part FOSY is 1.1 for MoS calculation. With applying these values on the equation (5.1) for metallic structure the result is become 2.066 which is a positive number and has a good score.

The stress distribution under the loads for aluminium semi-monocoque central cone assembly is shown at Figure 5.30 and the deformations and shape of the structure is shown at Figure 5.31.

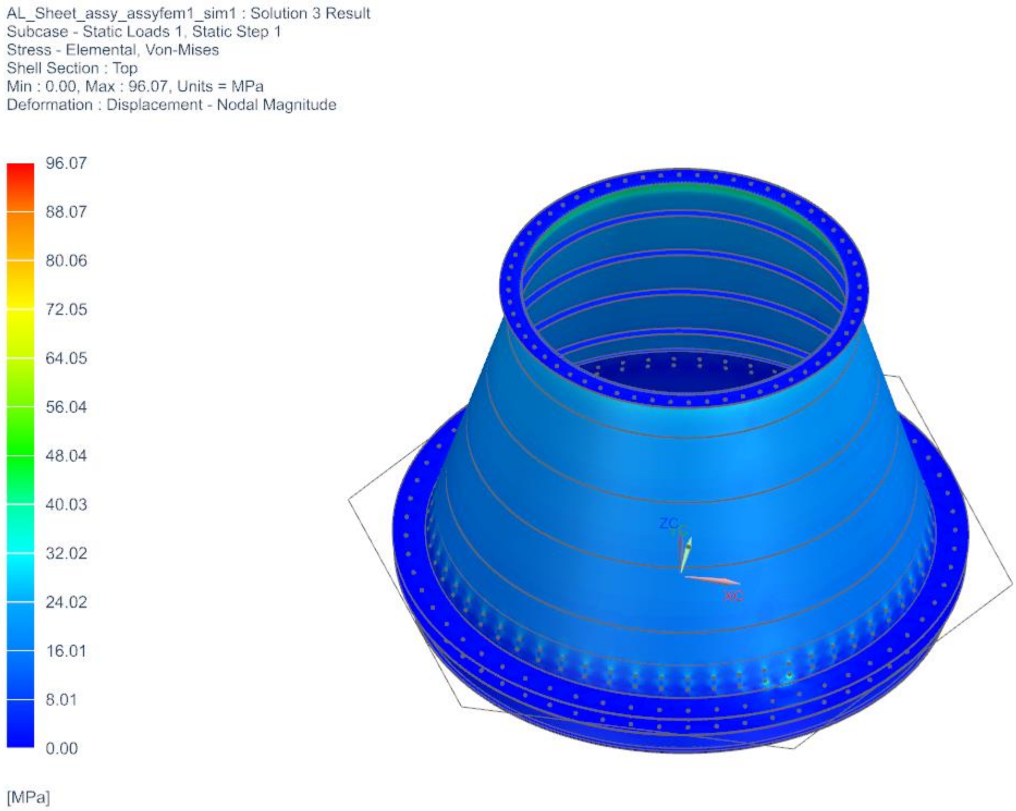

Figure 5.30 : Stress distribution of aluminium semi-monocoque central cone assy.

Stresses are concentrates on the holes of connections between central cone and other components of the assembly. Also, the load is affecting the top surface of the central cone most because it is applying on that plane as a simulation of satellite. The results are satisfying the requirements.

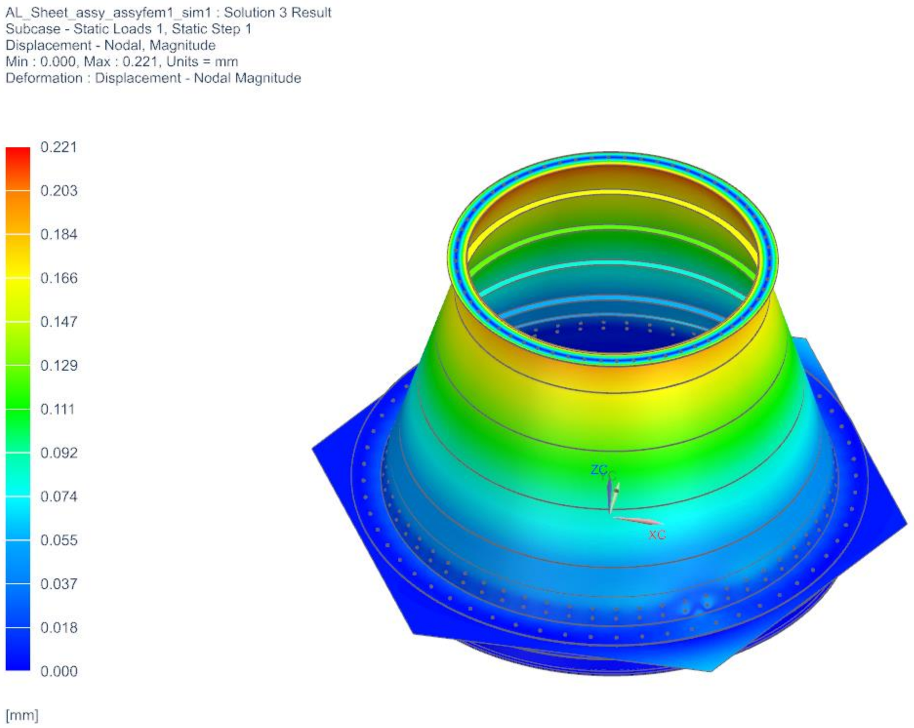

Figure 5.31 : Deformations of aluminium semi-monocoque central cone assy.

5.5.1.2 Static structural analysis of CFRP semi-monocoque central cone assembly

For CFRP semi-monocoque central cone assembly there is no margin of safety calculation because of the material is composite but Tsai-Wu failure theory used with Simcenter Nastran solver. The failure index of the results should be examined for all laminates one by one. The absolute value of the results should between 0 and 1 and it would be better to far from 1. With considering this information, the same load conditions and boundaries applied on CFRP semi-monocoque central cone assembly. Deformations on the structure and worst ply result of Tsai-Wu calculation is presented at Table 5.26.

Table 5.26 : Static structural analysis results of CFRP semi-monocoque central cone assy.

Central Cone Assy.	CFRP Semi-monocoque
Deformation (mm)	0.145
Tsai-Wu Failure Index (worst ply)	0.303
Von-Mises MPa (worst ply)	185.40

0.303 is the worst absolute Tsai-Wu failure index result for CFRP semi-monocoque central cone. It is satisfying the requirements of failure criteria. Also, deformations of the structure are minimal for all assembly. The worst ply Tsai-Wu results are shown at Figure 5.32 and deformations for central cone assembly is shown at Figure 5.33. For other plies, results are generally around the worst ply but have less value than 0.303. That worst ply is also the first ply of the composite. It is predictable to get worst results from the first ply of the composite because of the first touch to force from satellite.

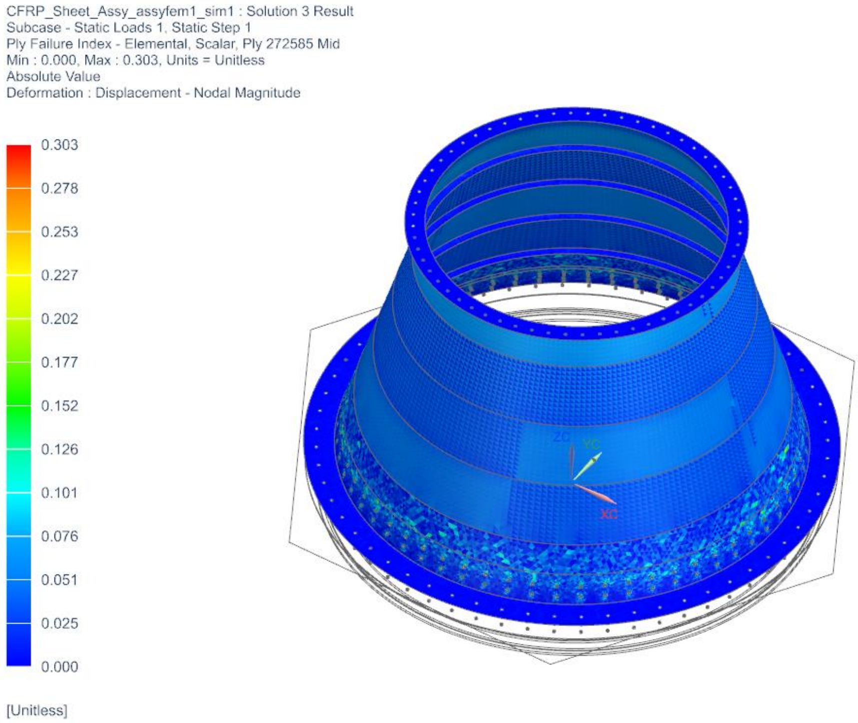

Figure 5.32 : Tsai-Wu failure index results of CFRP semi-monocoque worst ply

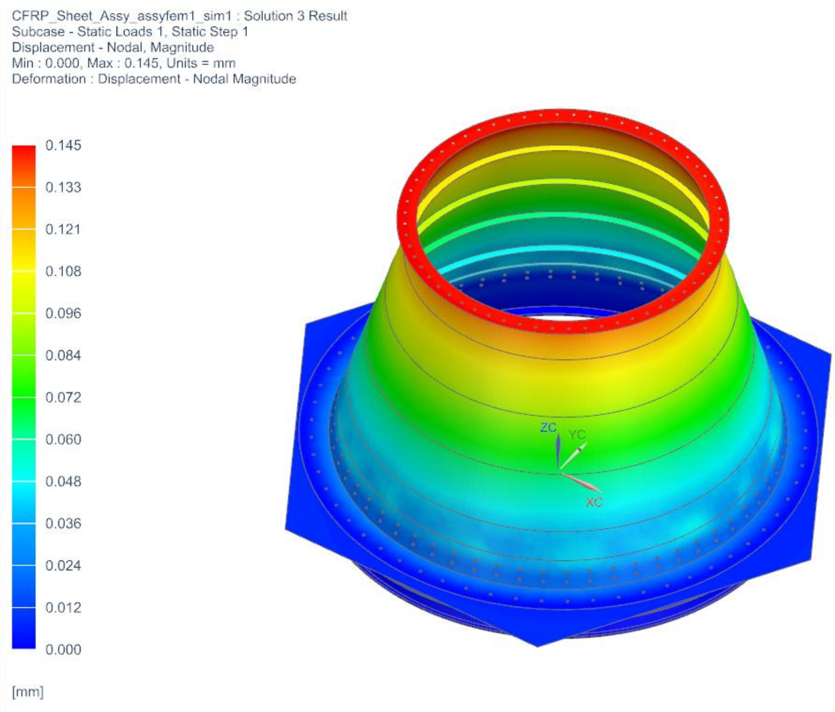

Figure 5.33 : Deformations of CFRP semi-monocoque central cone assy.

5.5.2 Static structural analysis of grid central cone assemblies

5.5.2.1 Static structural analysis of Aluminium grid central cone assembly

The analysis and margin of safety calculations for aluminium grid central cone assembly is similar to aluminium semi-monocoque central cone. They both are using the same equation as equation (5.1) to get margin of safety value. The Von-Mises stress results, deformation on the structure and $MoS_{Metallic}$ calculation results are listed at Table 5.27.

Table 5.27 : Static structural analysis results for Aluminium grid central cone assy.

Central Cone Assy.	Aluminium Grid
Von-Mises (MPa)	65.28
Deformation (mm)	0.268
$MoS_{Metallic}$	5.531

The material applied on the aluminium grid central cone is AL 7050 which has 469 MPa tensile yield stress value. The yielding properties of the AL 7050 is much better than AL 2024, that is why the $MoS_{Metallic}$ results of the Aluminium grid central cone is better than semi-monocoque one. Also, the Von-Mises stresses of the grid central cone is lower than the semi-monocoque one which makes grid cone more safety. The Von-Mises stress distribution on the central cone and deformation of the system is shown at Figure 5.34 and Figure 5.35.

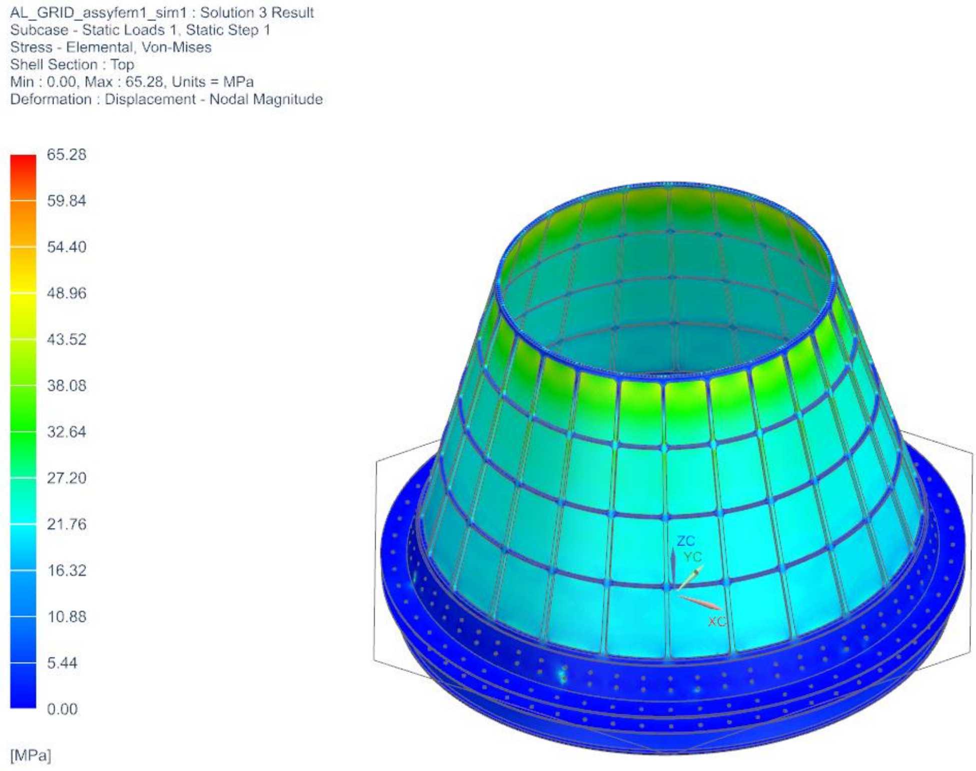

Figure 5.34 : Von-Mises stress distribution on Aluminium grid central cone

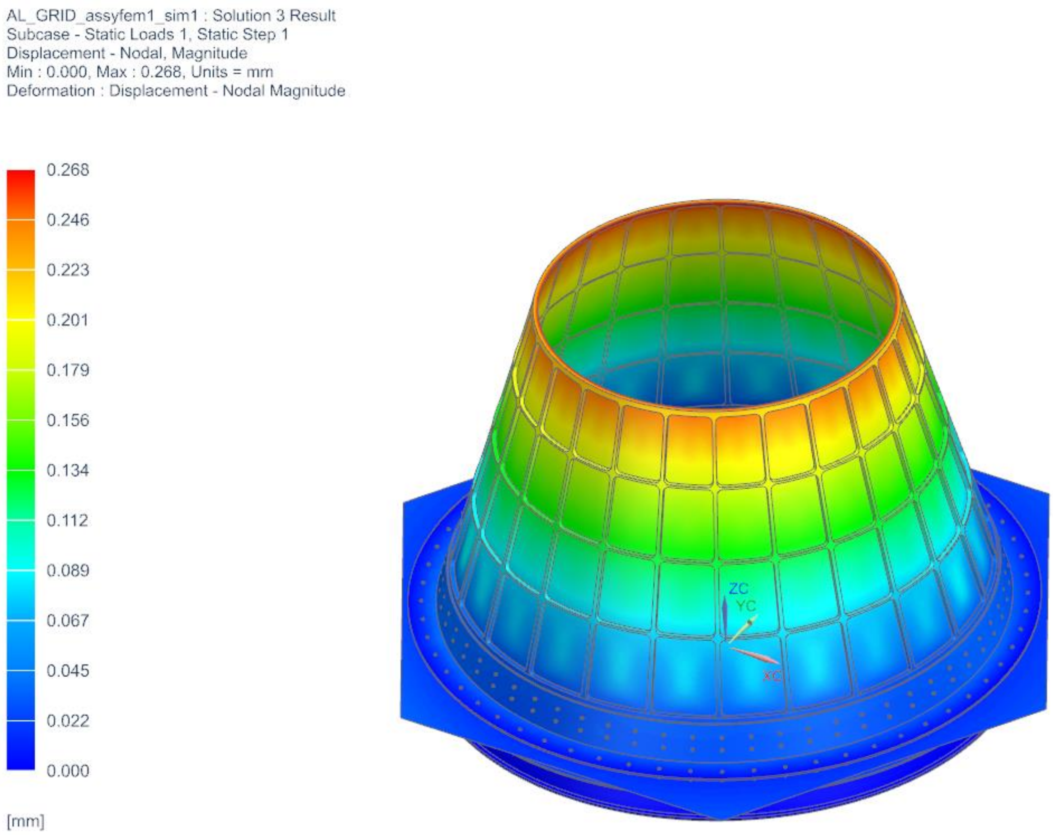

Figure 5.35 : Deformation of Aluminium grid central cone assy.

Connection points of the grids have stress concentration on the aluminium grid central cone but same with semi-monocoque central cone the most stress concentrated locations are hole circumference and top surface of the central cone as expected. Deformation results are also similar with semi-monocoque central cone assemblies which can be negligible.

5.5.2.2 Static structural analysis of CFRP grid central cone assembly

As a composite structure, CFRP grid central cone assembly is also using Tsai-Wu failure criteria to predict the possible failure on the structure under defined load case similar with CFRP semi-monocoque central cone. At Table 5.28, the static structural analysis results of the system are shown as worst ply stress level, worst ply Tsai-Wu score and deformation of the assembly.

Table 5.28 : Static structural analysis results of CFRP grid central cone assy.

Central Cone Assy.	CFRP Grid
Deformation (mm)	0.367
Tsai-Wu Failure Index (worst ply)	0.661
Von-Mises MPa (worst ply)	162.50

The forced part of the structure is the grids around the shell of central cone. Even the results of the analysis are satisfying the requirements, they are quite worse than previous central cone assemblies with having highest value of deformation and Tsai-Wu Failure Index score. It is still smaller than 1 which makes strength of the CFRP grid central cone is enough for 1000kg LEO satellite. The worst ply Tsai-Wu results are shown at Figure 5.36.

The behaviour of the assembly under the 100 kN force which is a simulation of the 1000 kg LEO satellite with 10g is shown at Figure 5.37. The deformation values are small enough to neglect.

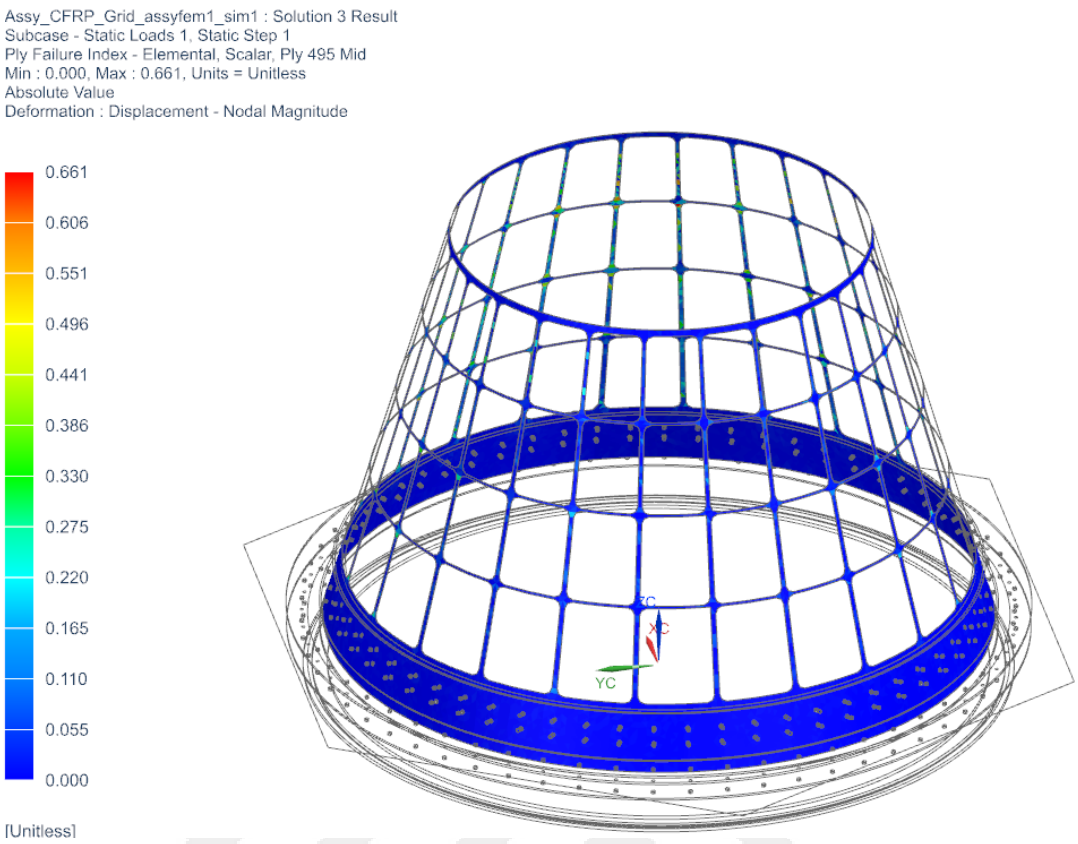

Figure 5.36 : Tsai-Wu failure index results of CFRP grid cone worst ply

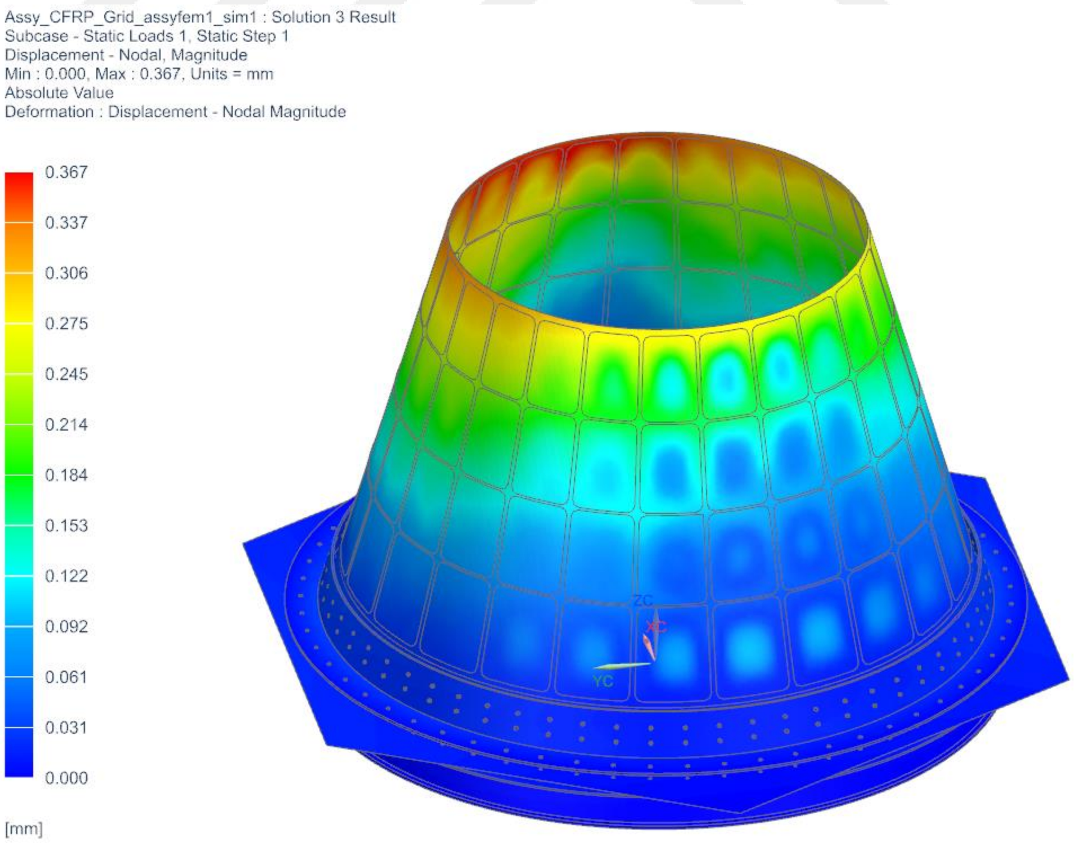

Figure 5.37 : Deformations of CFRP grid central cone assy.

5.5.3 Static structural analysis of sandwich central cone assemblies

There are some differences for sandwich central cone assemblies to determine the strength of the structure. The reason of it there are different kind of structural parts at sandwich structure which are skins and core of the structure. For metallic sandwich central cone, simple $MoS_{Metallic}$ calculation applied for skins and $MoS_{Honeycomb}$ calculation done for core of sandwich. For CFRP sandwich cone, Tsai-Wu failure criteria used for skins of sandwich and same with metallic sandwich cone, $MoS_{Honeycomb}$ is used for core of sandwich central cone.

5.5.3.1 Static structural analysis of Aluminium sandwich central cone assmebly

For aluminium skins of the sandwich central cone as applied for other metallic central cones equation (5.1) is used to calculate margin of safety values of them. For sandwich core structure which is honeycomb, there are different kind of calculation for margin of safety which is equation (5.2). With using interlaminar shear stresses of the honeycomb the margin of safety value is determined. Equation (5.1) is applied the worst stress resulted skin of the sandwich structure and equation (5.2) is applied for core structure directly. For metallic skins of the aluminium sandwich central cone Von-Mises stress values, $MoS_{Metallic}$ calculation results, deformation of the system, shear stresses of the honeycomb and $MoS_{Honeycomb}$ calculation results are listed at Table 5.29.

Table 5.29 : Static structural analysis results of Aluminium sandwich central cone assy.

Central Cone Assy.	Aluminium Sandwich
Von-Mises (MPa) (worst skin)	208.09
Deformation (mm)	0.532
$MoS_{Metallic}$ (worst skin)	0.415
τ_{xz} (MPa) (honeycomb)	2.77
τ_{yz} (MPa) (honeycomb)	1.69
$MoS_{Honeycomb}$	0.311

Material of the skins of sandwich central cone is AL 2024 which has yielding stress of 324 MPa. All the MoS results are positive that is why there is no problem for the design but it is on the limits of the design requirements for skin strength. The core of the sandwich is AL 5056 with density of 8.1 which has 6.52 MPa for FsL and 3.86 MPa for FsW. Deformation results are the worst results for now between other 4 central cone design which are metallic and CFRP semi-monocoque and grid central cone assemblies. Stress distribution of the worst skin is shown at Figure 5.38.

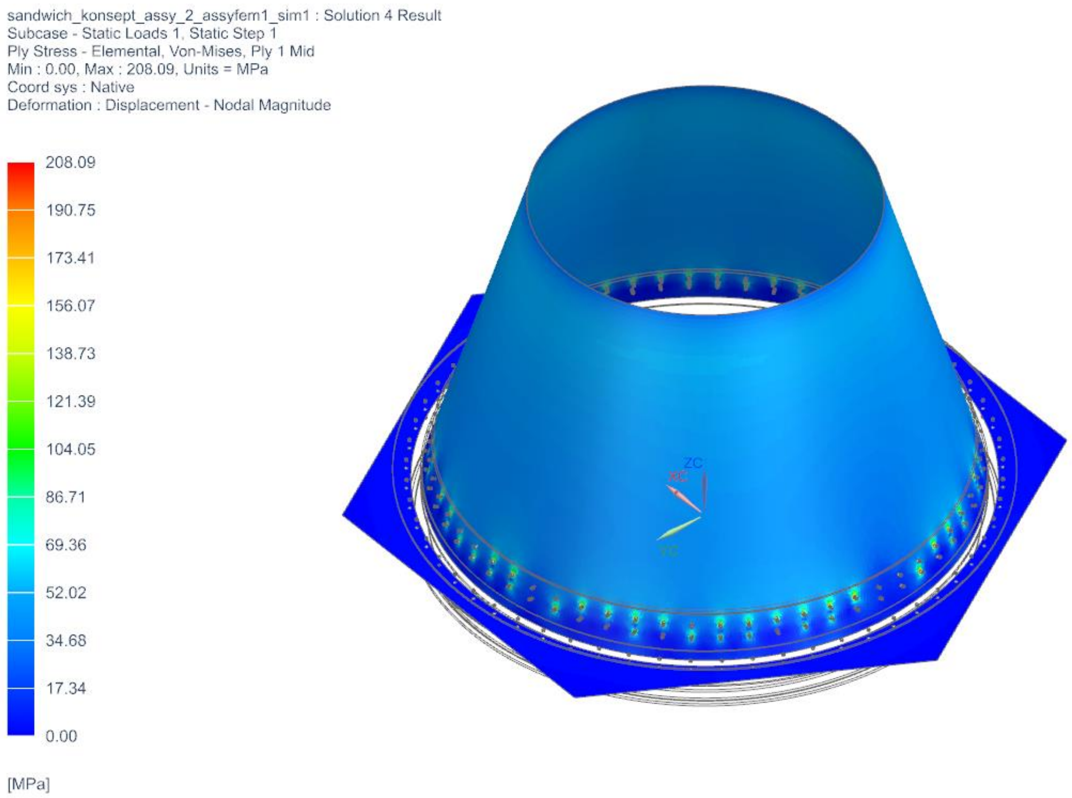

Figure 5.38 : Von-Mises stress distribution on Aluminium sandwich central cone

Interlaminar shear stress distributions for xz and yz directions are shown at Figure 5.39 and Figure 5.40 respectively.

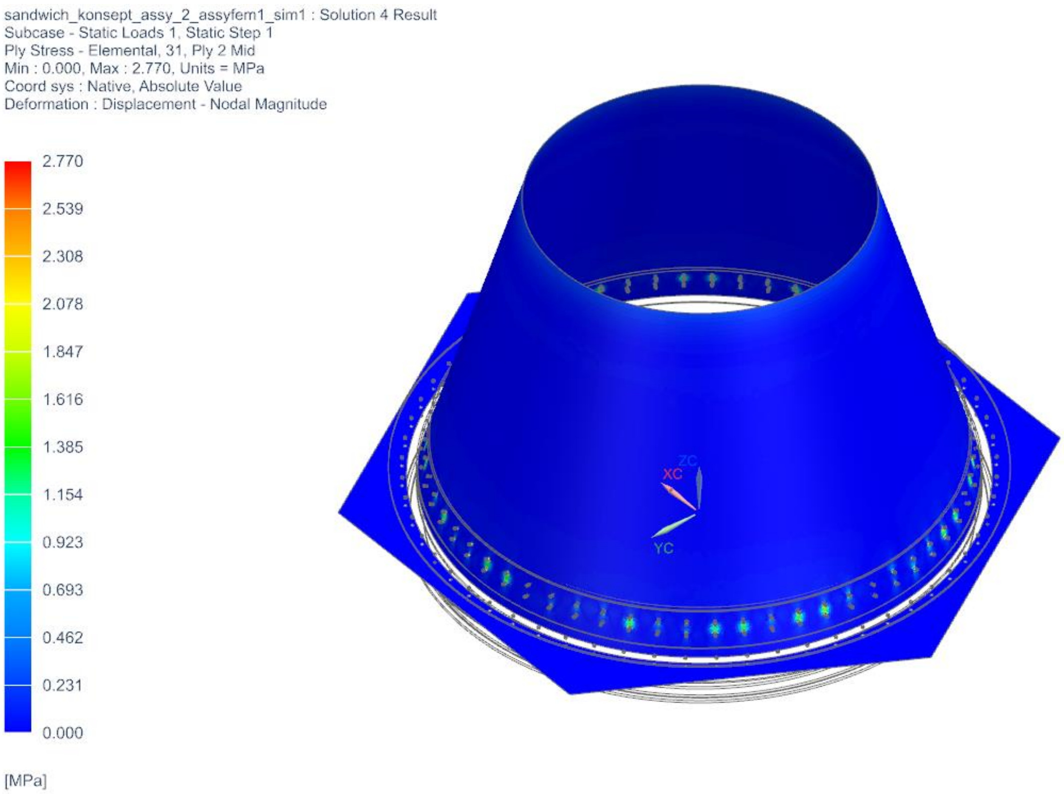

Figure 5.39 : Interlaminar shear stress results of Aluminium sandwich central cone with direction of τ_{xz}

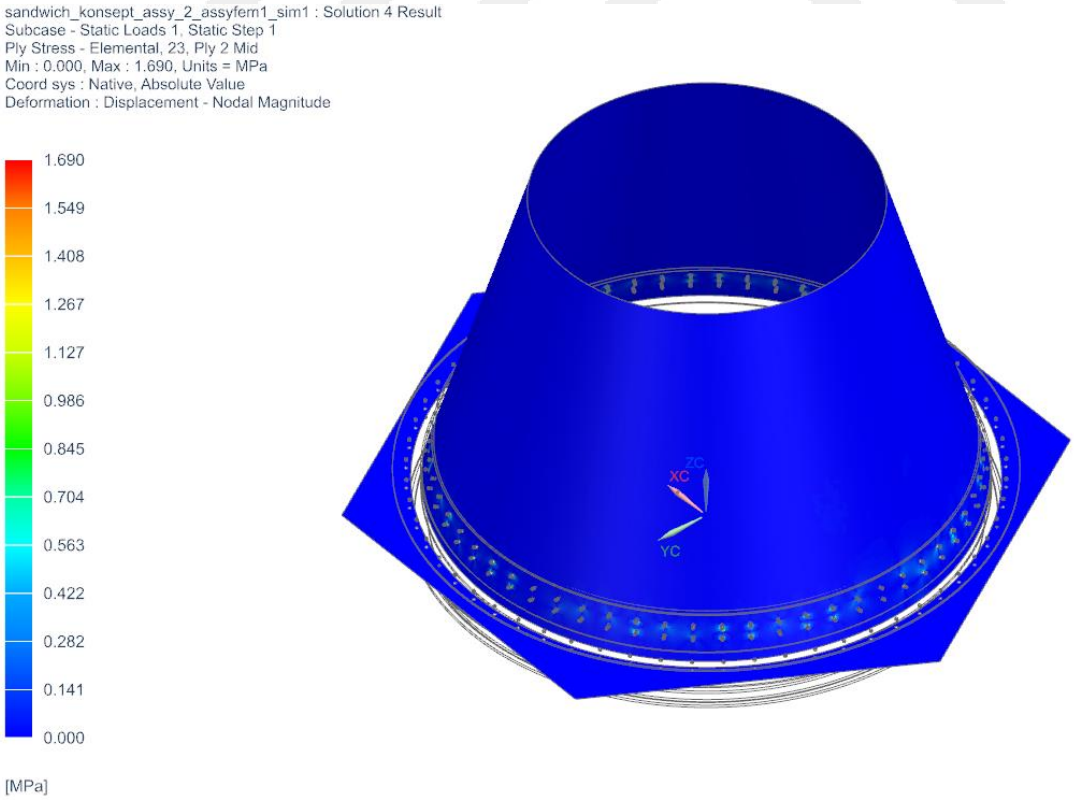

Figure 5.40 : Interlaminar shear stress results of Aluminium sandwich central cone wit direction of τ_{yz}

The behaviour of the assembly under the 100 kN force which is a simulation of the 1000 kg LEO satellite with 10g is shown at Figure 5.41.

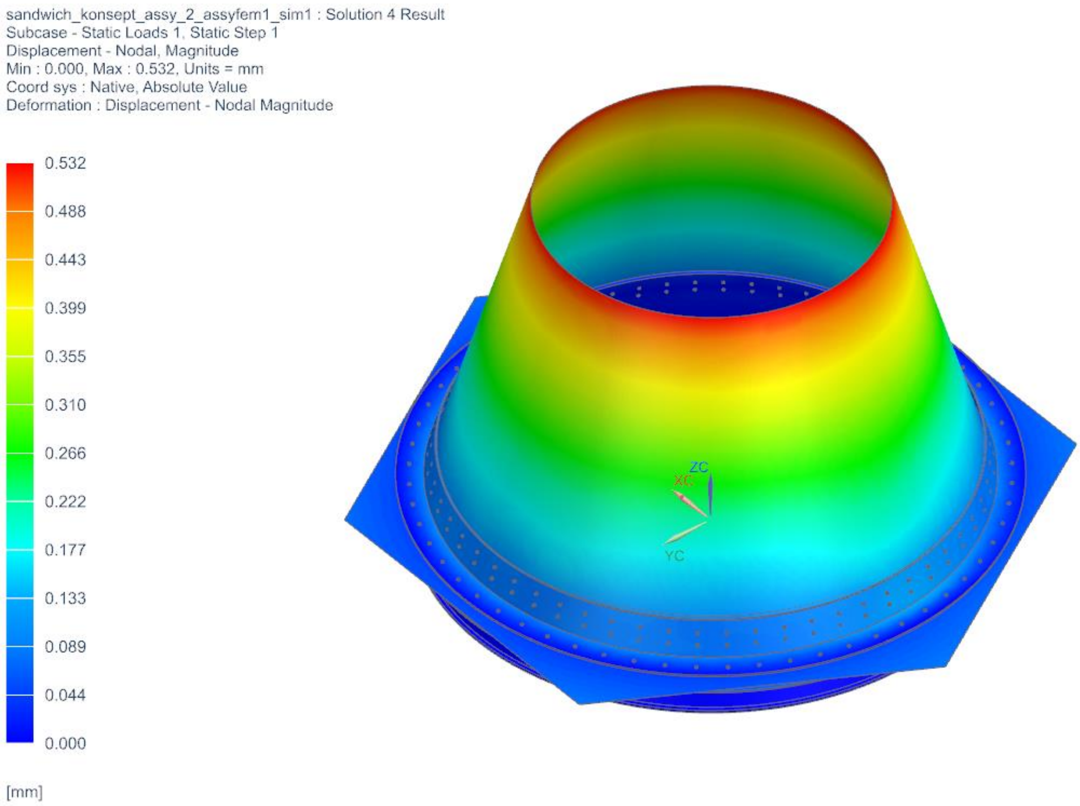

Figure 5.41 : Deformations of Aluminium sandwich central cone assy.

5.5.3.2 Static structural analysis of CFRP sandwich central cone assembly

For CFRP skins of the sandwich central cone, Tsai-Wu failure criteria applied and worst ply of the composite selected. Same procedure done for core of sandwich structure with aluminium sandwich central cone core interlaminar shear stress margin of safety calculations. For CFRP skins of the CFRP sandwich central cone Tsai-Wu failure index results for worst ply, deformation of the system, shear stresses of the honeycomb and $MoS_{Honeycomb}$ calculation results are listed at Table 5.30.

Table 5.30 : Static structural analysis results of CFRP sandwich central cone assy.

Central Cone Assy.	Aluminium Sandwich
Deformation (mm)	0.154
Tsai-Wu Failure Index (worst ply)	0.407
τ_{xz} (MPa) (honeycomb)	1.896
τ_{yz} (MPa) (honeycomb)	1.353
$MoS_{Honeycomb}$	0.266

AL 5056 with density of 6.1 is used for CFRP sandwich's core which has 4.76 MPa for FsL and 2.76 MPa for FsW. The strength values of the material are lower than AL 5056 (8.1) which is used for aluminium sandwich central cone but with lower density the weight advantage is came to CFRP sandwich central cone. Also, all the margin of safety and Tsai-Wu results are satisfying the design requirements. The worst ply Tsai-Wu results are shown at Figure 5.42.

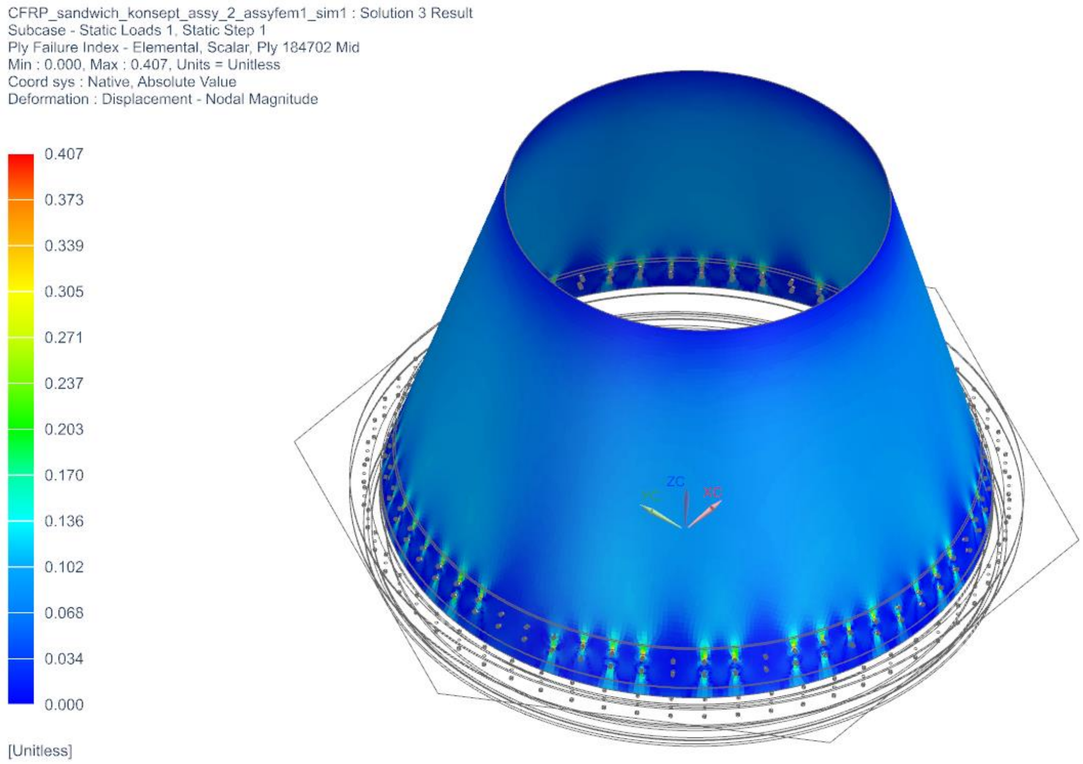

Figure 5.42 : Tsai-Wu failure index results of CFRP sandwich cone worst ply

Interlaminar shear stress distributions for xz and yz directions are shown at Figure 5.43 and Figure 5.44 respectively.

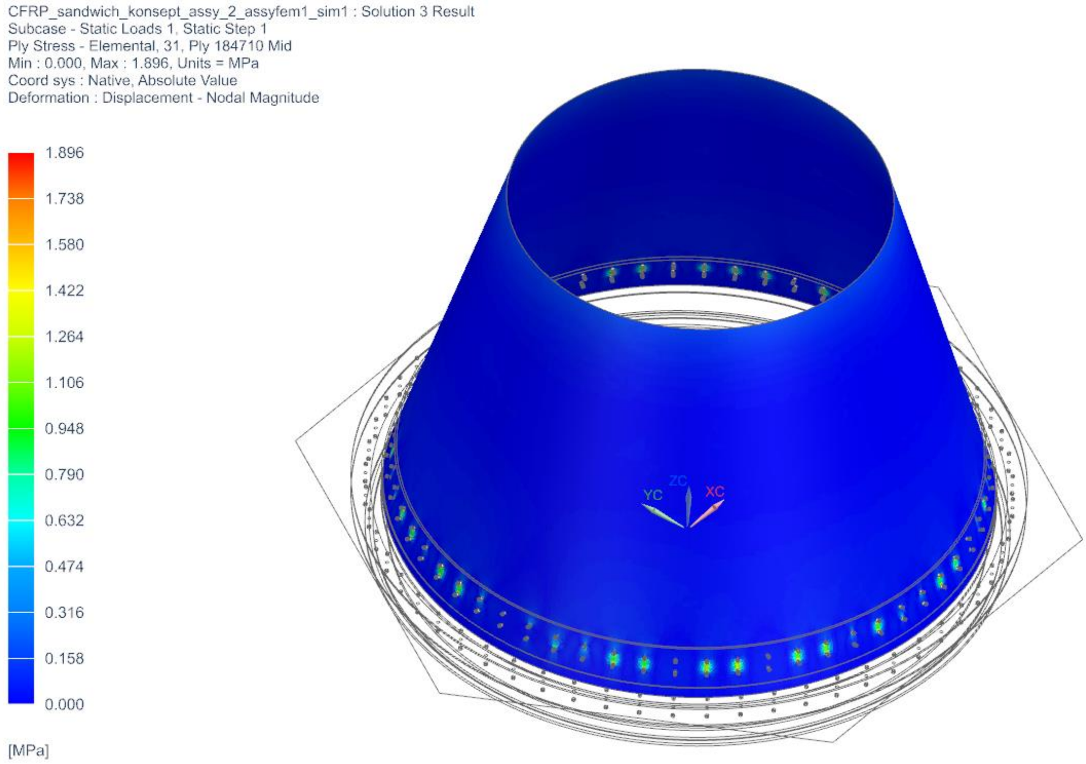

Figure 5.43 : Interlaminar shear stress results of CFRP sandwich central cone with direction of τ_{xz}

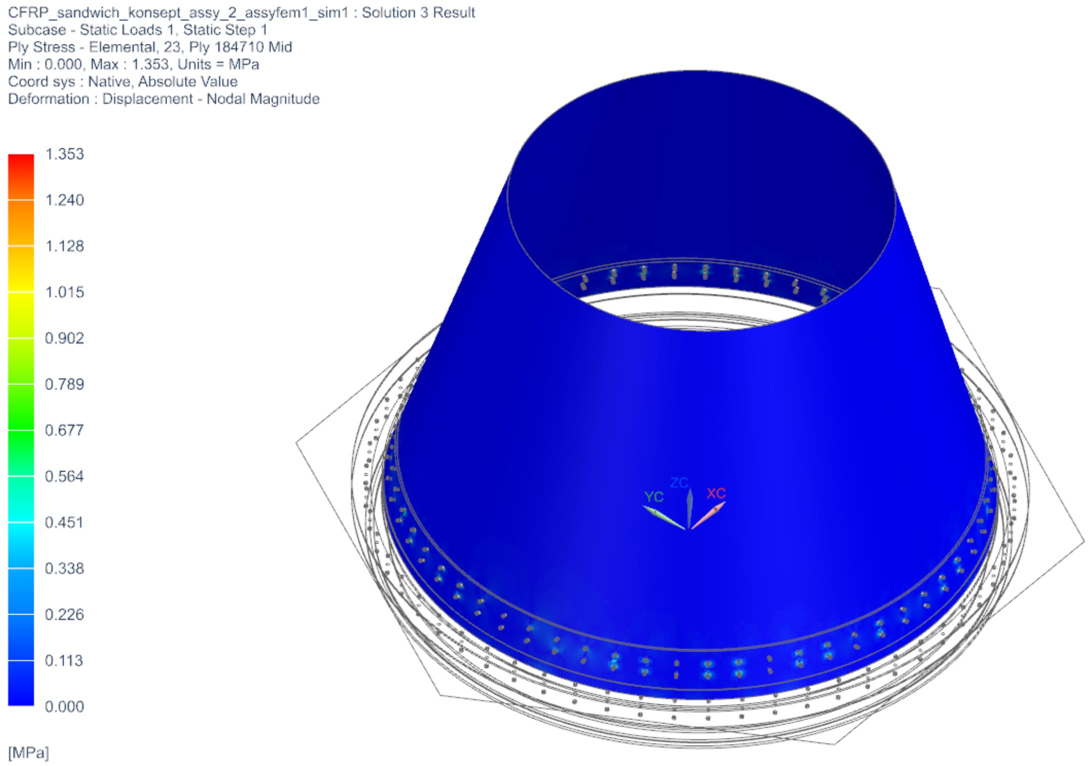

Figure 5.44 : Interlaminar shear stress results of CFRP sandwich central cone with direction of τ_{yz}

Deformation of the CFRP sandwich central cone assembly under the defined load case which is same with other central cone assemblies is shown at Figure 5.45. Because of the low number of displacements, the deformation effect can be negligible for thesis.

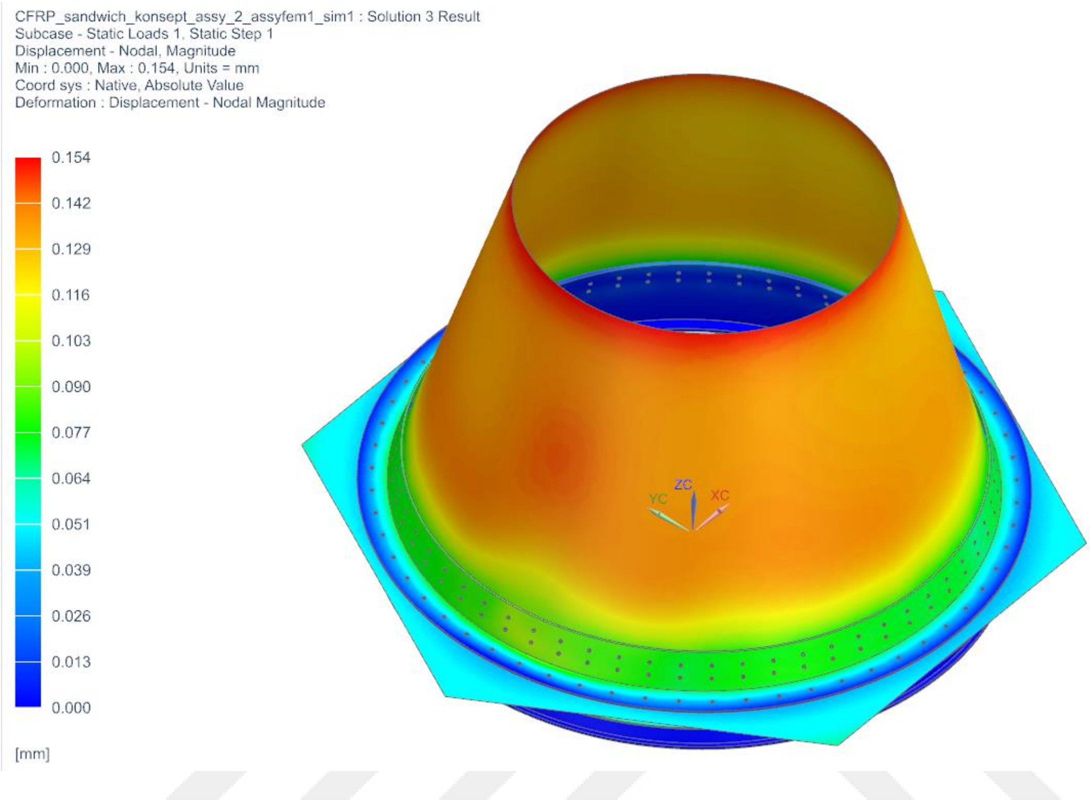

Figure 5.45 : Deformations of CFRP sandwich central cone assy.

5.5.4 Comparison of static structural analysis results of central cone assemblies

It is hard to compare the results of the static structural analysis because of having different type of approach to examine the design concepts of central cones. Margin of safety calculation approaches of central cones are changing with material and design type of the structure. The comparison of central cones with same material depends on the $MoS_{Metallic}$ calculation results, Tsai-Wu failure index score or $MoS_{Honeycomb}$ calculation results. On the other hand, the results of the margin of safety calculations can be compared as general without considering the material of the structure. Same with the margin of safety calculations Tsai-Wu results of the CFRP central cones can be compared between each other to get trade-off study. Deformations of the central cone assemblies are small enough to neglect as comparison or failure that is why in the comparison of the static structural analysis only the margin of safety calculations taken into account.

The comparison of the central cone assemblies is shown at Table 5.31.

Table 5.31 : Comparison of static structural analysis results

Central Cone Assy.	AL Monocoque	CFRP Monocoque	AL Grid	CFRP Grid	AL Sandwich	CFRP Sandwich
$MoS_{Metallic}$	2.066	-	5.531	-	0.415	-
$MoS_{Honeycomb}$	-	-	-	-	0.311	0.266
Tsai-Wu	-	0.303	-	0.661	-	0.407

From the results of the static structural analysis results, Aluminium grid central cone has the highest number of margin of safety result between all the central cone assemblies. From the metallic central cones worst results of $MoS_{Metallic}$ came with Aluminium sandwich central cone skins. The interlaminar shear stress of the honeycomb sandwich central cones are almost similar between aluminium sandwich central cone and CFRP sandwich central cone but aluminium one has better result. From the CFRP central cones, semi-monocoque central cone is the best with being far from 1 by considering the Tsai-Wu failure index. All the central cone designs are satisfying the design requirements of the thesis.

5.6 Buckling Analysis of Central Cone Assemblies

In the buckling analysis of the central cone assemblies, the critical buckling load factor (λ) is the main criteria for the comparation of the structures. Design limit loads of the structures are defined with applying a load case on the central cone assemblies. The load case for buckling analysis is same with static structural analysis. The reference satellite is 1000kg LEO satellite and 10g applied to this mass. The buckling strength of the central cones used for sorting.

Factor of safety for buckling analysis is selected from ECSS [34] as 2 which is FOSU for satellite parts local buckling safety factor. Material or design concepts of the central cones are not a factor to calculate margin of safety for buckling analysis. For all central cone assemblies' same margin of safety calculation applied which is shown at equation (5.3).

$$MoS_{Buckling} = \frac{\lambda}{FOS} - 1 \tag{5.3}$$

5.6.1 Buckling analysis of semi-monocoque central cone assemblies

5.6.1.1 Buckling analysis of Aluminium semi-monocoque central cone assembly

Defined load which is 100kN downward force applied on the aluminium semi-monocoque central cone assembly to find the critical load factor of the central cone. With using Simcenter Nastran SOL 105 Linear Buckling solver, the critical load factor is found. Critical load factor is the design limit load divided by defined load. That is why it is important to find how much load we can apply to buckle the structure. Linear buckling analysis results of the aluminium semi-monocoque central cone is listed at Table 5.32.

Table 5.32 : Buckling analysis results of Aluminium semi-monocoque central cone assy.

Central Cone Assy.	Aluminium Semi-monocoque
Buckling Mode (λ)	9.95
$MoS_{Buckling}$	3.975

The results are satisfying the design requirement. That is because 9.95 times defined load which is 10g with 1000kg satellite can make the central cone fail. Being on the positive side of the margin of safety is enough. The buckling mode shape of the structure is shown at Figure 5.46.

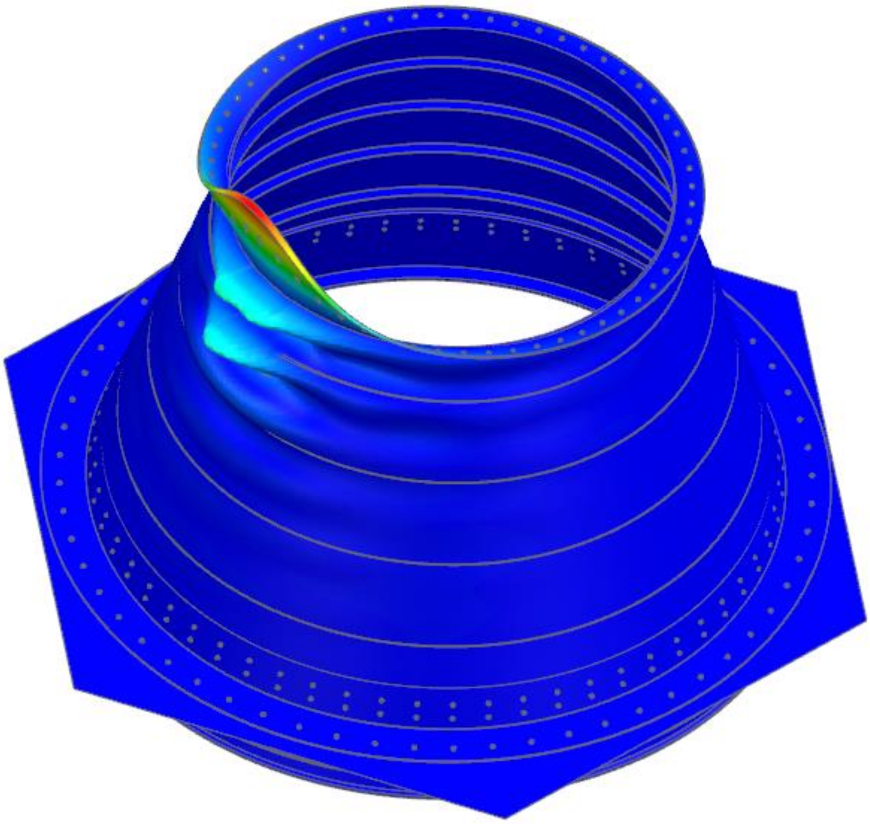

Figure 5.46 : Buckling mode shape of aluminium semi-monocoque central cone assy.

Top surface of the central cone is deforming under the defined load times 9.95 for aluminium semi-monocoque central cone. The optimization of the top surface of the central cone can help to increase the critical buckling load of structure.

5.6.1.2 Buckling analysis of CFRP semi-monocoque central cone assembly

Same analysis performed for CFRP semi-monocoque central cone assembly too. The results of the buckling analysis are listed at Table 5.33.

Table 5.33 : Buckling analysis results of CFRP semi-monocoque central cone assy.

Central Cone Assy.	CFRP Semi-monocoque
Buckling Mode (λ)	13.01
$MoS_{Buckling}$	5.505

Results of the CFRP semi-monocoque central cone is better than aluminium one regarding to critical load factor. The mode shape of the CFRP semi-monocoque central cone is shown at Figure 5.47. Results are satisfying the design requirements because of positive margin of safety.

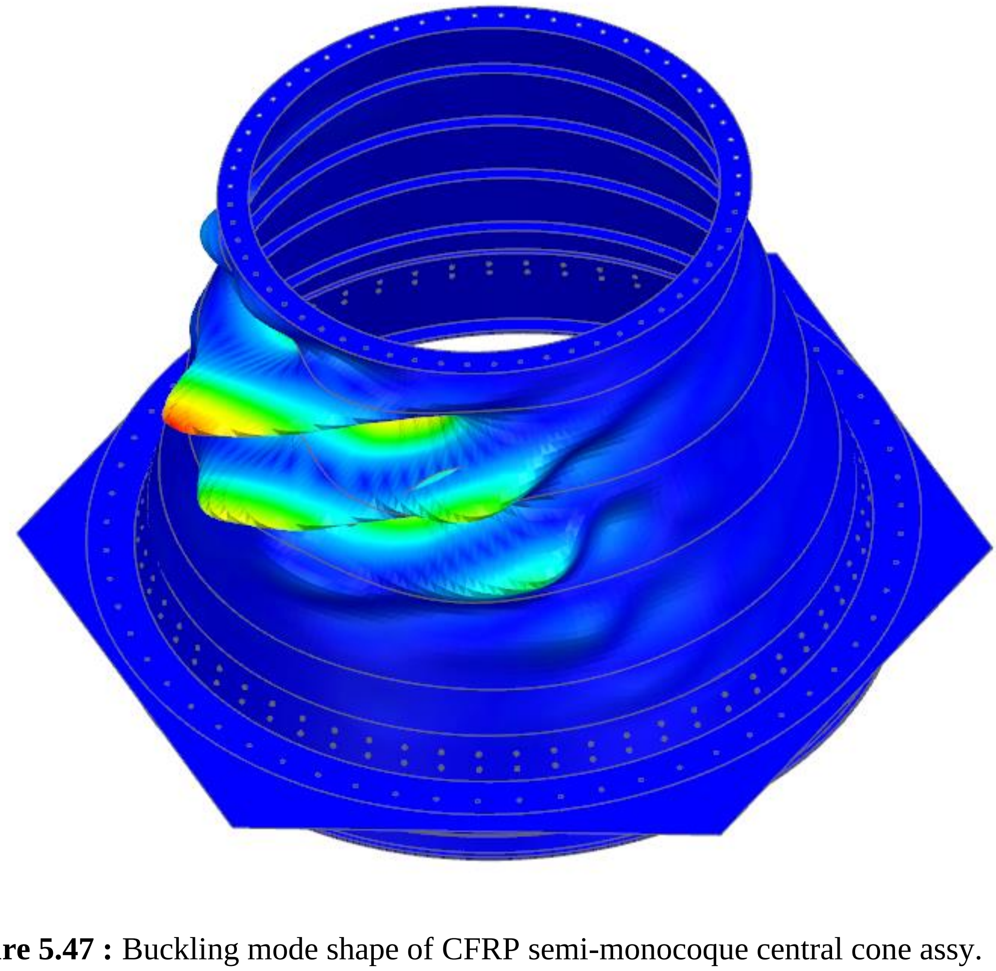

Figure 5.47 : Buckling mode shape of CFRP semi-monocoque central cone assy.

The shells without ribs are having the modes on 13.01 times defined load for CFRP semi-monocoque central cone.

5.6.2 Buckling analysis of grid central cone assemblies

5.6.2.1 Buckling analysis of aluminium grid central cone assembly

Aluminium grid central cone has great $MoS_{Metallic}$ for static structural analysis, but bucking analysis is totally different than static analysis. Geometry of the structure is also affecting the results of the buckling analysis. The results are listed at Table 5.34.

Table 5.34 : Buckling analysis results of Aluminium grid central cone assy.

Central Cone Assy.	Aluminium Grid
Buckling Mode (λ)	5.12
$MoS_{Buckling}$	1.56

Semi-monocoque central cone assemblies have better buckling strength than aluminium grid central cone. The result of the analysis is positive that is why it is not a problem for grid cone but, still critical limit load of the aluminium grid central cone is only 5.12 times defined load. The mode shape of the aluminium grid central cone assembly under 100 kN is shown at Figure 5.48.

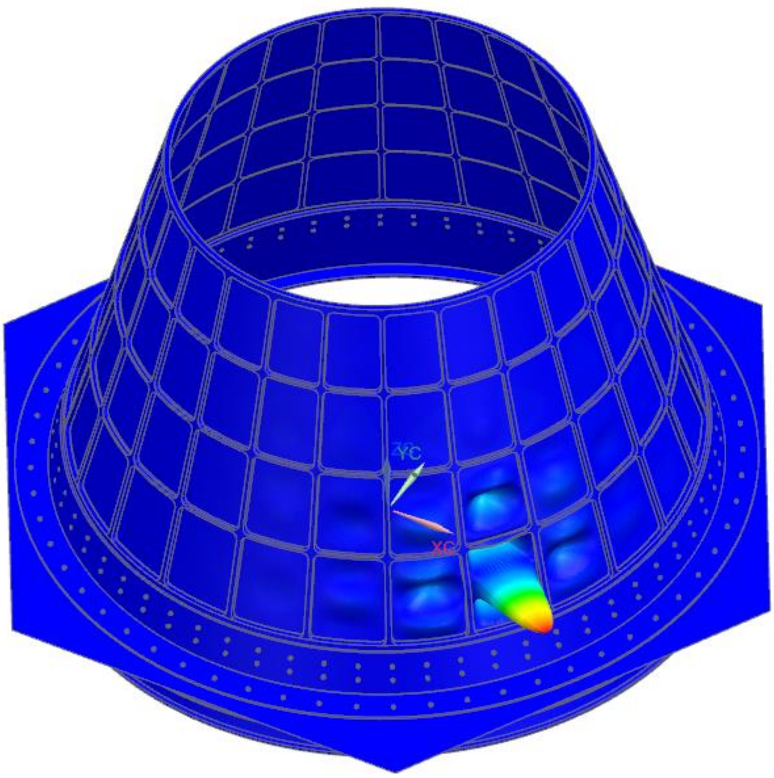

Figure 5.48 : Buckling mode shape of aluminium grid central cone assy.

The shell behind the grids has modes on 5.12 times defined load of the thesis. Increasing the thickness of the shell can rise the buckling mode which is critical load factor of the aluminium grid central cone. Thickness optimization can make the results better for this central cone.

5.6.2.2 Buckling analysis of CFRP grid central cone assembly

From static structural analysis, CFRP grid central cone has the worst result between all the design concepts of central cones. Same with the aluminium grid central cone, the buckling analysis results are expected to be low for CFRP grid cone too. The results of the analysis is shown at Table 5.35.

Table 5.35 : Buckling analysis results of CFRP central cone assy.

Central Cone Assy.	CFRP Grid
Buckling Mode (λ)	2.78
$MoS_{Buckling}$	0.39

Despite having the positive margin of safety, results of the CFRP grid central cone are close to 0 which is not preferred. Only the 2.78 times defined load can buckle the structure. The lamination of the CFRP or thickness of the shells can be optimized for having more buckling strength. The mode shape of the buckling results is shown at Figure 5.49.

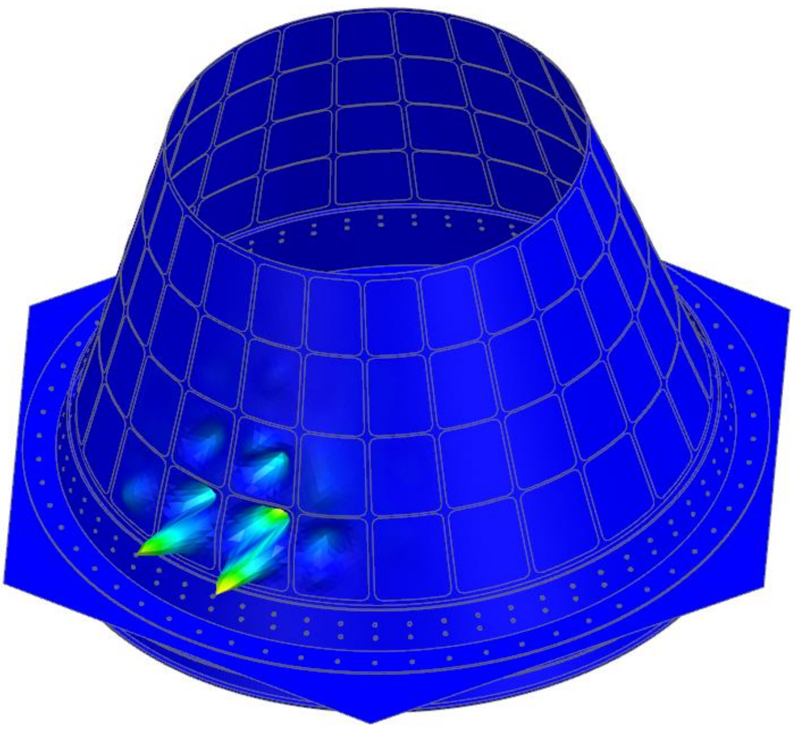

Figure 5.49 : Buckling mode shape of CFRP central cone assy.

5.6.3 Buckling analysis of sandwich central cone assemblies

5.6.3.1 Buckling analysis of Aluminium sandwich central cone assembly

One of the best advantages of the sandwich structures are having great number of buckling strengths. That is why it is expected to see best buckling analysis results for sandwich central cones. Same load conditions applied to aluminium sandwich central cone assembly and results are listed at Table 5.36.

Table 5.36 : Buckling analysis results of Aluminium sandwich central cone assy.

Central Cone Assy.	Aluminium Sandwich
Buckling Mode (λ)	32.62
$MoS_{Buckling}$	15.31

As expected, aluminium sandwich central cone has great results under the load conditions for buckling analysis. 32.62 times defined load can fail the structure which is almost perfect for assembly. Mode shape of the buckling analysis results is shown at Figure 5.50. The deformation on the central cone is homogeneously spread throughout the central cone.

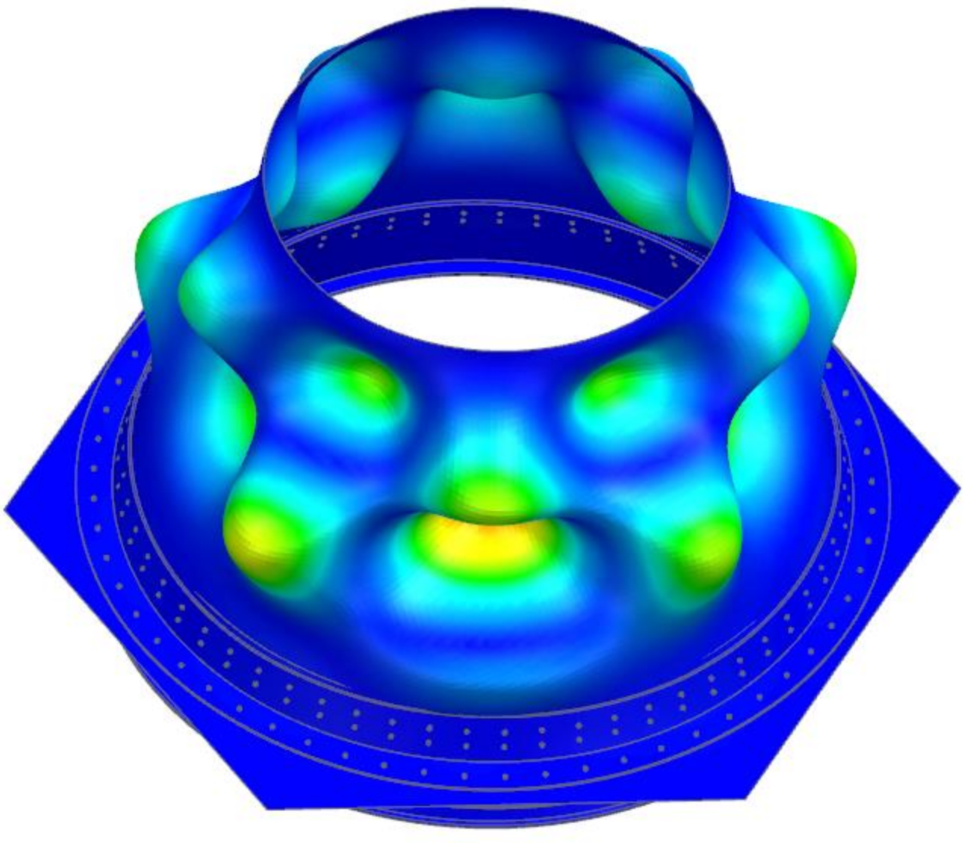

Figure 5.50 : Buckling mode shape of Aluminium sandwich central cone assy.

5.6.3.2 Buckling analysis of CFRP sandwich central cone assembly

Static structural analysis results of sandwich central cones were parallel to each other. The buckling analysis results of the CFRP central cone assembly is shown at Table 5.37.

Table 5.37 : Buckling analysis results of CFRP sandwich central cone assy.

Central Cone Assy.	CFRP Sandwich
Buckling Mode (λ)	45.39
$MoS_{Buckling}$	21.695

CFRP Sandwich central cone assembly is the best central cone assembly regarding to buckling analysis. 45.39 times defined load can buckle the structure. The mode shape and deformations are shown at Figure 5.51.

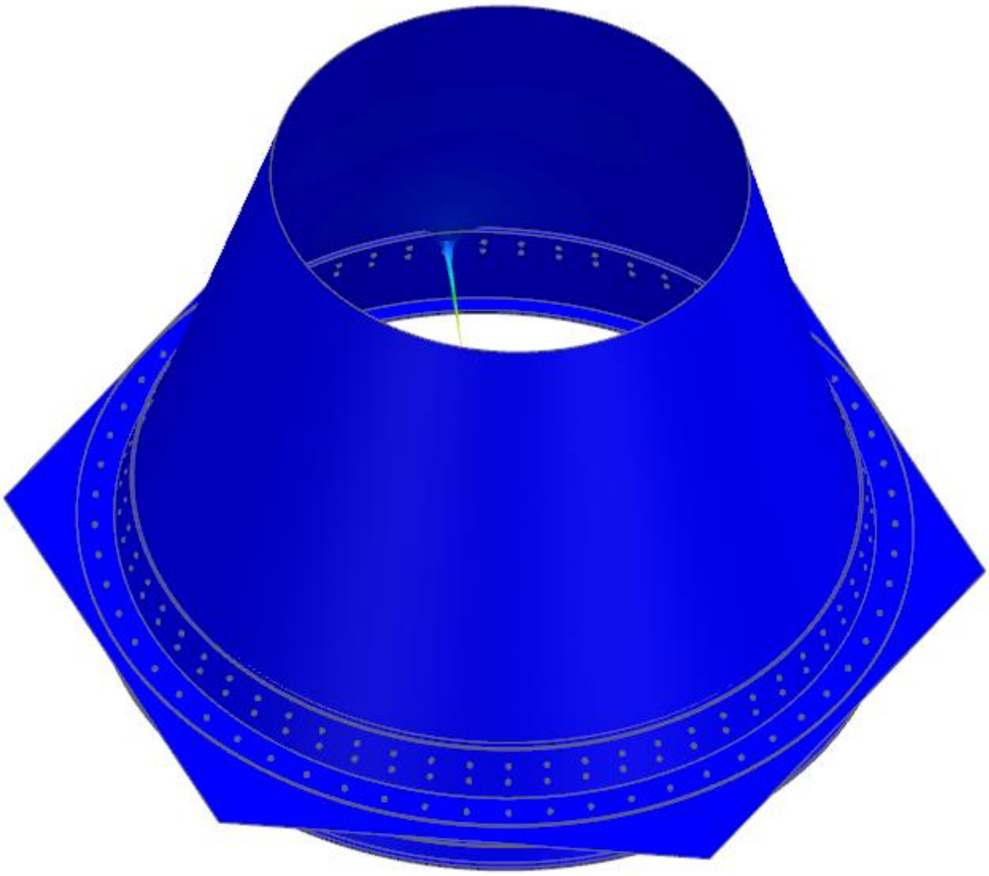

Figure 5.51 : Buckling mode shape of CFRP sandwich central cone assy.

The deformation is local buckling which is located on the central cone and LVA connection. On the surface of the sandwich cone there is no deflection which means that is not a global buckling for that λ.

5.6.4 Comparison of buckling analysis results of central cone assemblies

The results of the margin of safety buckling are directly the comparison object for this section. Having large number of $MoS_{Buckling}$ makes the structure safer. The comparison of the central cone assemblies is listed at Table 5.38.

Table 5.38 : Comparison of buckling analysis results of central cone assemblies

Central Cone Assy.	AL monocoque	CFRP Monocoque	AL Grid	CFRP Grid	AL Sandwich	CFRP Sandwich
$MoS_{Buckling}$	3.395	5.505	1.56	0.39	15.31	21.695

From the results of buckling analysis, sandwich design concept is the optimum design concept for buckling as expected. CFRP sandwich central cone has the highest $MoS_{Buckling}$ value among other central cones. Aluminium sandwich central cone is following the CFRP sandwich central cone. Semi-monocoque central cone assemblies are the second-best central cone design concept for buckling strength, but same with sandwich cones CFRP semi-monocoque central cone is more suitable than Aluminium semi-monocoque central cone for buckling. Worst results came to grid central cones and the last central cone of the thesis for buckling analysis is CFRP grid central cone. At the end of the all the buckling analysis, it shows that all the central cone assembly designs are satisfying the design requirement under the defined load which is 100 kN downward force on the top of the central cones.

5.7 Trade-off Study for Central Cone Assemblies

After finishing the first stage of the design and analysis phase, first trade-off study can be done. The objective of this trade-off study is determining the first two optimum design of central cone designs for a satellite with 1000kg mass. After deciding the first two optimum design, there will be some optimizations on them to get most appropriate design concept for defined subject.

In the first trade-off study, the headings are mass of central cones, mass of central cone assemblies, modal analysis results of central cone, modal analysis results of central cone assemblies, static structural analysis results of the central cone assemblies and finally buckling analysis results of central cone assemblies. Another important part of the trade-off study is deciding the weights of the categories. There are two mass comparison and stiffness comparison in the thesis that is why for each mass comparison weight is 1 and for each stiffness comparison weight is 1.25. For static structural analysis and buckling analysis result comparisons the weights are 2.75. Total score of the weight is 10 and being close to 10 makes the central cone more optimal. First trade-off study results are shown at Table 5.39.

Table 5.39 : Trade-off study results of central cone design concepts

Central Cone Assy.	Weight	AL Monocoque	CFRP Monocoque	AL Grid	CFRP Grid	AL Sandwich	CFRP Sandwich
Mass	1	5	9	4	7	10	10
Assy. Mass	1	6	10	4	6	8	8
Stiffness	1.25	8	10	6	7	7	8
Assy. Stiffness	1.25	8	10	6	8	8.5	9.25
MoS_{Static}	2.75	8	7	10	5	6	6.5
$MoS_{Buckling}$	2.75	6	6.5	5	3.5	9	10
Total	10	6.95	8.1125	6.425	5.5125	7.8625	8.4937

CFRP sandwich central cone has the highest score from the trade-off study with considering the categories and weights of them. Mass of the central cone, buckling analysis results and assembly stiffness values are great for CFRP sandwich central cone. Assembly mass and stiffness of the central cone can be optimized after some design iterations but static structural analysis results of the CFRP sandwich central cone is the weak point of the structure. CFRP semi-monocoque central cone also has great scores at assembly mass, stiffness of the cone and stiffness of the assembly. The buckling analysis and static structural analysis results of he CFRP semi-monocoque central cone can be improve. Aluminium sandwich central cone is following that two central cone designs. Aluminium semi-monocoque and aluminium grid central cone has similar results in total but CFRP grid cone has the lowest score in each other. At the end of the trade-off study CFRP sandwich central cone and CFRP semi-monocoque central cone are selected for stage 2 of the thesis.

5.8 Design Iterations Phase

In the design iterations phase, CFRP sandwich and CFRP semi-monocoque central cones will be optimized. The main purpose of the iterations is decreasing the mass of central cones and assemblies without losing too much strength or stiffness. Removing assembly components, lamination of the plies, thickness of the central cones can be the iteration options for the selected central cones. At the end of the iterations, there will be second trade-off study for these two central cones to determine which one is more accurate for more than 1000 kg LEO satellites.

5.8.1 Design iterations of CFRP sandwich central cone

Assembly mass of the CFRP sandwich central cone was more than CFRP semi-monocoque central cone because of having NC bracket in its design. To reduce the mass of assembly NC bracket can be removed to understand the effect of it. Also, for decrease the central cone mass honeycomb density can be reduce with using low density honeycomb with lower strength properties. The optimizations applied on the CFRP sandwich central cone assembly are:

- Removing NC bracket
- Changing AL 5056 (6.1) honeycomb to AL 5056 (4.5) honeycomb

CFRP sandwich central cone assembly is shown at Figure 5.52 after removing NC bracket in its design. By removing the NC bracket connections of horizontal structural panel and central cone is also removed too.

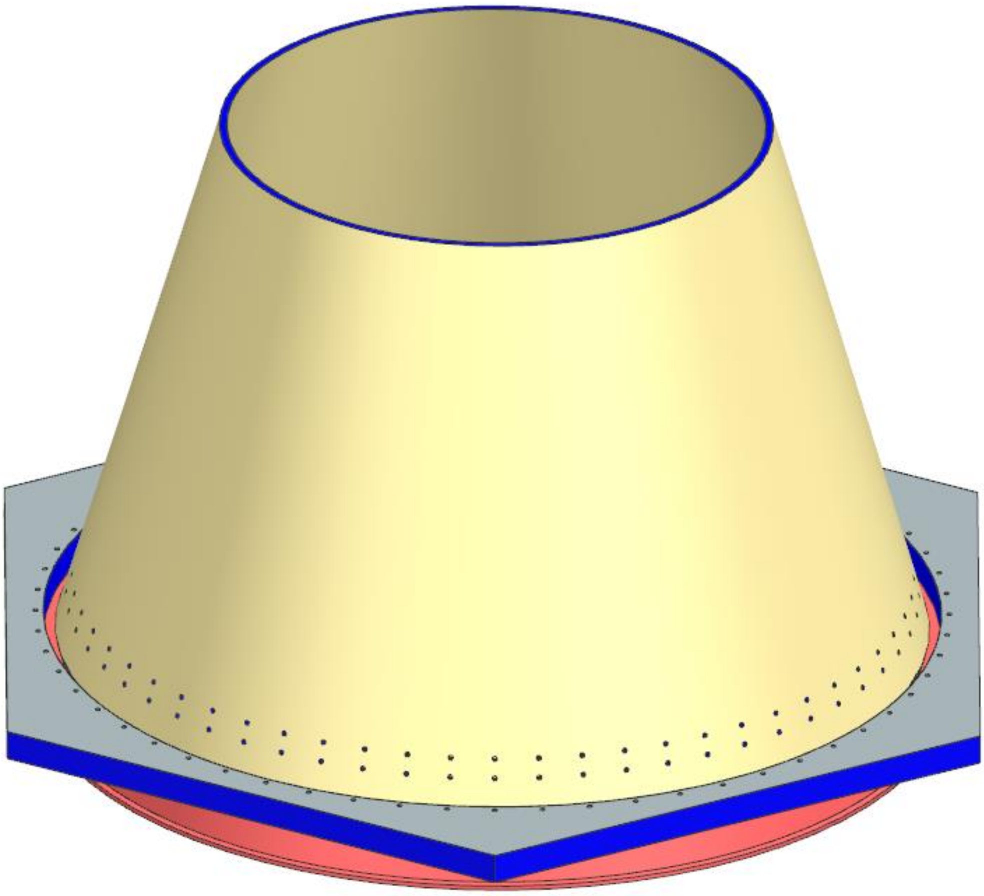

Figure 5.52 : CFRP sandwich central coen assembly design without NC bracket

AL 5056 (4.5) material properties are listed at Table 5.40 [25].

Table 5.40 : Honeycomb AL 5056 (4.5) material properties [25]

Honeycomb	5056 AL (4.5)
Density	72 kg/m^3
Shear Modulus (G13)	483 MPa
Shear Modulus (G23)	193 MPa
FsL	3.03 MPa
FsW	1.76 MPa

Changes of the designs are affecting positively masses of central cone and assembly. New mass values of the CFRP sandwich central cone are shown at Table 5.41.

Table 5.41 : Mass values of CFRP sandwich central cone

Central Cones	CFRP Sandwich
Mass (kg)	7.72
Assy. Mass (kg)	28.13

The mass advantage gained with these iterations is 6.29 kg with considering the previous design of CFRP sandwich central cone assembly. Same analysis with phase 1 of the thesis applied on the optimized CFRP sandwich central cone with same load cases. That analyzes are modal analysis of central cone, modal analysis of central cone assembly, static structural analysis of central cone assembly and buckling analysis of the central cone assembly.

Modal analysis of optimized CFRP sandwich central cone results with previous analysis results on preliminary designed CFRP sandwich central cone is shown at Table 5.42. For modal analysis only the first natural frequencies of the structures are compared because only that is the design requirement.

Table 5.42 : Modal analysis result comparison of CFRP sandwich central cone

Central Cones	CFRP Sandwich
Previous Mode 1 (Hz)	329.76
Optimized Mode 1 (Hz)	338.18

Result of the modal analysis also improved with 8.26 Hz. Weight advantage of the optimized central cone is affecting the improvement of the modal analysis results. The mode shape of the optimized CFRP sandwich central cone is show at Figure 5.53. The mode shape of the CFRP sandwich central cone is similar with the preliminary designed one.

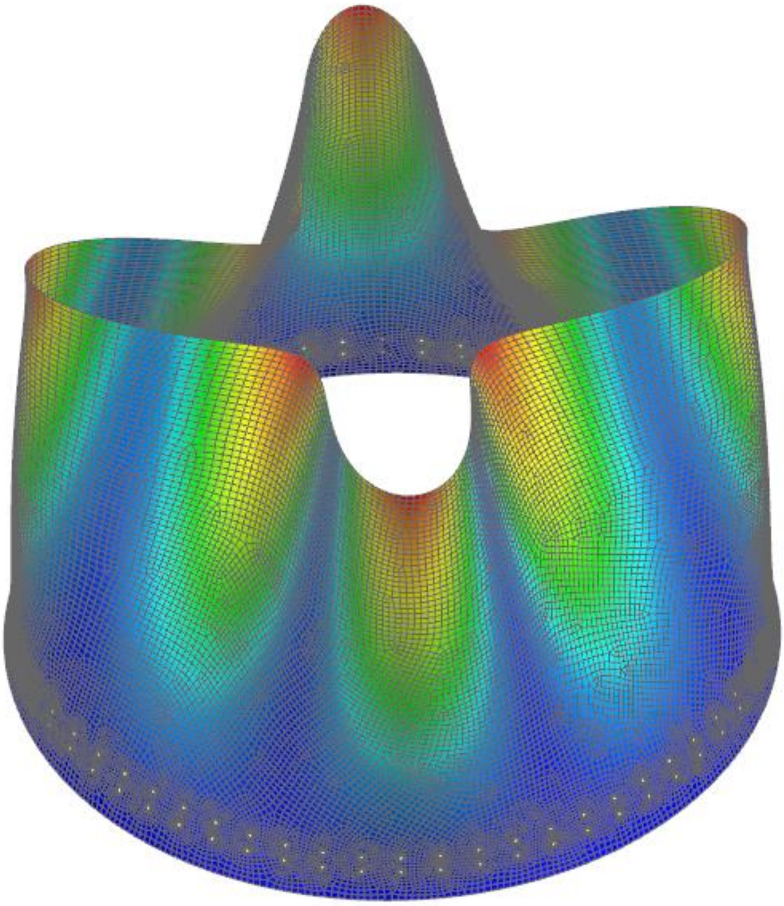

Figure 5.53 : Mode shape of optimized CFRP sandwich central cone Mode 1

Second analysis of the iteration is assembly modal analysis. The result comparison of the assembly modal analyzes are listed at Table 5.43.

Table 5.43 : Modal analysis result comparison of CFRP sandwich central cone assemblies

Central Cones Assy.	CFRP Sandwich
Previous Mode 1 (Hz)	553.05
Optimized Mode 1 (Hz)	578.83

Same with central cone modal analysis results, assembly modal analysis results are also improved with optimizations. The improvement of the result is 25.78 Hz. The mode shape of the optimized CFRP sandwich central cone assembly is show at Figure 5.54. Mode shape of the mode 1 is similar with the preliminary designed CFRP sandwich central cone assembly.

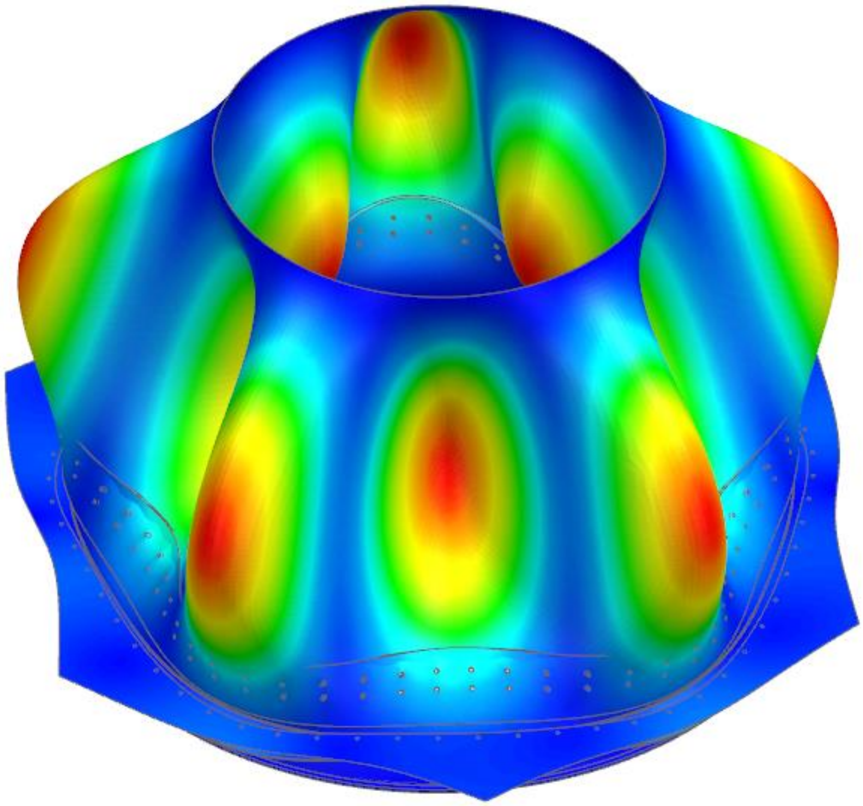

Figure 5.54 : Mode shape of optimized CFRP sandwich central cone assembly Mode 1

For static structural analysis, $MoS_{Honeycomb}$ and Tsai-Wu failure theorem results are the key factors of the comparison. For $MoS_{Honeycomb}$ interlaminar shear stresses are important parameters to get bigger margin of safety results. The result comparison of the static structural analyzes is shown at Table 5.44.

Table 5.44 : Static structural analysis of CFRP sandwich central cone assy.

Central Cone Assy.	Previous CC	Optimized CC
Deformation (mm)	0.154	0.121
Tsai-Wu Failure Index (worst ply)	0.407	0.246
τ_{xz} (MPa) (honeycomb)	1.896	0.641
τ_{yz} (MPa) (honeycomb)	1.353	0.549
$MoS_{Honeycomb}$	0.266	1.123

Both parameters which are Tsai-Wu failure index and $MoS_{Honeycomb}$ values are improved in the optimized central cone. For Tsai-Wu score, being close to 0 and far from 1 is better solution and for margin of safety high number of results are better. Deformation of the structure is shown at Figure 5.55.

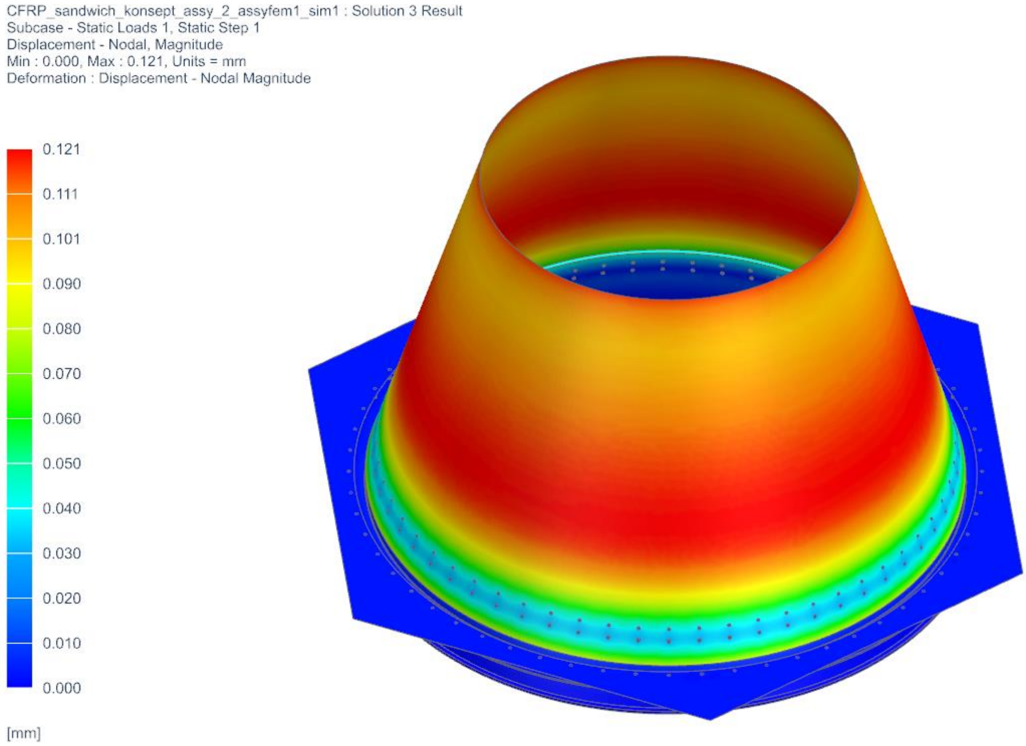

Figure 5.55 : Optimized CFRP sandwich central cone static structural analysis results (deformation)

Interlaminar shear stress results of the optimized central cone is shown at Figure 5.56 and Figure 5.57 respectively.

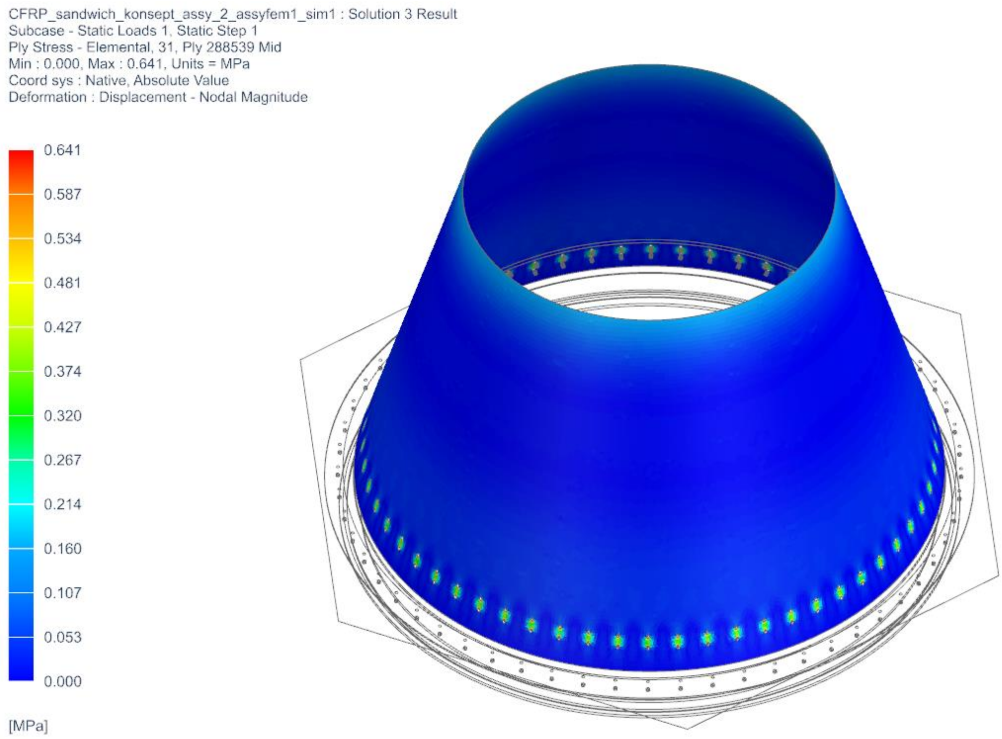

Figure 5.56 : Interlaminar shear stress results of CFRP sandwich central cone with direction τ_{xz}

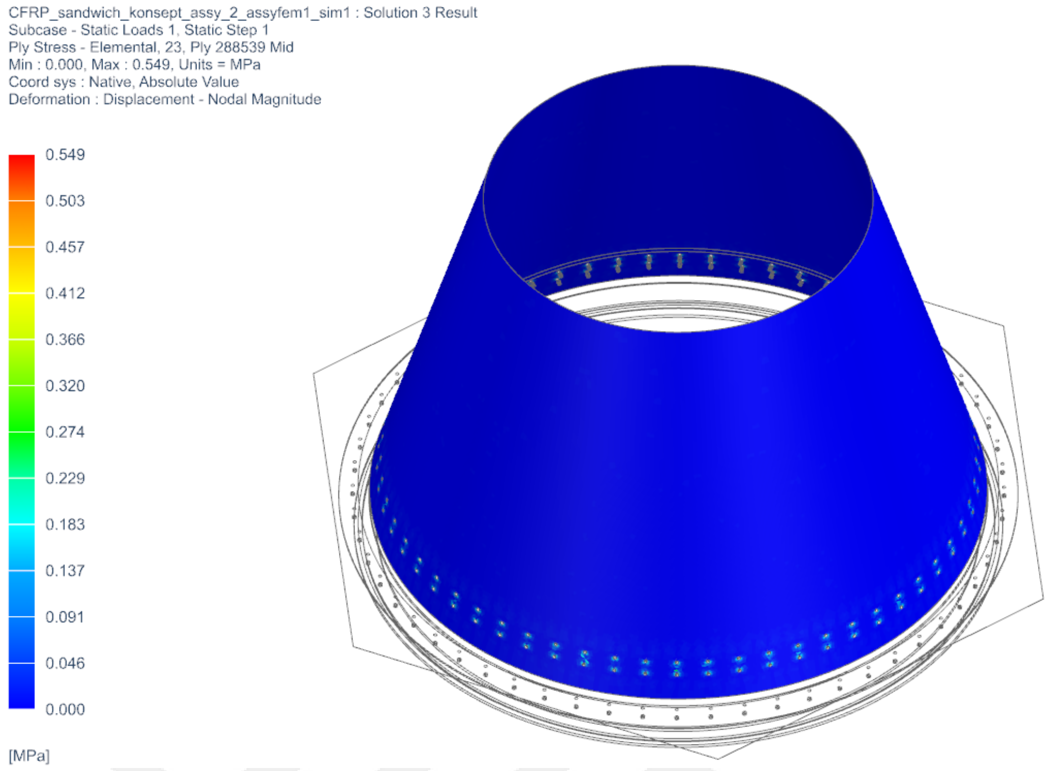

Figure 5.57 : Interlaminar shear stress results of CFRP sandwich central cone with direction of τ_{yz}

Tsai-Wu failure results for worst ply in the CFRP sandwich central cone is shown at Figure 5.58.

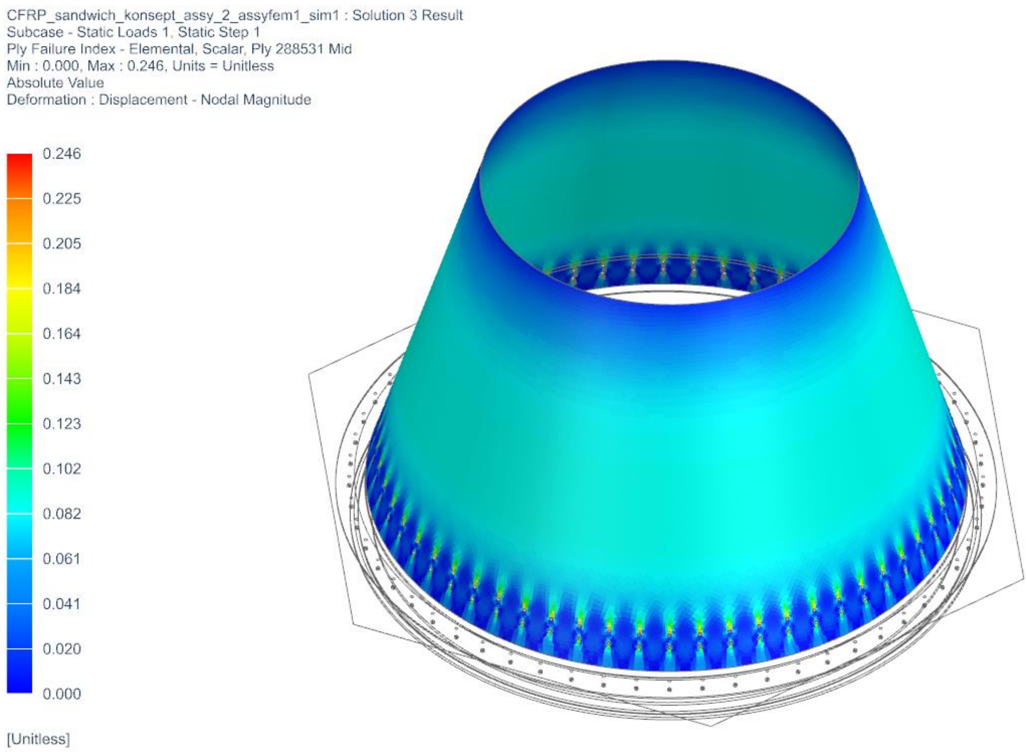

Figure 5.58 : Tsai-Wu failure index results of CFRP sandwich cone worst ply

Last analysis performed with optimized CFRP sandwich central cone is buckling analysis of it. Having bigger critical buckling factor after the analysis is the preferred result for this analysis. Result comparison of the buckling analysis results are shown at Table 5.45.

Table 5.45 : Buckling analysis result comparison for CFRP sandwich central cone assy.

Central Cone Assy.	Previous CC	Optimized CC
Buckling Mode (λ)	45.39	51.85
$MoS_{Buckling}$	21.695	24.925

Same with other analyzes results, buckling analysis result is also improved with the optimization. Mode shape and deformations after buckling analysis is shown at Figure 5.59. The shape of the modes of buckling analysis result for optimized solution is homogenous deformation. At preliminary design, the deformation was local at the connection area of the central cone to LVA and NC bracket.

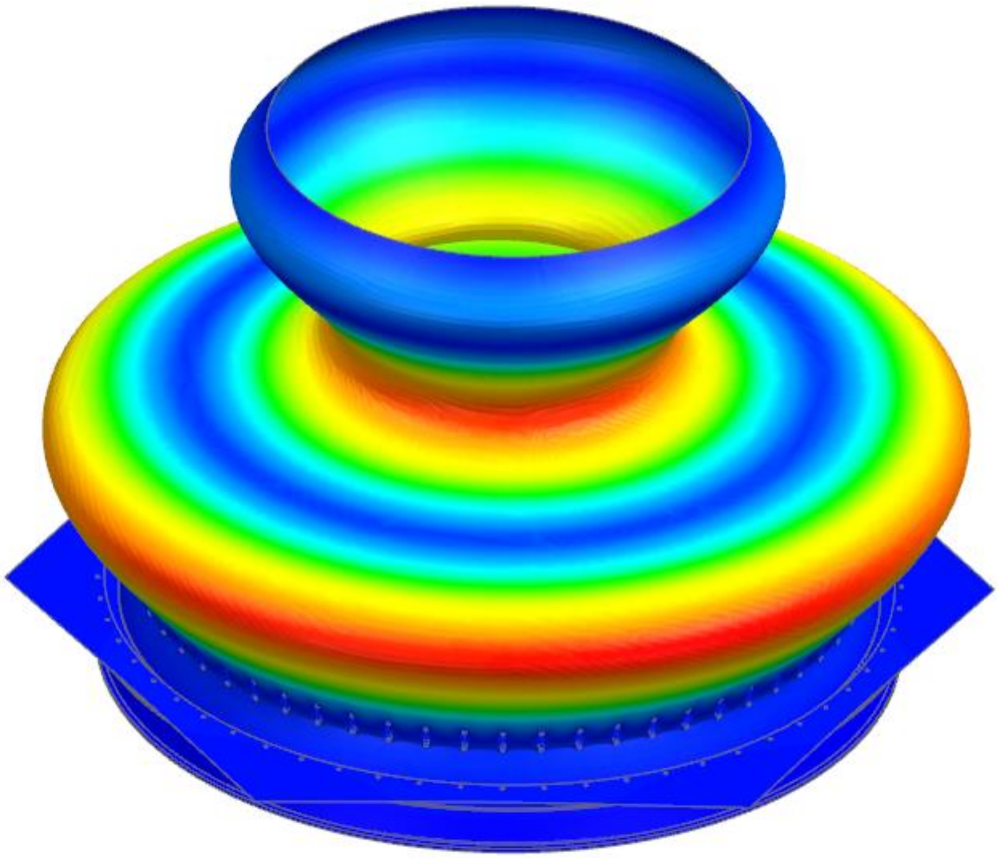

Figure 5.59 : Buckling mode shape of optimized CFRP sandwich central cone assy.

5.8.2 Design iterations of CFRP semi-monocoque central cone

In the optimization of the CFRP semi-monocoque central cone, the number of plies is decreased to reduce the mass of central cone. This design change is affecting the thickness of the central cone. In the previous design, thickness of the central cone shell was 3mm and ribs inside of the cone was 2mm. All the thickness values are reduced to 1.6 mm for CFRP semi-monocoque central cone. With this operation, mass results of central cone and assembly are shown at Table 5.46.

Table 5.46 : Mass values of CFRP semi-monocoque central cone

Central Cones	CFRP Sandwich
Mass (kg)	7.04
Assy. Mass (kg)	27.63

Thickness optimization results with 2.37 kg mass save for the design of central cone. Same analyzes with phase 1 and CFRP sandwich central cone performed for CFRP semi-monocoque central cone too. The comparison of the results is shown with tables.

Modal analysis results are shown at Table 5.47 for CFRP semi-monocoque central cone.

Table 5.47 : Modal analysis result comparison for CFRP semi-monocoque central cone optimization

Central Cones	CFRP Sandwich
Previous Mode 1 (Hz)	485.55
Optimized Mode 1 (Hz)	495.49

Results are close to each other but improved 9.94 Hz with mass optimization. The modal analysis results of the CFRP semi-monocoque central cone in the phase 1 comparisons was the best between the all-central cone designs and with the design optimization that stiffness value is increased more. Mode shape of the analysis is shown at Figure 5.60.

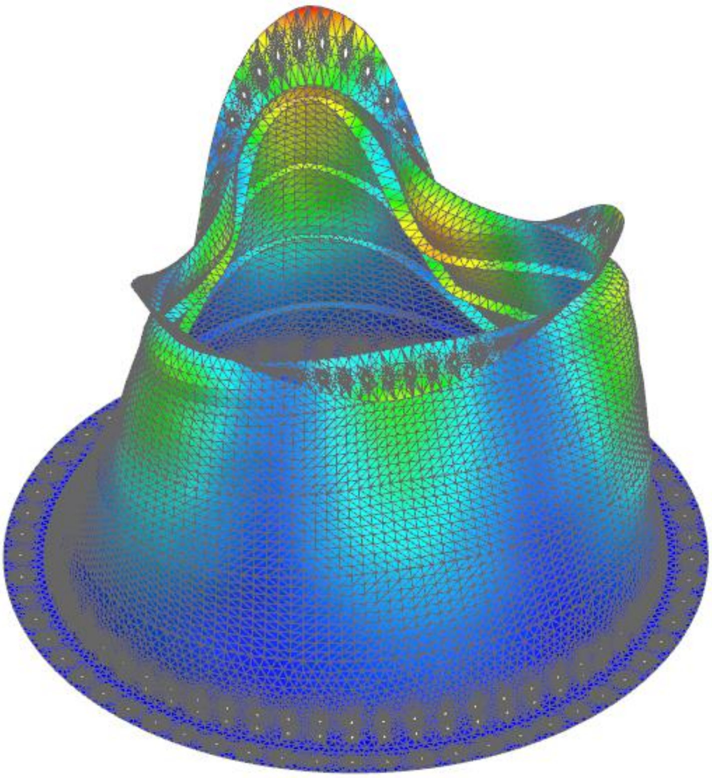

Figure 5.60 : Mode shape of optimized CFRP semi-monocoque central cone

Assembly modal analysis results are shown at Table 5.48. Results are improved 73.18 Hz which is different than the CFRP sandwich central cone assembly. The gain of stiffness draws attention. Mode shape of natural frequency of CFRP semi-monocoque central cone assembly is shown at Figure 5.61.

Table 5.48 : Modal analysis result comparison for CFRP semi-monocoque central cone assembly optimization

Central Cones Assy.	CFRP Sandwich
Previous Mode 1 (Hz)	615.47
Optimized Mode 1 (Hz)	688.65

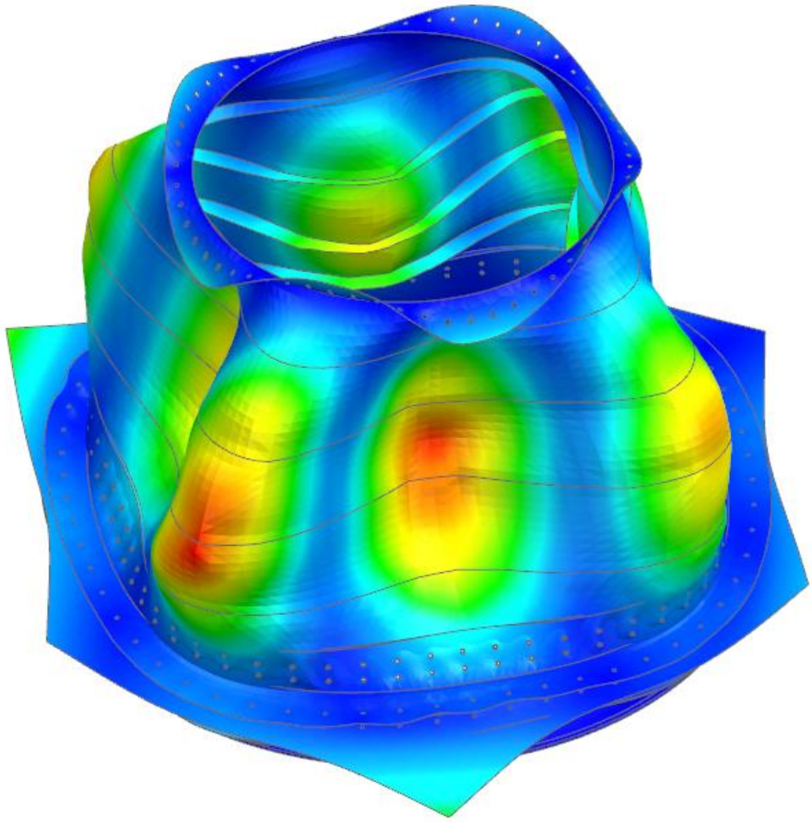

Figure 5.61 : Mode shape of optimized CFRP semi-monocoque central cone assembly Mode 1

Static structural analysis results for CFRP semi-monocoque central cone is depends on the Tsai-Wu failure calculation results. In the phase 1 of the thesis, Tsai-Wu results of the CFRP semi-monocoque central cone was the best results between the other CFRP central cones. The analysis result comparison is at Table 5.49.

Table 5.49 : Static structural analysis result comparison for CFRP semi-monocoque central cone assy.

Central Cone Assy.	Previous CC	Optimized CC
Deformation (mm)	0.145	0.162
Tsai-Wu Failure Index (worst ply)	0.303	0.293

Deformation of the central cone is increased but it can be neglect the results because of the small change. Also, it is expected to have this kind of deformation increase because of the thickness changes of the CFRP semi-monocoque central cone. Tsai-Wu failure results are better with the optimization of the central cone. Deformation of the central cone is shown at Figure 5.62 and Tsai-Wu results at worst ply of the CFRP semi-monocoque central cone is shown at Figure 5.63.

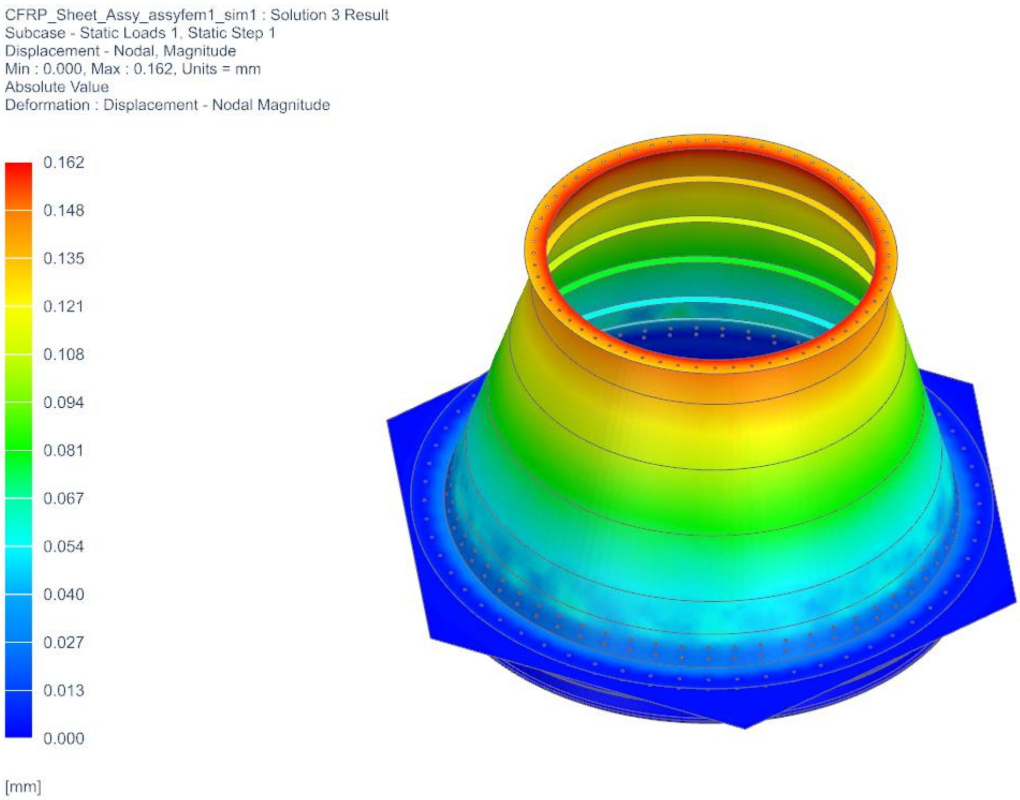

Figure 5.62 : Optimized CFRP smei-monocoque central cone static structural analysis results (deformation)

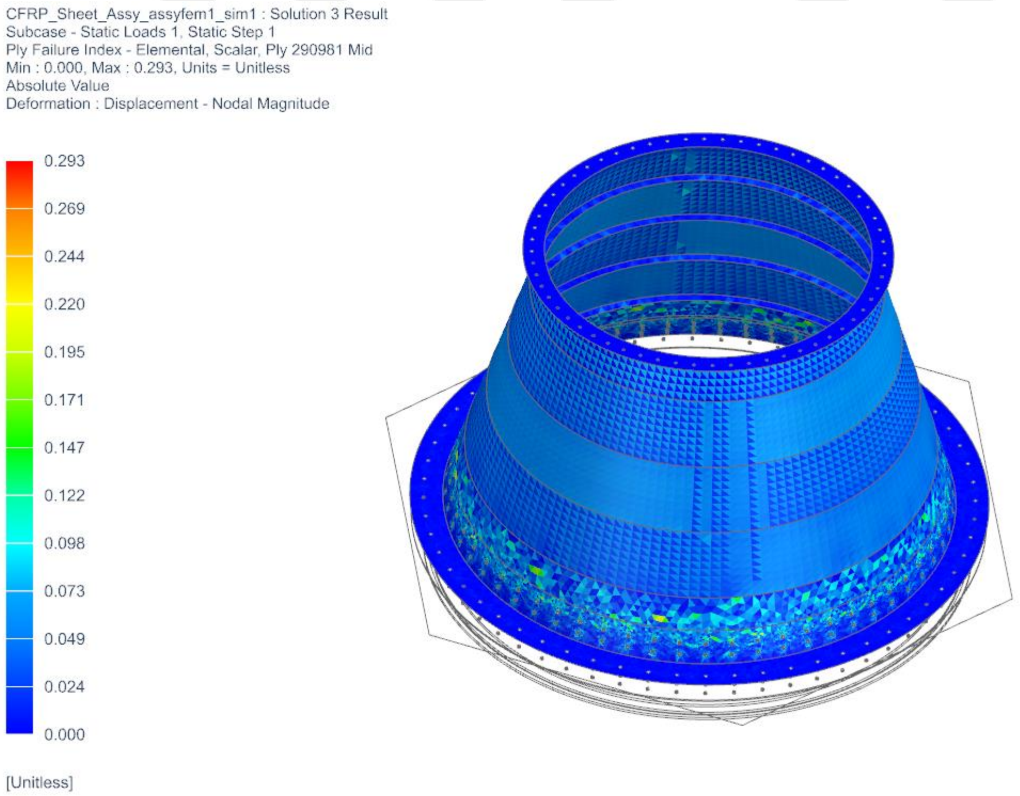

Figure 5.63 : Tsai-Wu failure index results of CFRP semi-monocoque cone worst ply

Last analysis performed for CFRP semi-monocoque central cone is buckling analysis. The result comparison is shown at Table 5.50.

Table 5.50 : Buckling analysis result comparison of the CFRP semi-monocoque central cone optimization

Central Cone Assy.	Previous CC	Optimized CC
Buckling Mode (λ)	13.01	8.74
$MoS_{Buckling}$	5.505	3.37

From all the analysis performed in the phase 2 of the thesis, only analysis result with decreased with optimization is buckling analysis of CFRP semi-monocoque central cone which is normal because of the thinner central cone. Mode shape and deformations after buckling analysis is shown at Figure 5.64. The deformation is kind of local buckling with considering the mode shape of the analysis.

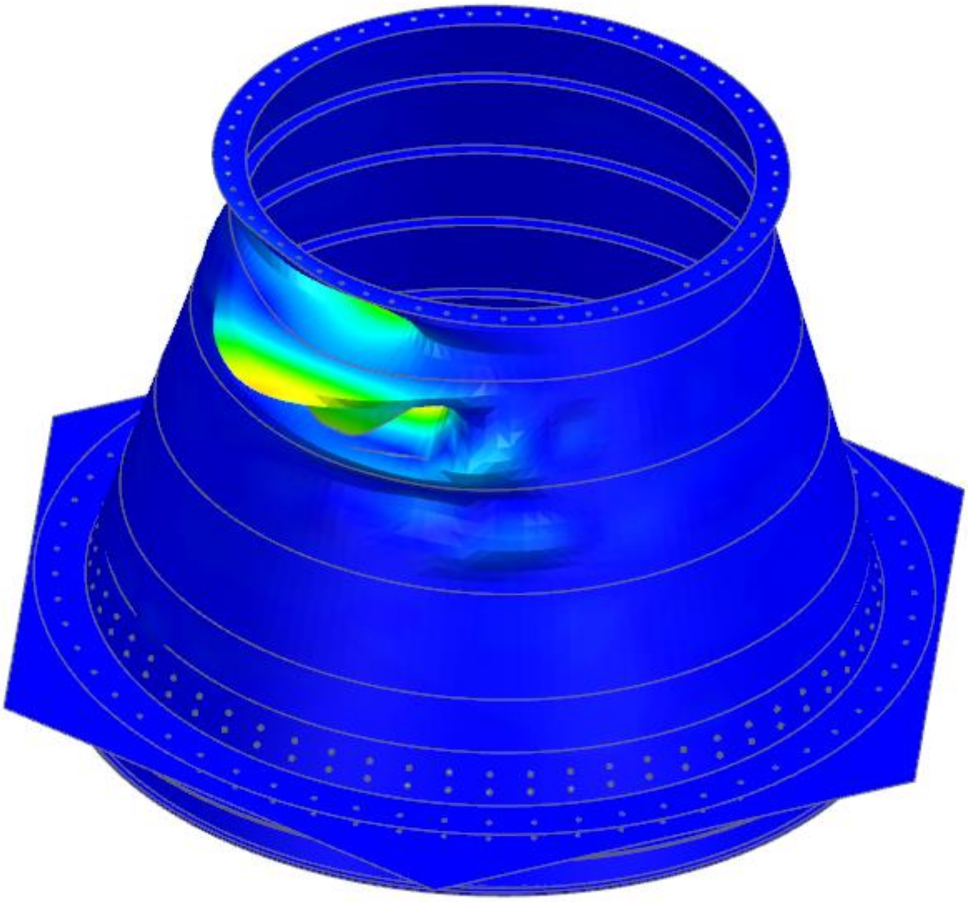

Figure 5.64 : Buckling mode shape of optimized CFRP semi-monocoque central cone assy.

5.9 Trade-off Study for Optimized Central Cones

In the second trade-off study of the thesis, only two optimized central cones compared between each other to determine optimal design for referenced satellite which is around 1000kg at Low Earth Orbit. Because of the having only two central cones, the point scales are given with considering their own results. Having better solution in each category having 10 points from 10, and other central cone gets the points depends on how close its results. That is why, for all the categories one of the central cones has the 10 points which is top point. Weight of the trade-off study is same with previous trade-off study which is done for six central cones. Trade-off study table is shown at Table 5.51.

Table 5.51 : Trade-off study results of optimized central cones

Central Cone Assy.	Weight	CFRP Monocoque	CFRP Sandwich
Mass	1	10	9.5
Assy. Mass	1	10	9.5
Stiffness	1.25	10	8.5
Assy. Stiffness	1.25	10	9
MoS_{Static}	2.75	9.5	10
$MoS_{Buckling}$	2.75	7	10
Total	10	9.0375	9.5875

Mass and assembly mass results of central cones are extremely close to each other but CFRP semi-monocoque central cone has less mass in its design. Only difference in their masses is 0.68 kg for both categories. After mass comparisons, stiffness comparisons are done. In the modal analysis results, CFRP semi-monocoque central cone has advantage to have better stiffness values which is first natural frequency value. On the other hand, for static structural and buckling analysis results CFRP sandwich central cone has better results. For margin of safety static results are close to each other but sandwich central cone has better results. For critical buckling factor, sandwich central cone has huge difference from semi-monocoque central cone. Both central cones have great results in the performed analyzes and both of them meets the design requirements. As a result of all the categories, with 0.55-point difference CFRP sandwich central cone became the optimal design for the thesis.

6. CONCLUSIONS AND RECOMMENDATIONS

In the thesis, the main object was finding the optimal design solution as central cone of a satellite which is more than 1000kg at Low Earth Orbit. In the study, the design requirements and restrictions, launcher and satellite effect on central cone, design, analysis and trade-off philosophy are described. In this section, the phases of the thesis are summarized with results and recommendations.

6.1 General Conclusions

Before starting the design of any structure for satellites, the design requirements and limitations should be defined to foresee what kind of design solution study need. In the beginning of the thesis, the mechanical loads which satellite is affecting from launchers are defined with considering some possible launchers for a LEO satellite. Material types and design concepts are also described for primary structures of satellite. Six different design of central cones which are three different design concepts and two types of material for each decided to compare in the study. Materials are aluminium and CFRP for each design concept, and design concepts are semi-monocoque, grid and sandwich types. There are two main phases of the thesis, in the first phase of the study six different central cone compared in the trade-off study and top two central cone selected for optimizations. In the second phase of the thesis that two central cones optimized and compared again with the same trade-off study to define optimal central cone.

In the design phase of the central cones, Siemens NX used to design all central cones and the assembly components of them. The components of the assemblies are LVA, horizontal structural panel and NC bracket if it is needed. First comparations of the study is done in the design phase of the thesis by comparing the masses of central cones and their assemblies. From first mass comparations, sandwich central cones are the lighter central cones. In the assembly mass comparisons, CFRP semi-monocoque central cone is the lighter central cone assembly because of not having NC bracket in semi-monocoque assembly designs.

In the analysis phase of the study, defined types of the analysis will be performed which are modal analysis, static structural analysis and buckling analysis. Creation of the FEM of central cones and other assembly components are shown. Modal analysis is performed for just central cones itself and their assemblies.

First analysis was modal analysis on central cones, and CFRP semi-monocoque central cone has best results. CFRP sandwich central cone and Aluminium semi-monocoque central cone are following the CFRP semi-monocoque central cone with their results. Assembly modal analyzes are performed for all six central cone assemblies, and again CFRP semi-monocoque central cone has the highest stiffness from the results.

For static structural analysis, there are some margin of safety formulas to compare different types of design concepts and materials. Also, a load case is defined with regarding to consider reference satellite with 1000kg mass. In the preliminary results of the static analyzes, Aluminium grid central cone assembly has the highest margin of safety value. Aluminium semi-monocoque central cone is the second best in terms of static structural strength of the central cone assemblies.

Same with the static structural analysis, a margin of safety philosophy is used in their calculations with same load cases. Both sandwich central cone assemblies got highest buckling strength results, but CFRP sandwich central cone is the best design concept for buckling.

All central cones are compliance the design requirements defined in the beginning of the study. After finishing all design and analysis phase works, trade-off study calculations performed to select two central cones to optimize more for get optimal design concept. In the results of trade-off study CFRP sandwich central cone and CFRP semi-monocoque central cone selected as top two central cone design concept for the second phase of the thesis.

In the design iterations phase the main purpose is reducing the mass of the central cones and their assemblies without loosing any strength or stiffness. For CFRP sandwich central cone 0.49 kg saved and for its assembly 6.29 kg weight reduced with the iterations. The iterations are removing the NC bracket in the CFRP sandwich central cone assembly and changing the honeycomb type and density. Even the mass reduced the stiffness results are raised with the optimizations for the CFRP sandwich central cone. Also, with same load cases of first phase of the study, static structural and buckling analysis performed. Results are improved with the optimizations on the assembly and central cone. For CFRP semi-monocoque central cone number of plies are reduced and thickness of the central cone changed with that. As a result of this optimization new central cone and its assembly are 2.37kg lighter than first design of CFRP semi-monocoque central cone. Modal analysis results are also improved with the optimizations. There is only buckling analysis results reduce but not dramatically for CFRP semi-monocoque central cone. At the end of the design iterations, there is a second trade-off analysis for these two central cones. With 9.5875 points from 10, CFRP sandwich central cone selected as optimum design concept for LEO satellites around 1000kg which is Göktürk-Y satellite as a reference.

6.2 Recommendations

In this study, the design concepts of the central cones are examined and analysed with some optimizations. As a result of the study CFRP sandwich central cone is selected as optimum design concept for large LEO satellites, but results of CFRP semi-monocoque central cone is also close to sandwich one.

In the future work, the optimization on CFRP sandwich or semi-monocoque central cone can be the main objective to improve the results of them. On the other hand, the recommended future study can be production and tests of CFRP sandwich central cone. There can be a production and test campaign to correlate the results of the study. There can be two types of test campaigns for possible future study on this thesis. First one of them is after production of CFRP sandwich central cone, the main focus can be the central cone with defined load cases in this study. Also, the load cases can be improved by adding new load cases with regarding to other possible reference satellite projects. Second test type can be in a satellite test as a system level. In those tests central cone can prove itself in the satellite with the launcher load cases on them.

REFERENCES

[1] **Calvi, A., & Bastia, P.** (2016). Mechanical architecture and loads definition for the design and testing of the Euclid spacecraft. *Advances in Aircraft and Spacecraft Science*, 3(2), 225-242. doi:10.12989/aas.2016.3.2.225

[2] **Morozov, E.V and Lopatin, A.V**. (2017) Computer modelling and simulation of the mechanical response of composite lattice structures, 22nd International Congress on Modelling and Simulation, December 2017.

[3] **ESA** (2012) Sentinel-3: ESA's Global Land and Ocean Mission for GMES Operational Services Netherlands : ESA Communications

[4] **Abay M. M., Atak A., İzgü O., Şahin M.** (2019) Design and Optimization of Innovative CFRP Central Cylinder for Satellite *2019 9th International Conference on Recent Advances in Space Technologies (RAST)* (pp. 103-107) Istanbul, Turkey doi: 10.1109/RAST.2019.8767825.

[5] **Pavlov, L., Smeets, B., Simonian, S. M.** (2016). Optimization of a composite lattice satellite central cylinder structure using an efficient semi-automated approach. *57th AIAA/ASCE/AHS/ASC Structures, Structural Dynamics, and Materials Conference.* California, USA https://doi.org/10.2514/6.2016-1497

[6] **Afonso, S. M. B., Sienz, J., Belblidia, F.** (2005). Structural optimization strategies for simple and integrally stiffened plates and shells. *Engineering Computations*, 22(4), (pp. 429–452) https://doi.org/10.1108/02644400510598769

[7] **Guerrera A., Varbaro A.** (2014) *Reverse engineering and structural analysis of Ariane 5 payload adapters PAS 1194VS and PAS 1194C* (Master Thesis in Aerospace Engineering) Department of Civil and Industrial Engineering, School of Engineering, Universita Di Pisa, Italy

[8] **Günal A.B., Atak A., Şahin M.** (2019) Building a design decision methodology by combining quantitative and qualitative methods – A case study for central cylinder design selection. *10th Ankara International Aerospace Conference* Ankara, Turkey

[9] **Url-1** (n.d) https://www.hvkk.tsk.tr/Custom/Hvkk/243 retrieved March 5, 2023

[10] **Url-2** (n.d) https://alen.space/basic-guide-nanosatellites/ retrieved April 6, 2023

[11] **Url-3** (n.d) https://www.tusas.com/urunler/uzay/yer-gozlem-ve-kesif-uydulari/gokturk-2 retrieved March 11, 2023

[12] **Url-4** (n.d) https://solarsystem.nasa.gov/basics/chapter11-1/ retrieved February 20, 2023

[13] **Sarafin T. P.** (2003) *Spacecraft Structures and Mechanisms From Concept to Launch* Fourth Edition, Space Technology Series, United States of America

[14] **ECSS** (2008) *Space Engineering – Structural general requirements* (ECSS-E-ST-32C Rev.1) Retrieved from https://ecss.nl/standard/ecss-e-st-32c-rev-1-structural-general-requirements/

[15] **Arianespace** (2016) *Ariane – 5 User's Manual* (Issue 5 – Revision 2) Retrieved February 16, 2023 from https://www.arianespace.com/wp-content/uploads/2011/07/Ariane5_Users-Manual_October2016.pdf

[16] **Arianespace** (2018) *Soyuz User's Manual* (Issue 2 – Revision 1) Retrieved March 2, 2023 from https://www.arianespace.com/wp-content/uploads/2018/07/Vega-C-user-manual-Issue-0-Revision-0_20180705.pdf

[17] **SpaceX** (2021) *Falcon User's Guide* (September 2021) Retrieved March 3, 2023 from https://www.spacex.com/media/falcon-users-guide-2021-09.pdf

[18] **Arianespace** (2018) *Vega C User's Manual* (Issue 0 Revision 0) Retrieved March 4, 2023 from https://www.arianespace.com/wp-content/uploads/2018/07/Vega-C-user-manual-Issue-0-Revision-0_20180705.pdf

[19] **Sarafin T.P.** (2022) *Structural Design and Analysis for Aerospace Engineers* (Course Book) Instar Engineering and Consulting, Inc. Retrieved from https://www.instarengineering.com/pdf/courses/SDA_course_book-Nov2022.pdf

[20] **Vijker, J. J.** (2008) Material Selection in *Spacecraft Structures* (pp. 207-2). Springer. doi:10.1007/978-3-540-75553-1

[21] **Gaudenzi P.** (n.d.) *Mechanical behaviour of structural materials and structures for space* [PowerPoint Slides] Retrieved from

https://www.scribd.com/document/88549987/01-Mechanical-Behaviour-of-Structural-Materials-and-Structures-for-Space#

[22] **Url-5** (n.d) https://www.tusas.com/urunler/uzay/modernizasyon-programlari/gokturk-y retrieved February 18, 2023

[23] **ECSS** (2014) *Space Engineering – Materials* (ECSS-E-ST-32-08C Rev.1). Retrieved from https://ecss.nl/standard/ecss-e-st-32-08c-rev-1-space-engineering-materials-15-october-2014/

[24] **MMPDS** (2019) *Metallic Materials Properties Development and Standardization* (MMPDS-14)

[25] **Hexcel** (2017*) HexWeb CR III Corrosion Resistant Specification Aluminum Honeycomb* Retrieved from https://www.hexcel.com/user_area/content_media/raw/HexWeb_CRIII_DataSheet.pdf

[26] **ECSS** (2011) *Space Engineering – Structural Materials Handbook – Part 1: Overview and material properties and applications* (ECSS-E-HB-32-20_Part-1A) Retrieved from https://ecss.nl/hbstms/ecss-e-hb-32-20-part-1a-structural-materials-handbook-part-1-overview-and-material-properties-and-applications-20-march-2011/

[27] **Url-6** (n.d) https://en.wikipedia.org/wiki/Natural_frequency retrieved March 11, 2023

[28] **Hansen, C., Snyder, S., Qiu, X., Brooks, L., Moreau, D.** (2012) Modal Analysis in *Active Control of Noise and Vibration* (2nd ed.,Vol 1, pp. 213-229). CRC Press

[29] **ECSS** (2010) *Space Engineering – Buckling Analysis* (ECSS-E-HB-32-24A) Retrieved from https://ecss.nl/hbstms/ecss-e-hb-32-24a-buckling-of-structures/

[30] **Siemens NX** (Version 2000) [Computer Software] Siemens Industry Software Inc.

[31] **Chen S., McGregor O.P.L., Endruweit A., Harper L.T., Warrior N.A.** (2019). Simulation of the forming process for curved composite sandwich panels *International Journal of Material Forming, 13(6),* 967-980. https://doi.org/10.1007/s12289-019-01520-4

[32] **Simcenter 3D** (Version 2000) [Computer Software] Siemens Industry Software Inc.

[33] **Url-7** (n.d) https://www.fidelisfea.com/post/what-is-the-difference-between-a-kinematic-rbe2-and-a-distributing-rbe3-coupling-in-fea retrieved April 9, 2023

[34] **ECSS** (2019) *Space Engineering – Structural factors of safety for spaceflight hardware* (ECSS-E-ST-32-10C Rev.2 Corrigendum 1) Retrieved from https://ecss.nl/standard/ecss-e-st-32-10c-rev-2-corr-1-structural-factors-of-safety-for-spaceflight-hardware-1-august-2019/

APPENDICES

APPENDIX A:

PAS 1194 technical drawings with the interface of the spacecraft's LVA is shown at Figure A.1

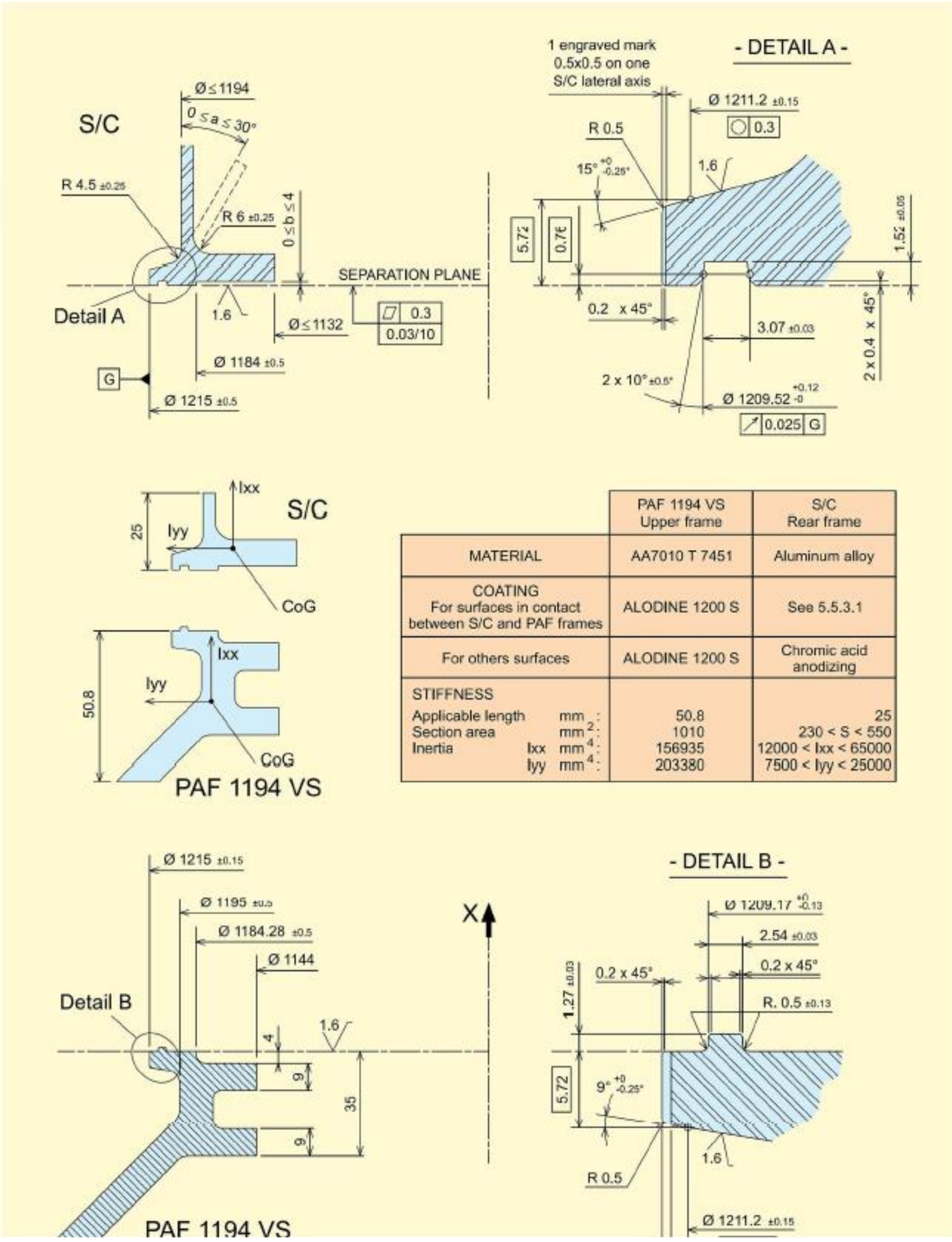

	PAF 1194 VS Upper frame	S/C Rear frame
MATERIAL	AA7010 T 7451	Aluminum alloy
COATING For surfaces in contact between S/C and PAF frames	ALODINE 1200 S	See 5.5.3.1
For others surfaces	ALODINE 1200 S	Chromic acid anodizing
STIFFNESS Applicable length mm : Section area mm^2 : Inertia Ixx mm^4 : Iyy mm^4 :	 50.8 1010 156935 203380	 25 230 < S < 550 12000 < Ixx < 65000 7500 < Iyy < 25000

Figure A.1 : PAS 1194 mechanical interface drawings

APPENDIX B:

CFRP semi-monocoque central cone composite lay-up is shown at Figure A.2 and Figure A.3. Central cone shell is 2mm that is why 20 plies are used for it. Upper and lower rings of the central cone is 3mm with 30 plies.

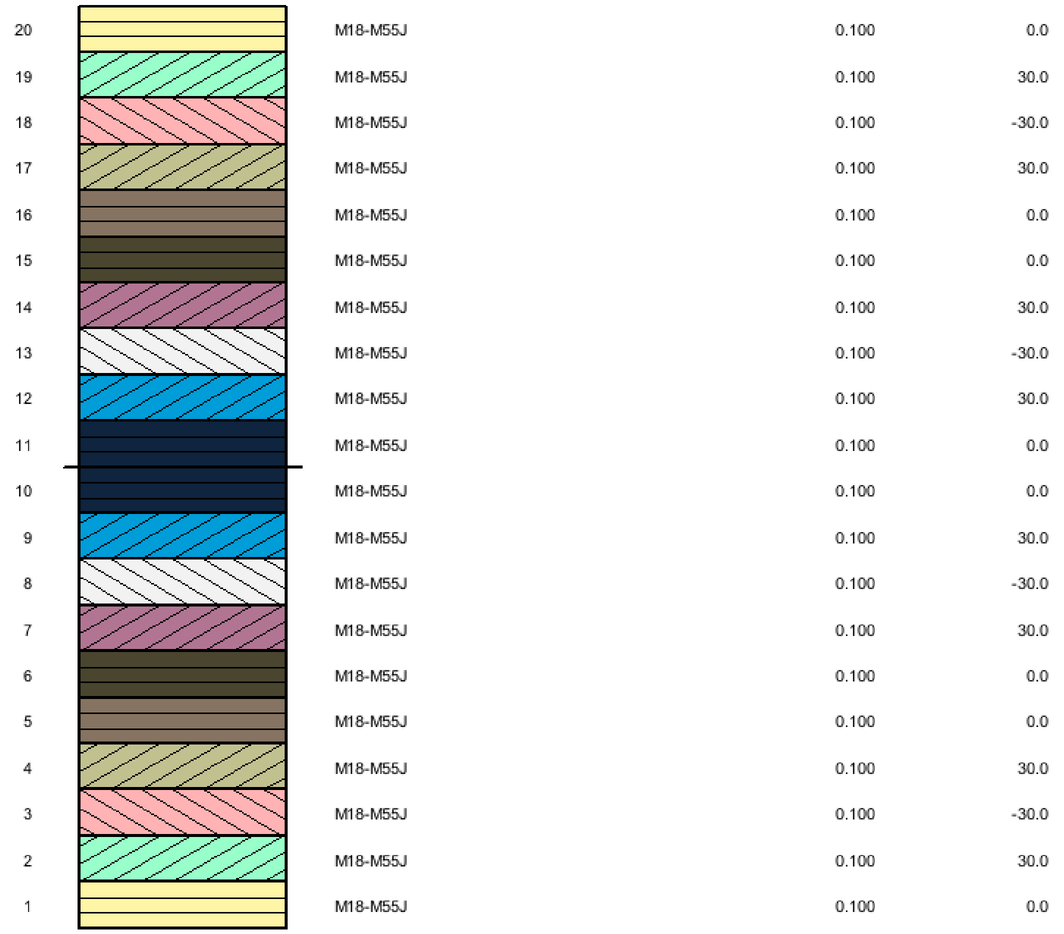

Figure A.2 : Composite lay-up of CFRP semi-monocoque central cone shell

30	M18-M55J	0.100	0.0
29	M18-M55J	0.100	30.0
28	M18-M55J	0.100	-30.0
27	M18-M55J	0.100	30.0
26	M18-M55J	0.100	0.0
25	M18-M55J	0.100	0.0
24	M18-M55J	0.100	30.0
23	M18-M55J	0.100	-30.0
22	M18-M55J	0.100	30.0
21	M18-M55J	0.100	0.0
20	M18-M55J	0.100	0.0
19	M18-M55J	0.100	30.0
18	M18-M55J	0.100	-30.0
17	M18-M55J	0.100	30.0
16	M18-M55J	0.100	0.0
15	M18-M55J	0.100	0.0
14	M18-M55J	0.100	30.0
13	M18-M55J	0.100	-30.0
12	M18-M55J	0.100	30.0
11	M18-M55J	0.100	0.0
10	M18-M55J	0.100	0.0
9	M18-M55J	0.100	30.0
8	M18-M55J	0.100	-30.0
7	M18-M55J	0.100	30.0
6	M18-M55J	0.100	0.0
5	M18-M55J	0.100	0.0
4	M18-M55J	0.100	30.0
3	M18-M55J	0.100	-30.0
2	M18-M55J	0.100	30.0
1	M18-M55J	0.100	0.0

Figure A.3 : Composite lay-up of CFRP semi-monocoque central cone upper and lower rings

APPENDIX C:

CFRP grid central cone composite lay-up is also divided in two parts. First part is shell behind the grids and second part is grids of the CFRP grid central cone. Lay-up and orientation of the shell of the central cone is shown at Figure A.4 and for grid part of the composite it is shown at Figure A.5.

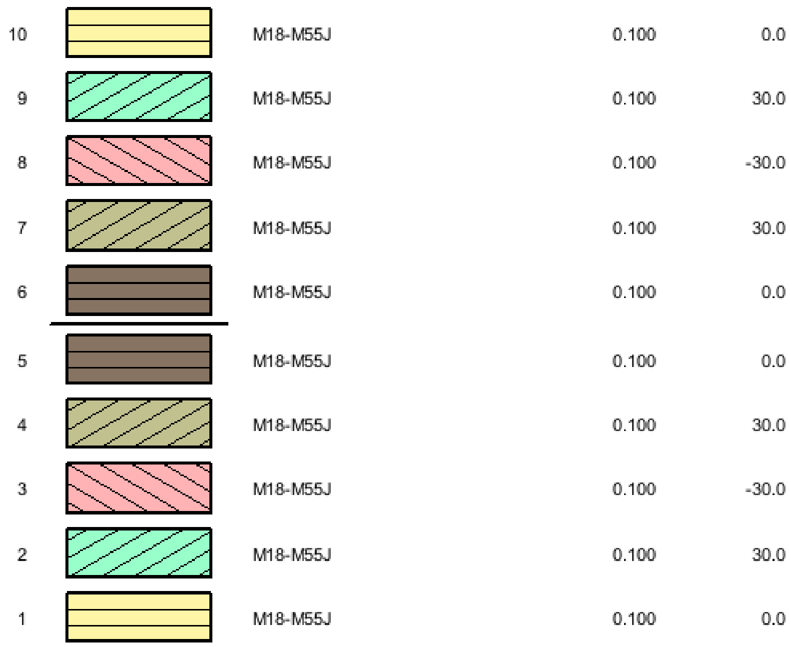

Figure A.4 : Composite lay-up of CFRP grid central cone shell

60	M18-M55J	0.150	0.0
59	M18-M55J	0.150	30.0
58	M18-M55J	0.150	-30.0
57	M18-M55J	0.150	30.0
56	M18-M55J	0.150	0.0
55	M18-M55J	0.150	0.0
54	M18-M55J	0.150	30.0
53	M18-M55J	0.150	-30.0
52	M18-M55J	0.150	30.0
51	M18-M55J	0.150	0.0
50	M18-M55J	0.150	0.0
49	M18-M55J	0.150	30.0
48	M18-M55J	0.150	-30.0
47	M18-M55J	0.150	30.0
46	M18-M55J	0.150	0.0
45	M18-M55J	0.150	0.0
44	M18-M55J	0.150	30.0
43	M18-M55J	0.150	-30.0
42	M18-M55J	0.150	30.0
41	M18-M55J	0.150	0.0
40	M18-M55J	0.150	0.0
39	M18-M55J	0.150	30.0
38	M18-M55J	0.150	-30.0
37	M18-M55J	0.150	30.0
36	M18-M55J	0.150	0.0
35	M18-M55J	0.150	0.0
34	M18-M55J	0.150	30.0
33	M18-M55J	0.150	-30.0
32	M18-M55J	0.150	30.0
31	M18-M55J	0.150	0.0
30	M18-M55J	0.150	0.0
29	M18-M55J	0.150	30.0
28	M18-M55J	0.150	-30.0
27	M18-M55J	0.150	30.0
26	M18-M55J	0.150	0.0
25	M18-M55J	0.150	0.0
24	M18-M55J	0.150	30.0
23	M18-M55J	0.150	-30.0
22	M18-M55J	0.150	30.0
21	M18-M55J	0.150	0.0
20	M18-M55J	0.150	0.0
19	M18-M55J	0.150	30.0
18	M18-M55J	0.150	-30.0
17	M18-M55J	0.150	30.0
16	M18-M55J	0.150	0.0
15	M18-M55J	0.150	0.0
14	M18-M55J	0.150	30.0
13	M18-M55J	0.150	-30.0
12	M18-M55J	0.150	30.0
11	M18-M55J	0.150	0.0
10	M18-M55J	0.150	0.0
9	M18-M55J	0.150	30.0
8	M18-M55J	0.150	-30.0
7	M18-M55J	0.150	30.0
6	M18-M55J	0.150	0.0
5	M18-M55J	0.150	0.0
4	M18-M55J	0.150	30.0
3	M18-M55J	0.150	-30.0
2	M18-M55J	0.150	30.0
1	M18-M55J	0.150	0.0

Figure A.5 : Composite lay-up of CFRP grid central cone grid

APPENDIX D:

The lay-up of CFRP sandwich central cone is shown at Figure A.6.

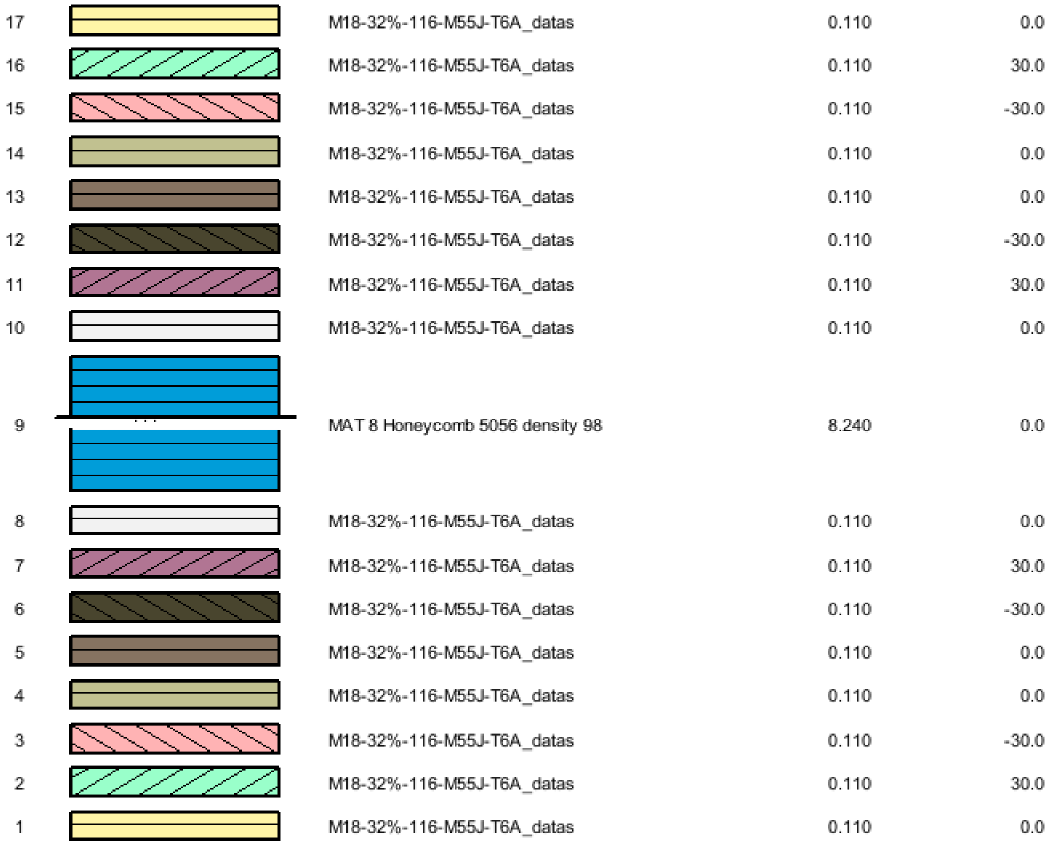

Figure A.6 : Composite lay-up of CFRP sandwich central cone

CURRICULUM VITAE

Name Surname : Semih Türkoğlu

E-Mail :

EDUCATION :

- **B.Sc. :** 2019, Istanbul Technical University, Faculty of Aeronautics and Astronautics, Astronautical Engineering

PROFESSIONAL EXPERIENCE AND REWARDS:

- 2019 – Design Engineer at Turkish Aerospace